12-2016

Towards Structuring Smart Grid: Energy Scheduling, Parking Lot Allocation, and Charging Management

Mehdi Rahmani-Andebili
Clemson University, mehdir@g.clemson.edu

TOWARDS STRUCTURING SMART GRID: ENERGY SCHEDULING, PARKING LOT ALLOCATION, AND CHARGING MANAGEMENT

A Dissertation
Presented to
the Graduate School of
Clemson University

In Partial Fulfillment
of the Requirements for the Degree
Doctor of Philosophy
Electrical Engineering

---

by
Mehdi Rahmani-Andebili
December 2016

Accepted by:
Haiying Shen, Committee Chair
William R. Harrell
Carl W. Baum
Lea Jenkins

ABSTRACT

Nowadays, the conventional power systems are being restructured and changed into smart grids to improve their reliability and efficiency, which brings about better social, economic, and environmental benefits. To build a smart grid, energy scheduling, energy management, parking lot allocation, and charging management of plug-in electric vehicles (PEVs) are important subjects that must be considered. Accordingly, in this dissertation, three problems in structuring a smart grid are investigated.

The first problem investigates energy scheduling of smart homes (SHs) to minimize daily energy consumption cost. The challenges of the problem include modeling the technical and economic constraints of the sources and dealing with the variability and uncertainties concerned with the power of the photovoltaic (PV) panels that make the problem a mixed-integer nonlinear programming (MINLP), dynamic (time-varying), and stochastic optimization problem. In order to handle the variability and uncertainties of power of PV panels, we propose a multi-time scale stochastic model predictive control (MPC). We use multi-time scale approach in the stochastic MPC to simultaneously have vast vision for the optimization time horizon and precise resolution for the problem variables. In addition, a combination of genetic algorithm (GA) and linear programming (GA-LP) is applied as the optimization tool. Further, we propose cooperative distributed energy scheduling to enable SHs to share their energy resources in a distributed way. The simulation results demonstrate remarkable cost saving due to cooperation of SHs with one another and the effectiveness of multi-time scale MPC over

single-time scale MPC. Compared to the previous studies, this work is the first study that proposes cooperative distributed energy scheduling for SHs and applies multi-time scale optimization.

In the second problem, the price-based energy management of SHs for maximizing the daily profit of GENCO is investigated. The goal of GENCO is to design an optimal energy management scheme (optimal prices of electricity) that will maximize its daily profit based on the demand of active customers (SHs) that try to minimize their daily operation cost. In this study, a scenario-based stochastic approach is applied in the energy scheduling problem of each SH to address the variability and uncertainty issues of PV panels. Also, a combination of genetic algorithm (GA) and linear programming (GA-LP) is applied as the optimization tool for the energy scheduling problem of a SH. Moreover, Lambda-Iteration Economic Dispatch and GA approaches are applied to solve the generation scheduling and unit commitment (UC) problems of the GENCO, respectively. The numerical study shows the potential benefit of energy management for both GENCO and SH. Moreover, it is proven that the GENCO needs to implement the optimal scheme of energy management; otherwise, it will not be effective. Compared to the previous studies, the presented study in this paper is the first study that considers the interaction between a GENCO and SHs through the price-controlled energy management to maximize the daily profit of the GENCO and minimize the operation cost of each SH.

In the third problem, traffic and grid-based parking lots allocation and charging management of PEVs is investigated from a DISCO's and a GENCO's viewpoints.

Herein, the DISCO allocates the parking lots to each electrical feeder to minimize the overall cost of planning problem over the planning time horizon (30 years) and the GENCO manages the charging time of PEVs to maximize its daily profit by deferring the most expensive and pollutant generation units. In both planning and operation problems, the driving patterns of the PEVs' drivers and their reaction respect to the value of incentive (discount on charging fee) and the average daily distance from the parking lot are modeled. The optimization problems of each DISCO and GENCO are solved applying quantum-inspired simulated annealing (SA) algorithm (QSA algorithm) and genetic algorithm (GA), respectively. We demonstrate that the behavioral model of drivers and their driving patterns can remarkably affect the outcomes of planning and operation problems. We show that optimal allocation of parking lots can minimize every DISCO's planning cost and increase the GENCO's daily profit. Compared to the previous works, the presented study in this paper is the first study that investigates the optimal parking lot placement problem (from every DISCO's view point) and the problem of optimal charging management of PEVs (from a GENCO's point of view) considering the characteristics of electrical distribution network, driving pattern of PEVs, and the behavior of drivers respect to value of introduced incentive and their daily distance from the suggested parking lots.

In our future work, we will develop a more efficient smart grid. Specifically, we will investigate the effects of inaccessibility of SHs to the grid and disconnection of SHs in the first problem, model the reaction of other end users (in addition to SHs) based on the price elasticity of demand and their social welfare in the second problem, and propose

methods for energy management of end users (in addition to charging management of PEVs) and model the load of end users in the third problem.

DEDICATION

I would like to dedicate my dissertation to my parents for their continued support and patience.

ACKNOWLEDGMENTS

I would like to thank my adviser, Dr. Shen, for her guidance and support. Also, I have special thanks to Dr. Harrell, Dr. Baum, and Dr. Jenkins for their valuable comments on my dissertation.

TABLE OF CONTENTS

Page

Table of Contents (Continued) Page

Table of Contents (Continued) Page

LIST OF TABLES

List of Tables (Continued)

Table Page

LIST OF FIGURES

List of Figures (Continued)

Figure Page

List of Figures (Continued)

Figure Page

List of Figures (Continued)

Figure Page

List of Figures (Continued)

Figure Page

List of Figures (Continued)

Figure Page

CHAPTER ONE

INTRODUCTION

Nowadays, the main challenges of the world today are quickly using up the vast but finite amount of fossil fuels and the related environmental issues including global warming, climate changes, and atmosphere pollution. The U.S. Energy Information Administration (EIA) estimates that 37% of end use electricity in the U.S. is consumed in the residences [4]. In addition, the buildings are responsible for 36% of the carbon emissions in the U.S. [4-5]. Moreover, a recent study demonstrates that almost 27% of total energy consumption and 33% of greenhouse gas emissions in the world are related to the transportation sector [46]. To handle these problems, the conventional power systems are being restructured and changed into smart grids to improve their reliability and efficiency, which brings about better social, economic, and environmental benefits such as decreasing electricity price and minimizing carbon emissions. Smart grids are the electrical systems that coordinate the needs and capabilities of all generators, grid operators, end users and electricity market stakeholders to operate all parts of the system as efficiently as possible, minimizing costs and environmental impacts while maximizing system reliability [1].

To build a smart grid, energy scheduling, energy management, parking lot allocation, and charging management of plug-in electric vehicles (PEVs) are important subjects that must be considered. Accordingly, in this dissertation, three problems in building a smart grid are investigated. As can be seen in Figure 1.1, the defined problems

in the dissertation include cooperative distributed energy scheduling of smart homes (SHs), price-controlled energy management of SHs, and traffic and grid-based parking lot allocation and charging management of PEVs. In the following, we briefly introduce the motivation and our research work on each problem.

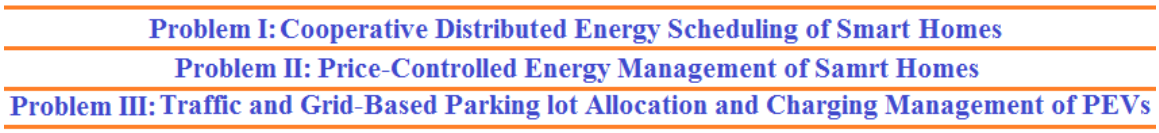

Figure 1.1: Different problems investigated in the dissertation.

1.1 Problem I: Cooperative Distributed Energy Scheduling of Smart Homes

1.1.1 Motivation of Cooperative Distributed Energy Scheduling

Building sector has a considerable potential for decreasing cost of energy use, increasing energy efficiency, and decreasing the carbon footprint by including renewables [2-3]. A SH is defined as a well-designed structure with sufficient access to assets, communication, controls, data, and information technologies for enhancing the occupants' quality of life through comfort, convenience, reduced costs, and increased connectivity [6-7]. Advances in the technology are able to change a conventional home into a SH that allows the occupant to control the energy consumption of the home [8-9]. A SH might have a variety of sources including DG, photovoltaic (PV) panels installed on the roof of SH, and a battery or a PEV as an energy storage.

On the other hand, SHs are equipped with devices and sources that coordinate with one another to achieve a common set of goals that benefit the occupants [10]. SHs are able to connect to each other, share their energy sources, and exchange electricity. In other words, each SH can provide energy to other SHs or purchase energy from them.

Also, every SH can deliver its extra energy to the grid and sell it to the local DISCO, but at a lower price compared to the purchasing price from the local DISCO [11].

Figure 1.2 illustrates the schematic diagram related to the first problem of dissertation. In the first problem, the SHs that include renewable energy resources, diesel generator (DG), and energy storage cooperate with one another to minimize their daily operation costs, as can be seen in Figure 1.2.

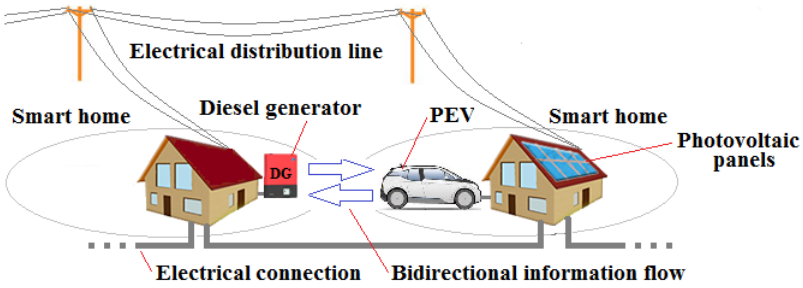

Figure 1.2: The schematic diagram of first problem (cooperative distributed energy scheduling of SHs).

Generally, there are two approaches for solving the energy scheduling problem of SHs that include centralized energy scheduling and cooperative distributed energy scheduling. However, the centralized energy scheduling approach has the so-called curse of dimensionality when the problem is large or complex [12]. In other words, the computational complexity and computation latency of problem grow exponentially when the size of problem is increased. Moreover, this phenomenon is very likely to happen when the problem is a dynamic optimization problem due to presence of the renewable energy resources or demand fluctuations, since the problem must be optimized at every time step. Therefore, the centralized energy scheduling approach is not efficiently applicable when the problem has a large number of variables or the states of problem is

changed dynamically. In addition, the privacy of SHs might be jeopardized in a centralized energy scheduling approach because all the economic and technical information of the SHs must be available for the control center [13].

An important question for energy scheduling problem of a SH is: *At every time step, how much energy to use from the available energy sources of the SH such as DG, PV panels installed on the roof of SH, and energy storage; how much energy to purchase/sell from/to which SHs; how much energy to purchase/sell from/to local DISCO to supply the demanded energy of the SH so that the daily energy consumption cost of SH is minimized.*

The challenges of problem include:

- Power of a renewable energy resource such as PV panels is uncertain that makes the problem a stochastic optimization problem.
- Another issue for the power of a renewable energy resource is variability of its power that make the problem a dynamic (time-varying) optimization problem.
- There are several economic and technical constraints for the energy sources of SH such as power limits and minimum up/down time limits of DG, power limits of the battery of PEV, state of charge (SOC) limit and depth of discharge (DOD) limit of the battery of PEV, life loss cost of the battery of PEV, and the unavailability of PEV for the SH when the PEV is being used by the driver. These constraints make the problem a mixed-integer nonlinear programming (MINLP) problem.

1.1.2 Proposed Approach for Cooperative Distributed Energy Scheduling of Smart Homes

The aforementioned challenges are addressed by applying the following proposed techniques.

Cooperative distributed energy scheduling: In the proposed cooperative distributed optimization for energy scheduling problem of SHs, at every time step, every SH randomly choses one of its connected SHs, as its counterpart, and solves its own energy scheduling problem with the aim of minimum total cost considering its energy sources and the available power of the connected SH and its proposed price. Then, every SH randomly changes its cooperator and updates its energy scheduling problem. This process is repeated several times until no significant improvement is observed in the value of objective function of each SH. The price of transacted energy between two SHs is evaluated based on the marginal cost of the installed DG in the power exporter SH; however, if there is no DG in the power exporter SH, the price is determined based on the marginal cost of the installed DG in the power importer SH. In addition, if both SHs have a DG, the price of electricity transaction is determined based on the average value of the marginal costs of the DGs.

- *Addressing uncertainty of power of the PV panels:* In order to deal with the uncertainty concerned with the power of the PV panels, a stochastic approach that includes predicting value of the solar irradiances over the optimization time horizon and defining the appropriate scenarios for the estimated solar irradiances is applied.

- *Dealing with time-varying power of the PV panels:* In order to handle the variability concerned with the power of the PV panels, an adaptive and dynamic technique, that is, multi-time scale MPC with five-minute and one-hour time scales is applied in the problem. The duration of optimization time horizon for both five-minute scale and one-hour time scale is assumed to be 12 time steps. The applied multi-time scale MPC with short time step (five minutes) and long time step (one hour) has characteristics of vast vision for the optimization time horizon (12 hours) and precise resolution for the problem variables (five-minute time step).
- *Modeling economic and technical constraints of the energy resources:* All the economic and technical constraints of the energy resources of SH including DG, battery of the PEV, and PV panels are modeled.
- *The optimization tool:* A combination of genetic algorithm (GA) and linear programming (GA-LP) is applied as the optimization tool to solve the energy scheduling problem of every SH. Herein, the GA, which deals with the discrete variables of the problem, addresses the nonlinearity of the problem and the LP, which handles the continuous variables of the problem, quickly finds the globally optimal solution.

1.2 Problem II: Price-Controlled Energy Management of Smart Homes

1.2.1 Motivation of Price-Controlled Energy Management

The main challenges of the world today are quickly using up the vast but finite amount of fossil fuels and the related environmental issues including global warming, climate changes, and atmosphere pollution [24]. Energy management has a significant potential for achieving benefits from economic and environmental viewpoints, thus it is

considered as the first priority in all the energy policy decisions [25-26]. It is able to reduce overall costs of energy supply, increase spinning and non-spinning reserves margin, and mitigate electricity price volatility [25]. Also, it achieves environmental goals by deferring commitment of polluted generation units, leading to increased energy efficiency and reduced greenhouse gas emissions [25].

Generation scheduling problem of generation units involves finding the least-cost dispatch of available generation power units to meet the electrical load demand [27]. In addition, UC problem is an optimization problem that produces physical generator commitment decisions to minimize the overall cost of serving forecasted net load demand subject to operational constraints on generation units and power system [28].

The schematic diagram of the second problem is shown in Figure 1.3. In the second problem, price-controlled energy management of SHs are investigated in the generation scheduling and unit commitment (UC) problems of a generation company (GENCO) to maximize the daily profit of GENCO. Herein, one part of demand of system is related to active end users (responsive to energy management schemes) such as SHs and another part of demand of is concerned with passive and conventional end users that do react to the energy management schemes. In this regard, the GENCO submits the price-controlled energy management scheme to SHs. Then, the SHs react and re-schedule their energy resources (DG, battery, PV panels, and electricity transaction with GENCO) and the GENCO receives feedback from the SHs and solve its generation scheduling and UC problems for every scheme of energy management. Finally, the optimal scheme of

energy management is determined based on the value of maximum daily profit of GENCO.

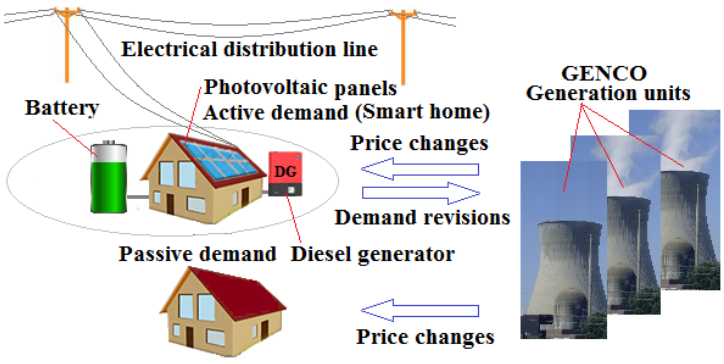

Figure 1.3: The schematic diagram of second problem (price-controlled energy management of SHs).

1.2.2 Proposed Approach for Price-Controlled Energy Management of Smart Homes

However, in the above mentioned studies, the reaction and re-scheduling energy resources of SHs with respect to the energy management schemes have not been investigated from a GENCO's viewpoint. In this study, the value of electricity price at peak period is changed by the GENCO to encourage the SHs to re-schedule their energy resources and re-shape their demand pattern. By implementing this price-controlled energy management, the overall profit of the GENCO not only depends on the cost of generation scheduling and UC problems but also the values of new electricity prices and the amount of sold electrical energy to the end users. Therefore, finding an optimal scheme for the energy management needs to be investigated.

A SH can include distributed energy resources such as PV panels and DG. On the other hand, a SH, as a part of the smart grid on the demand side, can deliver its extra energy to the grid and sell it to the power system, but at a lower price compared to the

purchasing price from the system [11]. However, there are some challenges in solving the energy scheduling problem of a SH that include variability and uncertainty issues of power of PV panels installed on the roof of a SH. Herein, we address these issues by applying a scenario-based stochastic optimization approach. Also, a combination of GA and linear programming (GA-LP) is applied as the optimization tool for the energy scheduling problem of a SH.

Determining the demand of system (sum of demands of SHs and passive end users) that depends on the fluctuated demand of SHs (due to variable power of PV panels and reaction of SHs to energy management scheme) is the one of the challenges of the generation scheduling and UC problems of the GENCO. In addition, modeling the economic and technical constraints of generation units are the others challenges of the GENCO that make the problem a MINLP problem. In this study, Lambda-Iteration Economic Dispatch and GA approaches are applied to solve the generation scheduling and UC problems of the GENCO, respectively.

1.3 Problem III: Traffic and Grid-Based Parking Lot Allocation and Charging Management of PEVs

1.3.1 Motivation of Parking Lot Allocation and Charging Management

A recent study demonstrates that almost 27% of total energy consumption and 33% of greenhouse gas emissions in the world are related to the transportation sector [46]. Replacing internal combustion based vehicles with PEVs is a promising strategy to mitigate the energy security and environmental issues, since PEVs can be charged by electricity generated by renewables as the free and clean resources of energy [47]. Based

on the study presented in [48-49], PEVs utilization is being increased rapidly in some developed countries because of the advancement in battery technology.

However, replacing conventional vehicles with PEVs might create new issues for every power system such as causing congestion in feeders, resulting in overload in power distribution, transmission, and generation systems, and even making spikes in electrical energy market prices due to uncontrolled charging of PEVs [50-51]. Therefore, the above mentioned issues must be mitigated by proper coordination and cooperation of responsive PEVs with the utilities and system operators. Moreover, in addition to the above mentioned achievements, the optimal parking allocation for PEVs in the distribution network and optimal charging management of responsive PEVs can bring about other benefits for the DISCO and GENCO.

Figure 1.4 shows the schematic diagram of the third problem of dissertation. In the third problem, the PEVs' drivers are motivated by the distribution companies (DISCOs) to charge their vehicles through the suggested optimal parking lots to minimize the overall cost of each DISCO over the planning time horizon (30 years). In fact, the drivers are encouraged by considering a discount on the charging fee of their vehicles. The reaction of PEVs' drivers is modeled based on the value of incentive and the value of their daily average distance from the suggested parking lot using several mathematical functions.

Moreover, the charging time of PEVs parked in the parking lots are managed by a GENCO to maximize its daily profit by deferring the most expensive and pollutant generation units. GENCO pays extra credit to the drivers of PEVs to motivate them for

letting GENCO to manage the charging time of PEVs. Herein, the value of credit is equal to the percentage of charging fee of PEVs. The drivers' behavior modeling performed by the GENCO is the same as the approach done by a DISCO, but, herein, the value of extra credit is applied instead of discount on charging fee of PEVs.

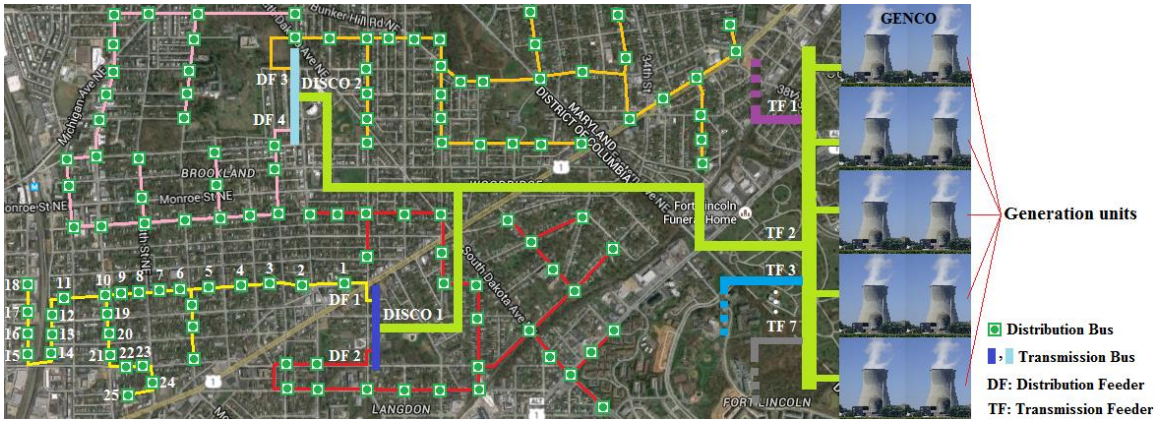

Figure 1.4: The schematic diagram of third problem (traffic and grid-based parking lot allocation and charging management of PEVs).

1.3.2 Proposed Approach for Traffic and Grid-Based Parking Lot Allocation and Charging Management of PEVs

In this study, the problem of parking lot placement is investigated by the cooperation of DISCOs and a GENCO in two different problems including planning and operation problems. Herein, the DISCOs solve the planning problem and allocate the parking lots in the optimal locations of every feeder of the electrical distribution network to achieve the minimum overall cost over the planning horizon (30 years). The cost terms of objective function of DISCO include the total investment for purchasing and installing parking lots in the optimal locations, the present worth value of maintenance cost of the installed parking lots over the operation period, the present worth value of incentive

(discount on charging fee) considered for the PEVs' drivers over the operation period, the present worth value of energy loss cost over the operation period, and the present worth value of expected energy not supplied (EENS) cost over the operation period. In addition, in order to achieve realistic results, economic and technical factors such as yearly inflation and interest rates, yearly growth rate for application of PEVs, yearly load growth rate, and daily and hourly variations of the load demand are taken into consideration in the planning problem. Moreover, the security constraints of the grid including the loading limit of branches (a branch is one part of the feeder, which is between two buses) and the voltage magnitude limits of the buses are considered over the operation period.

On the other hand, the GENCO manages the charging time of PEVs parked in the allocated parking lots (by DSICO) to maximize its daily profit by deferring the most expensive and pollutant generation units while satisfying the same daily charging demand of PEVs. In both planning problem solved by every DISCO and operation problem solved by the GENCO, the driving patterns of PEVs' drivers and their reaction with respect to the value of incentive and the amount of average daily distance of the PEVs from the parking lot are modeled. The value of incentive (the percentage of discount on charging fee of the PEVs) is considered by every DISCO to motivate the drivers to charge their vehicles through the parking lots. In addition, the value of incentive (as the extra credit, which is equal to the percentage of charging fee) is considered by the GENCO to encourage the drivers to let the GENCO decide on the charging time of their PEVs.

Furthermore, GA and quantum-inspired simulated annealing (SA) algorithm (QSA algorithm) are applied to solve the operation problem of GENCO and planning problem of each DISCO, respectively.

CHAPTER TWO

LITERATURE REVIEW AND RELATED WORK

In this chapter, the literature review and related work for the problems are presented separately. The problems include cooperative distributed energy scheduling of smart homes, price-controlled energy management of smart homes, and traffic and grid-based parking lot allocation and charging management of PEVs.

2.1 Related Work for Energy Scheduling of Smart Homes

Energy scheduling of a SH includes finding the optimal schedule, at every time step of the operation period, for the energy resources of the SH such as DG, battery, PV panels, and access to the local electrical grid. There are several papers that have investigated the energy resources scheduling problem for a single SH or a set of SHs [14-23]. These studies have not considered some of the aforementioned challenges (presented in 1.1.1) of the energy resources scheduling problem. In other words, in [15], [19], and [21-22], the presence of renewable energy resources has been neglected; in [14-15], [17], [19], and [22], energy storage has not been modeled; and in [14-15] and [17-19], the presence of DG has not been taken into consideration.

In addition, the defined scheduling problems do not have any dynamic and adaptive characteristics in [14], [16], [19], and [20-21]. In other words, the problems have been optimized once for the whole operation period (one day), while the optimization of the problems must be updated at every time step of the operation period (e.g., at every

hour, every five minutes) due to the time-varying feature of the power of renewables or load demand. Also, multi-time scale optimization approach has not been applied in any of the studies in [14-23]. In other words, the study presented in this part of dissertation is the first study that applies the multi-time scale stochastic MPC in the cooperative distributed energy resources scheduling problem of SHs.

The studies in [14-18] do not include cooperative distributed energy resources scheduling problem, since just one SH has been investigated. In [19-21] and [23], the energy scheduling problems have been solved for the set of SHs. However, the investigated problems are not cooperative distributed energy scheduling problems, since they have been solved by the centralized energy scheduling approaches. However, the centralized energy scheduling techniques have the so-called curse of dimensionality when the problem is large and complex [12], and also the privacy of the SHs is likely to be jeopardized in a centralized optimization approach since all the economic and technical information of SHs is submitted to the control center [13]. Compared to the previous works, this work is the first study that proposes cooperative distributed energy scheduling for SHs and applies multi-time scale optimization. Also, it comprehensively handles the aforementioned challenges presented in Section 1.1.1.

2.2 Related Work for Price-Controlled Energy Management

Some studies have summarized the existing research on demand response [29-30]. Demand response is generally referred to the response and reaction of end user customers to the energy management schemes. The study presented in [29] has investigated the

coordination of energy efficiency strategy (applying efficient appliances and device) and demand response, and also it has discussed the barriers for this coordination. In [30], the performed works for demand response in the U.S. electric power markets have been investigated.

In [31-35], energy management schemes have been investigated on the residential customers. In [31], a proposed controller that curtails peak load and saves electricity cost has been presented. In [32] and [34], an energy hub model (for supplying both electricity and heat demands) for a residential home has been presented. In [33], electricity peak demand reduction during summer, as an energy management scheme, in the Japanese residential sector has been investigated. In [35], the value of incentive is announced to the customers via the wireless sensors, installed in the residential systems, for load reduction. However, in above mentioned studies, the effects of energy management of end users on the generation scheduling problem of a GENCO has not been investigated.

The studies presented in [36-39] propose energy management schemes for direct load control of customers in order to increase the penetration of renewable energy resources (wind power) into the power system for different objective functions. In [36], the value of demand that must be shifted from peak period to off peak period is determined by the Independent System Operator (ISO) using direct load control to mitigate power transmission congestions and enhance the utilization of wind generation. In this paper, the problem has been defined as a MINLP to minimize the total operation cost of system. In [37], the elasticity of demand has been considered to adjust the demand profile in response to price changes to increase the amount of wind power that can be

economically injected. Also, herein, the wind power uncertainty is managed at a lower cost by adjusting electricity consumption in case of wind forecast errors. In [38-39], demand response has been incorporated with wind power to provide more cost-effective carbon emission reductions on a case study based on Texas power system. In these papers, it has been demonstrated that, while wind variability can increase the price, demand response can be an alternative to provide the opposite effect to help reduce that price volatility. Nonetheless, in the above mentioned studies, the energy management schemes have not been investigated in the generation scheduling problem and they have not been studied from a GENCO's point of view.

In [40-43], the optimal value of incentive is designed to motivate the end users to reduce their demand at peak period to minimize the daily cost of generation scheduling and UC problems. UC and generation scheduling problems determine the status of each generation unit for being "on" or "off" and the generation level of each unit, respectively. In [40-41], the reaction of end users has been modeled based on the price elasticity of demand and their social welfare in the UC and generation scheduling problem. In these papers, linear function has been considered in the benefit function of the end users customers. Also, it has been demonstrated that the cooperation of GENCO with the end users and implementing an optimal scheme of energy management in combined emission and generation scheduling problem has a high potential for reducing cost of power generation and carbon emission level of the thermal power plants. In [42-43], nonlinear models for benefit function of the end user customers have been considered in the generation scheduling and UC problems. In these papers, it is concluded that obtaining

the minimum cost for system using an unsuitable scheme of demand response program or unrealistic model of responsive load is not possible. In addition, in [43], it is recommended that comprehensive studies and modeling are needed to realistically characterize the responsive end users behavioral model. Nevertheless, in the above mentioned papers, the reaction of end users has been modeled using just some pure mathematical and static models, but the demand of active end users such as SHs dynamically change due to re-scheduling of their energy resources (for minimizing their operation cost) and variable power of renewables.

In [44-45], the benefits of energy management and demand response have been investigated in the power markets. In [44], the authors have studied the benefits of implementing demand response programs. These benefits include participant financial benefits (bill savings and incentive payments earned by customers), market-wide financial benefits (lower wholesale market prices), reliability benefits (operational security and adequacy savings), and market performance benefits (mitigating suppliers' ability to exercise market power on customers). In [45], the impact of demand response on market clearing and locational marginal price of a power system has been investigated. In this paper, demand response has been formulated as the linear price-sensitive demand bidding curves and demand response includes load shifting and load curtailment. Nonetheless, the energy management of SHs has not been investigated in generation scheduling and UC problems of the GENCO.

In [19-23], just the energy scheduling problem of a SH has been investigated; however, the effects of energy scheduling of SHs on the generation scheduling and UC problems of a GENCO have not been investigated.

Compared to the previous studies, the presented study in the second problem of dissertation is the first study that considers the interaction between a GENCO and SHs through the price-controlled energy management to maximize the daily profit of the GENCO and minimize the operation cost of each SH.

2.3 Related Work for Parking Lot Allocation and Charging Management

The economic and technical features of PEVs fleet have been discussed in [52-53]. Paper [52] presents a mobile information system to give relevant information to the PEV drivers by allowing them to access data sources through a mobile application. In [53], the operation costs of PEVs in a future power system and the benefits of smart charging and discharging of PEVs have been estimated.

In [54-57], the parking lot allocation problem has been investigated on real power systems. In [54], the charging demand of PEVs in Beijing has been estimated and a model for distributing charging stations has been presented. This paper concludes that the service radius of fast charging stations affects the distribution pattern of charging stations and it has less disturbance on the power system. In [55], parking lot information from more than 30,000 records of personal trips in the Puget Sound, Seattle, Regional Council's 2006 Household Activity Survey has been used to determine the public parking locations and durations. In this paper, the presented algorithm minimizes PEV drivers'

costs for station access while penalizing unmet demand. In [56], a study on the location of PEVs charging stations for an area of Lisbon, the capital city of Portugal, has been conducted considering the population and employment in the area. In [57], a dynamic model of development of a charging station for PEVs in the German metropolitan region of Stuttgart until 2020 has been presented. The presented model consists of simulating development of PEVs ownership, determining the demand of charging stations, calculating profitability of the infrastructure, and simulating the mobility of PEVs throughout the region. However, in these studies, the reaction of PEVs' drivers respect to the value of incentive and distance from parking lots has not been modeled. In addition, the parking lot placement for minimizing power loss and expected energy not supplied of a DISCO, and also charging management of PEVs for generation scheduling and UC of a GENCO has not been investigated.

In [58-62], parking lot allocation problem and PEVs charging management problem have been investigated considering minimum energy and power losses of the system. In [58], in addition to charging-recharging of PEVs, capacitor is installed in the electrical distribution system to supply the reactive power of distribution network. In [59], optimal charging stations of PEVs are determined based on the minimum total cost associated with the charging stations considering the environmental factors and service radius of charging stations. In [60], PEVs are charged in a coordinated way to find its positive effects on the feeder losses, load factor, and load variance of the system. In [61-62], charging stations, renewable energy resources (solar power), and distributed generation (such as DG) have been allocated simultaneously to minimize power loss of

the system. Nonetheless, in these studies, the behavior of PEVs' drivers has not been modeled and the problem has not been investigated from a GENCO's point of view.

In [63-67], the PEVs charging management and parking lot placement have been investigated for improving the reliability and performance of the system. In [63], parking lot allocation has been conducted to improve the reliability of distribution system and to incorporate the PEV fleet in the energy market transactions. However, in this paper, the behavior of PEV drivers just with respect to the value of incentive has been modeled and the geography of area, the driving pattern and traffic of PEVs have not been considered in the modeling. In [64], the effects of large-scale application of PEVs on the power systems of five Northern European countries (Denmark, Finland, Germany, Norway, and Sweden) towards 2030 have been investigated. In [65], environmental and social criteria have been considered in the life cycle of charging stations of PEVs to minimize total cost of the micro grid. In [67], solar parking lots have been allocated and sized in a distribution system to minimize the overall cost of DISCO considering the active and reactive power losses of system. In [66-67], the behavior of PEVs for being in the parking lots and the available energy of PEVs have been modeled based on the arrival time, departure time, and SOC of batteries of the PEVs. However, in [66-67], the reaction of PEVs' drivers respect to the value of incentive has been neglected and the optimal charging management of PEVs by a GENCO has not been considered. In addition, in [63-65, 67], the PEVs charging management problem has not been investigated from a GENCO's point of view.

In [68], since PEVs' batteries can be charged and discharged quickly, the PEVs have been incorporated in a power system to adjust the frequency and voltage deviations of system. Moreover, the presence of PEV fleet for power restoration [69] and back up energy resource for power outage management [70] have been investigated. In [69-70], in order to accelerate supplying the customers after removing a fault in the power distribution system, PEVs are incorporated as the backup sources to reduce the interruption duration of customers in the faulted zone. In the above mentioned studies, the economic behavior of PEVs' drivers, the type of driving patterns of drivers, and the traffic and geography of area have not been modeled or considered in PEVs charging management problems.

Compared to the previous works, the presented study in the third problem of dissertation is the first study that investigates the optimal parking lot placement problem (from every DISCO's view point) and the problem of optimal charging management of PEVs (from a GENCO's point of view) considering the characteristics of electrical distribution network, driving pattern of PEVs, and the behavior of drivers respect to value of introduced incentive and their daily average distance from the suggested parking lots.

CHAPTER THREE

PROBLEM I: COOPERATIVE DISTRIBUTED ENERGY SCHEDULING OF SMART HOMES

3.1 Proposed Technique for Cooperative Distributed Energy Scheduling of Smart Homes

In this section, different parts of the proposed technique for solving the cooperative distributed energy scheduling problem of the set of smart homes (SHs) applying multi-time scale stochastic MPC are presented and described.

3.1.1 Cooperative Distributed Energy Scheduling

Figure 3.1 illustrates the concept of cooperative distributed energy scheduling for a system with five SHs. As can be seen, each SH electrically connects to a number of other SHs for energy transaction. In other words, every SH can provide energy to its connected SHs and also purchase energy from them.

Herein, it is assumed that every SH needs to exchange the information just with its connected SHs. The information includes the value of available energy and the value of price for transacting power between two SHs. The price of transacted energy between two SHs is evaluated based on the marginal cost of the installed diesel generator (DG) in the power exporter SH; however, if there is no DG in the power exporter SH, the price is determined based on the marginal cost of the installed DG in the power importer SH. Also, if every SH has a DG, the price of electricity transaction is determined based on the average value of marginal costs of the DGs.

Based on the concept of introduced approach for the cooperative distributed energy scheduling, at every time step, in parallel to other SHs, every SH randomly selects its counterpart (one of the connected SHs), and solves its own energy scheduling problem with the aim of minimum total cost considering its energy sources and the received information from the selected cooperator (the available power of the connected SH and the proposed price). Then, every SH randomly changes its cooperator, share the updated information with its new cooperator, and optimize again its energy scheduling problem. This process is repeated several times until no significant improvement is observed in the value of objective function of each SH.

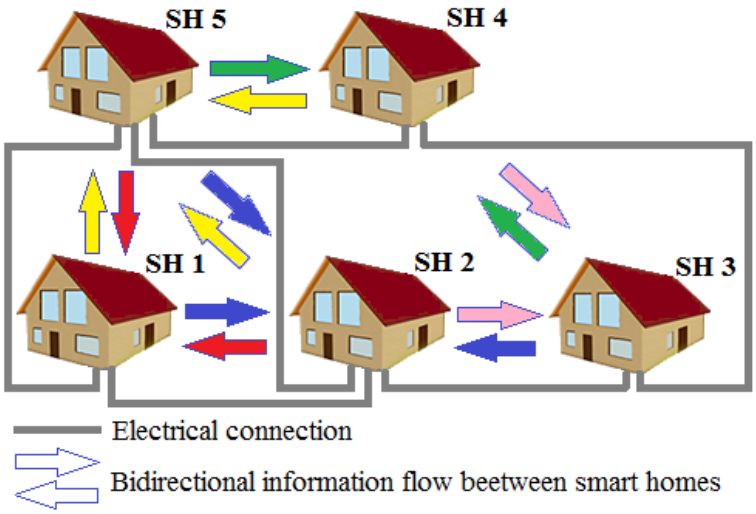

Figure 3.1: Applying cooperative distributed optimization on a system with five SHs.

Indicating how the updated information is utilized by the SHs can be explained by an example using Figure 3.1. Herein, it is supposed that at a specific time step (t_0), SH 4 has more generation than its demand due to extra generation of its photovoltaic (PV) panels, each of SH 5 and SH 1 has a DG that the marginal cost of every DG is less than

the price proposed by the distribution company (DISCO), the power generation of DG of SH 1 is more expensive compared to the generation of DG of SH 5, and the power generation of DG of SH 5 is in upper limit.

- In the first iteration, SH 1 and SH 5 cooperates with one another, but no power is transacted between them, since the DG of SH 5 cannot help to SH 1 because of the technical constraint (the power of DG of SH 5 is in its upper limit).
- In the next iteration, SH 5 cooperates with another connected neighbor (SH 4) and based on this cooperation, SH 5 decreases the generation level of its DG and absorbs power from SH 4, since SH 4 has extra power. Herein, SH 4 makes more profit by selling electricity to SH 5 instead of the local DISCO because of the NEM plan (In the NEM plan, the extra electricity of the customer is sold to the local DISCO in a less price compared to the purchasing price of electricity). Also, the cost of SH 5 is decreased because the marginal cost of its DG is reduced due to the lower level of generation of its DG. The fuel cost function and carbon emissions function of a DG are quadratic polynomials [28], [71]. Therefore, the generation of a DG is less expensive in the lower levels.
- Then, SH 1 cooperates with SH 5 and decreases the generation level of its DG and absorbs power from the DG of SH 5 (generation of the DG of SH 5 is cheaper). Herein, every SH is profited, since the electricity transaction is determined based on the average value of the generation costs of the DGs. In other words, the cost of SH 1 is decreased because its demand is supplied by a cheaper source and the income of SH 5 is increased because it sales electricity in a price which is more than the generation cost of its DG.

- Next, each SH randomly changes its cooperator and cooperates with it. This process is repeated several times until no remarkable reduction is realized in the value of the objective function of each SH.

Algorithm I presents the pseudo code for cooperative distributed energy scheduling problem of the set of SHs. Herein, $\mathbb{F}_{h,t}^{FL}$ is the stochastic forward-looking objective function for h^{th} SH at t^{th} time step. Also, $\left|\Delta\mathbb{F}_{h,t}^{FL}\right|$ is the difference between the values of $\mathbb{F}_{h,t}^{FL}$ in the current and previous iterations.

Algorithm I: The pseudo code for cooperative distributed energy scheduling of SHs.

$t = 1$
while $t \leq T$
  while $max\{\left|\Delta\mathbb{F}_{1,t}^{FL}\right|, \dots, \left|\Delta\mathbb{F}_{n_h,t}^{FL}\right|\} > \varepsilon$
    for $h = 1: n_h$ *//Selecting one counterpart for every SH*
      Randomly select a cooperator for h^{th} SH from its connected SHs.
      Remove h^{th} SH and its cooperator from the list.
    end
    for $h = 1: n_h$ *//Solving energy scheduling problem of every SH*
      Submit the information (the value of extra power and its price) of cooperator for h^{th} SH.
      Optimize the problem for h^{th} SH and calculate $\mathbb{F}_{h,t}^{FL}$ and $\left|\Delta\mathbb{F}_{h,t}^{FL}\right|$.
    end
  end
  $t \rightarrow t + 1$
end

3.1.2 Multi-Time Scale Stochastic MPC

3.1.2.1 Stochastic Approach

Stochastic approach and multi-time scale MPC are applied to address the uncertainty and variability concerned with the power of the PV panels, respectively. The

stochastic approach includes forecasting the solar irradiances and modeling the uncertainty of predictions by defining some effective scenarios.

3.1.2.1.1 Forecasting the Value of Uncertain States

The uncertain states of the problem include the values of solar irradiances (ρ) over the optimization time horizon predicted using the neural network available in MATLAB. The historical values of solar irradiances (for both five-minute and one-hour scales, but separately) are entered into the neural network to predict the values of solar irradiances over the optimization time horizon. The historical data of solar irradiances are the real solar irradiances recorded in Clemson, SC 29634, USA in July 2014. About 70% of the data is used for training the neural network and 30% of the data is used for validation and testing. The set of the predicted solar irradiances ($\tilde{\rho}$) can be presented as equation (3.1).

$$\{\tilde{\rho}_{t+1}, \dots, \tilde{\rho}_{t+n_\tau}\}, t \in \{t_1, t_2\}, \forall t_1 \in T_1, \forall t_2 \in T_2, T_1 = \{1, \cdots, n_{t1}\}, T_2 = \{1, \cdots, n_{t2}\} \quad (3.1)$$

Herein, the duration of forecasting time horizon for both five-minute and one-hour time scale stochastic MPC is 12 time steps (n_τ is equal to 12). The values of solar irradiances are predicted for every time step of the optimization time horizon for both time scales (five-minute scale (t_1) and one-hour scale (t_2)), as can be seen in equation (3.1). Herein, the value of n_{t1} and n_{t2} as the number of five-minute time steps and the number of one-hour time steps in the operation period (one day) are 288 and 24, respectively.

3.1.2.1.2 Modeling Uncertainties of the Forecasted Data

Figure 3.2 (a) illustrates the predicted and measured solar irradiances for the current time step (t) and past time steps ($1, 2, \cdots, t-1$), and also the predicted solar irradiances for every time step of the optimization time horizon ($t+1, \cdots, t+n_\tau$). As can be seen, the previously forecasted solar irradiances ($\tilde{\rho}$) are compared with the real solar irradiances (measured data) and the value of error of the predictions are calculated. Then, as can be seen in Figure 3.2 (b), the redundancy of prediction errors with respect to the value of prediction errors are plotted on a chart. After that, an appropriate distribution function is investigated for the prediction errors, as can be seen in Figure 3.2 (c).

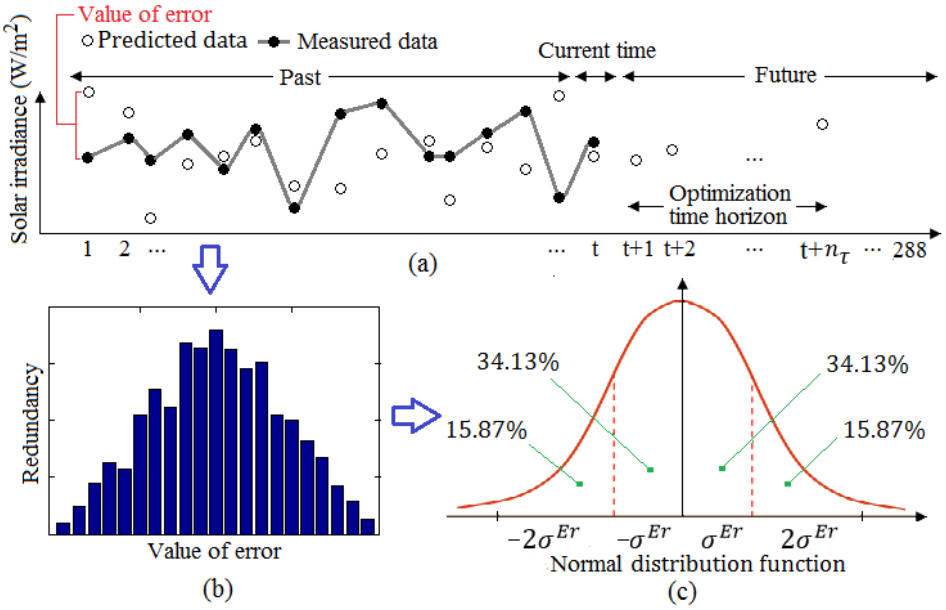

Figure 3.2: (a): The predicted data, measured data, and value of prediction error (b): The redundancy of prediction errors with respect to the value of prediction errors. (c): The Normal distribution function proportional to the prediction errors.

It is observed that the predication errors can be approximately fitted on a Normal distribution function with an appropriate standard deviation (σ^{Er}). Finally, the curve is divided into four areas to define four distinct values for the prediction inaccuracy with occurrence probabilities about 15.87%, 34.13%, 34.13%, and 15.87% related to $-2\sigma^{Er}$, $-\sigma^{Er}$, σ^{Er}, and $2\sigma^{Er}$, respectively, based on the concept of Normal distribution function. The value of σ^{Er} is updated in the next predictions in the optimization procedure of the problem $(1, 2, \cdots, t, \cdots, 288)$.

Although considering more scenarios for the value of solar irradiance over the optimization time horizon will result in more accurate outcomes for the problem, it may lead to an unmanageable optimization problem. In other words, the optimization problem cannot be solved due to the large number of the scenarios in the desirable time. This phenomenon happens because of the short time step (five minutes) considered in the optimization procedure of the problem, and also because of the application of multi-time scale MPC (the optimization problem must be updated at every time step for both five-minute and one-hour scales, separately). Therefore, in order to avoid dealing with an unmanageable optimization problem, four scenarios ($s \in S, S = \{1, \dots, n_s\}$, where n_s is 4) for solar irradiance are considered, as can be seen in equation (3.2). The occurrence probabilities of the defined scenarios (Ω^{PV}) are equal to 15.87%, 34.13%, 34.13%, and 15.87%, respectively.

$$\rho_{h,t,s} \in \left\{\tilde{\rho}_{h,t} - 2\sigma^{Er}, \tilde{\rho}_{h,t} - \sigma^{Er}, \tilde{\rho}_{h,t} + \sigma^{Er}, \tilde{\rho}_{h,t} + 2\sigma^{Er}\right\} \tag{3.2}$$

In other words, at every time step (with five-minute scale and one-hour scale, separately), the problem is solved four times and every time, one of the above mentioned values are considered for the value of solar irradiance.

3.1.2.2 Model Predictive Control (MPC)

3.1.2.2.1 Single-Time Scale MPC

MPC as a well-established technique in control engineering is capable of controlling a multi-variable constrained system by taking the control actions from the solution of an online optimization problem and repetitively predicting the behavior of system [72]. The concept of the single-time scale MPC is illustrated in Figure 3.3 [73]. As can be seen, at every time step (t), the optimization time horizon ($t+1, \cdots, t+n_\tau$) is updated, and then the value of the forward-looking objective function (F_t^{FL}) is optimized; however, just the variables of next time step ($t+1$) are accepted as the decision variables. The forward-looking objective function is sum of the values of the time step objective functions (F_t) over the optimization time horizon, as can be seen in equation (3.3). Next, the current time step is $t+1$ and the updated optimization time horizon is $t+2, \cdots, t+n_\tau+1$. Now, the value of the updated forward-looking objective function (F_{t+1}^{FL}) is minimized and the variables of the next time step ($t+2$) are accepted as the decision variables. This procedure that demonstrates the dynamic and adaptability characteristics of the MPC is repeated for every time step of the operation period (one day).

$$F_t^{FL} = \sum_{\tau=1}^{n_\tau} F_{t+\tau} \tag{3.3}$$

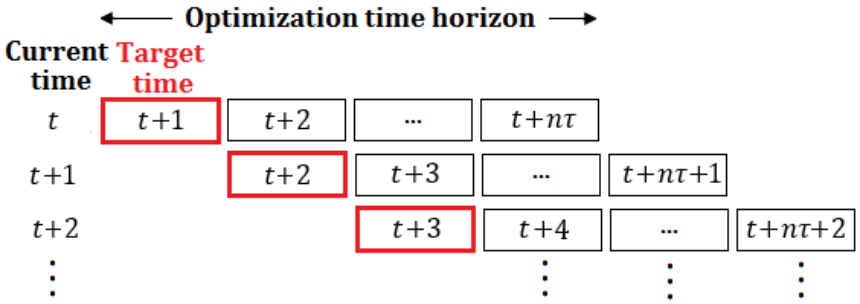

Figure 3.3: The concept of single-time scale MPC [73].

Algorithm II presents the pseudo code for single-time scale stochastic MPC for one SH with five-minute scale. Herein, T is equal to 288 as the number of five-minute time steps in one day (operation period). Herein, $P_{t,s}^{PV}$ is the output power of the PV panels installed on the roof of the SH at t^{th} time step and in s^{th} scenario for the estimated value of solar irradiance. Also, $\mathbb{F}_t^{FL}$ is the stochastic forward-looking objective function for the SH at t^{th} time step.

Algorithm II: The pseudo code for single-time scale stochastic MPC for a SH.

1: $t = 1$
2: **while** $t \leq T$ *//T=288*
3: **for** $s = 1{:}\, n_s$ *//Stochastic optimization*
4: Calculate $P_{t,s}^{PV}$ as a function of $\rho_{t,s}$ for the optimization time horizon based on equation (3.19).
5: Optimize the problem and calculate $F_{t,s}^{FL}$ based on equations (3.3) and (3.11).
6: **end**
7: Calculate $\mathbb{F}_t^{FL}$ based on equation (3.10).
8: Update the optimization time horizon: $t \rightarrow t+1$ in $t+1, \cdots, t+n_\tau$.
9: **end**

3.1.2.2.2 Multi-Time Scale MPC

The considered time scales in the multi-time scale stochastic MPC include five-minute scale and one-hour time scale. However, the energy scheduling problem of the SH is optimized in every five-minute time step of the operation period (one day as the operation period includes 288 time steps). Therefore, the considered one-hour time step (in the one-hour time scale stochastic MPC) is shrieked into five-minute time steps to be applied in the energy scheduling problem.

Figure 3.4 illustrates the applied multi-time scale MPC with t_1 (five-minute scale) and t_2 (one-hour scale) as its time steps. Also, the forward-looking objective function for the multi-time scale MPC is presented in equation (3.4). In the multi-time scale MPC, the decision variables of the problem are identified by comparing the value of weighted optimized stochastic forward-looking objective functions ($\mathbb{F}_{t_1}^{FL}$ and $\frac{5}{60} \times \mathbb{F}_{t_2}^{FL}$), as can be seen in equation (3.5). Herein, the value of optimized stochastic forward-looking objective function with one-hour time step is shrieked (by using $\frac{5}{60}$, as the multiplier), in order to make the values of the stochastic forward-looking objective functions (with five-minute and one-hour time steps) comparable. As can be seen in equation (3.5), the value of discrete and continuous variables achieved from the optimized $\mathbb{F}_{t_1}^{FL}$ (X_{t_1}) are chosen if $\mathbb{F}_{t_1}^{FL} \leq \frac{5}{60} \times \mathbb{F}_{t_2}^{FL}$; otherwise, the value of the discrete and continuous variables obtained from the optimized $\mathbb{F}_{t_2}^{FL}$ (X_{t_2}) are selected as the decision variables.

$$F_t^{FL} = \sum_{\tau=1}^{n_\tau} F_{t+\tau}, t \in \{t_1, t_2\}, \forall t_1 \in T_1, \forall t_2 \in T_2 \qquad (3.4)$$

$$X_t = \begin{cases} X_{t_1} & \mathbb{F}_{t_1}^{FL} \leq \frac{5}{60} \times \mathbb{F}_{t_2}^{FL} \\ X_{t_2} & \mathbb{F}_{t_1}^{FL} > \frac{5}{60} \times \mathbb{F}_{t_2}^{FL} \end{cases}, \forall t_1 \in T_1, \forall t_2 \in T_2 \quad (3.5)$$

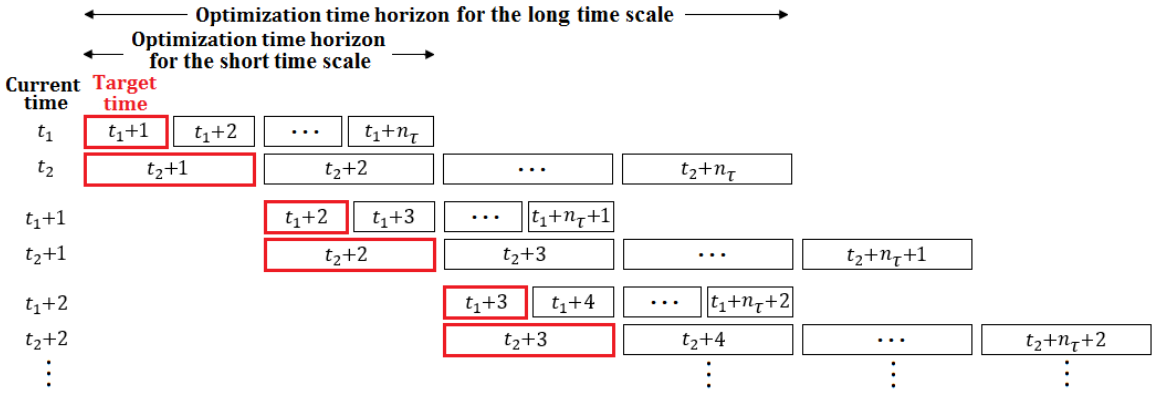

Figure 3.4: The concept of multi-time scale MPC.

Considering short time scale (five-minute) and large time scale (one-hour) in the multi-time scale MPC contribute to have precise resolution in the value of the variables and vast vision in the optimization time horizon, respectively. Based on this, the applied multi-time scale MPC has 12 hours vision as its optimization time horizon (the value of n_τ is 12) and precise resolution about five minutes for the variables.

It is noteworthy to mention that although a five minute-time scale MPC has better resolution for the problem variables, its optimization time horizon is 60 minutes (considering 12 as the value of n_τ), which is very short. In addition, a one-hour scale MPC has better optimization time horizon (12 hours), but the resolution for the problem variables (one hour) is not good. Therefore, a multi-time scale MPC can remove the disadvantages of the single-time scale MPC approaches. Algorithm III presents the

pseudo code for multi-time scale stochastic MPC for one SH with five-minute scale (t_1) and one-hour scale (t_2).

Algorithm III: The pseudo code for multi-time scale stochastic MPC for a SH.

1: $t_1 = 1$
2: $t_2 = 1$
3: **while** $t_1 \leq T_1$ & $t_2 \leq T_2$
4: **for** $s = 1: n_s$ *//Stochastic optimization for the first time scale (t_1)*
5: Calculate $P_{t_1,s}^{PV}$ as a function of $\rho_{t_1,s}$ for the optimization time horizon based on equation (3.19).
6: Optimize the problem for time scale t_1 and calculate $F_{t_1,s}^{FL}$ based on equations (3.4) and (3.11).
7: **end**
8: Calculate $\mathbb{F}_{t_1}^{FL}$ based on equation (3.10).
9: **for** $s = 1: n_s$ *//Stochastic optimization for the second time scale (t_2)*
10: Calculate $P_{t_2,s}^{PV}$ as a function of $\rho_{t_2,s}$ for the optimization time horizon based on equation (3.19).
11: Optimize the problem for time scale t_2 and calculate $F_{t_2,s}^{FL}$ based on equations (3.4) and (3.11).
12: **end**
13: Calculate $\mathbb{F}_{t_2}^{FL}$ based on equation (3.10).
14: **if** $\mathbb{F}_{t_1}^{FL} \leq \frac{5}{60} \times \mathbb{F}_{t_2}^{FL}$ *//Deciding about the value of variables*
15: Accept the optimal five-minute scale variables as the decision variables $\left(\mathrm{X}_t = \mathrm{X}_{t_1}\right)$.
16: **else**
17: Accept the optimal one-hour scale variables as the decision variables $\left(\mathrm{X}_t = \mathrm{X}_{t_2}\right)$.
18: **end**
19: Update the optimization time horizons for both time scales:
20: $t_1 \rightarrow t_1 + 1$ in $t_1 + 1, \cdots, t_1 + n_\tau$.
21: $t_2 \rightarrow t_2 + 1$ in $t_2 + 1, \cdots, t_2 + n_\tau$.
22: **end**

Figure 3.5 sequentially illustrates different parts of the proposed approach for solving the cooperative distributed energy scheduling problem of the set of SHs.

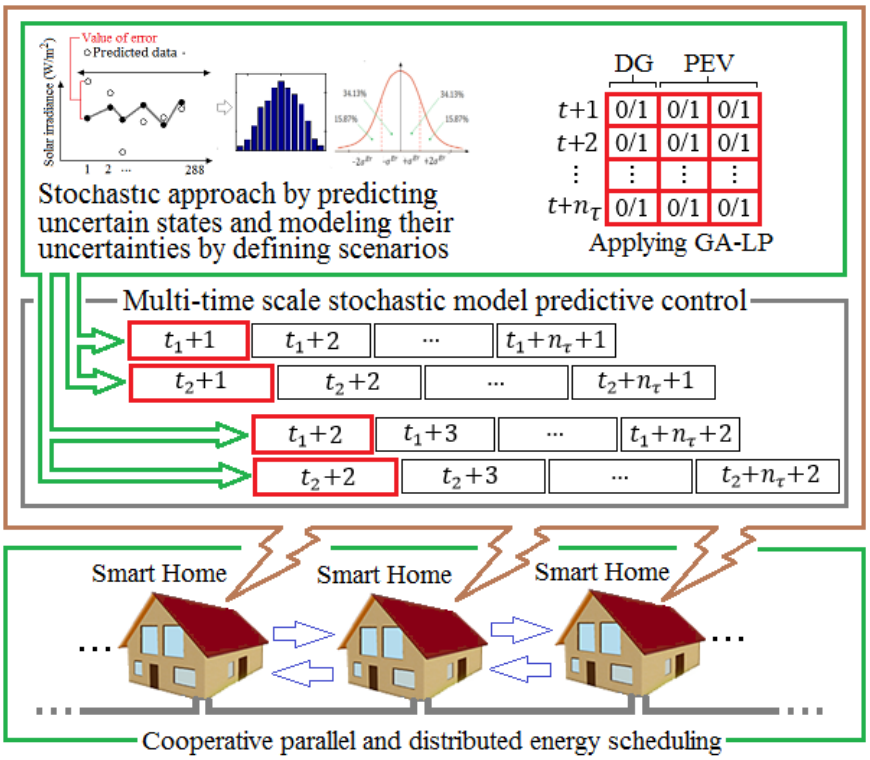

Figure 3.5: Different parts of the proposed approach for solving the cooperative distributed energy scheduling problem of the SHs.

3.1.3 Optimization Technique

The energy scheduling problem of a SH is a mixed-integer nonlinear programming (MINLP) problem. In this dissertation, GA-LP technique as the combination of GA and LP is applied to solve the energy scheduling problem of the SH. Other optimization algorithms could be used instead of GA; however, the capability of GA for parallel optimization and its competence in complex and nonlinear environments are the main reasons for the utilization of GA [74].

GA as the meta-heuristic technique that mimics the natural selection process belongs to the larger class of evolutionary algorithms (EA), which generate solutions to

optimization problems using techniques inspired by natural evolution including mutation, crossover, and selection operators. Mutation operator is used to maintain genetic diversity from one generation of a population of the chromosomes to the next. Mutation operator changes one or more gene values in a chromosome from its initial state. Also, crossover operator is used to vary the programming of the chromosomes from one generation to the next. Crossover operator is a process of taking two parent solutions and producing two offspring solutions from them. Additionally, selection is the stage of a GA in which the chromosomes are chosen from the population for breeding based on the best fitness criteria [74].

Herein, the GA is applied to address the nonlinearity of the problem and the LP is applied to quickly find the globally optimal solution. Moreover, the GA and LP techniques deal with the discrete variables (x^{DG}, x^{PEV}) and the continuous variables ($P^{DG}, P^{PEV}, P^{Grid}, P^{N}_{h'}, \forall h \in H'$) of the problem, respectively.

The discrete variables of the problem handled by the GA include the status of the DG (x^{DG}) and the status of the battery of the plug-in electric vehicle (PEV) (x^{PEV}) at every time step of the optimization time horizon (for five-minute and one-hour time steps, separately), as can be seen in equation (3.6). Herein, the values of "0" and "1" for x^{DG} mean "off" and "on", respectively. Also, the values of "-1", "0", and "1" for x^{PEV} mean charging, idle, and discharging, respectively.

$$\begin{Bmatrix} x^{DG}_{h,t} & \cdots & x^{DG}_{h,t+n_\tau} \\ x^{PEV}_{h,t} & \cdots & x^{PEV}_{h,t+n_\tau} \end{Bmatrix}, \forall h \in H, H = \{1, \dots, n_h\}, t \in \{t_1, t_2\}, \forall t_1 \in T_1, \forall t_2 \in T_2 \quad (3.6)$$

Based on this, the dimensions of the defined chromosome in the applied GA (for five-minute scale stochastic MPC or one-hour scale stochastic MPC) are $n_\tau \times 3$, as can be seen in Figure 3.6. Herein, one bit (gene) for indicating the status of DG ("0" for "off" and "1" for "on") and two bits for indicating the status of battery of PEV ("00" and "10" for idle, "01" for discharging, and "11" for charging) are considered.

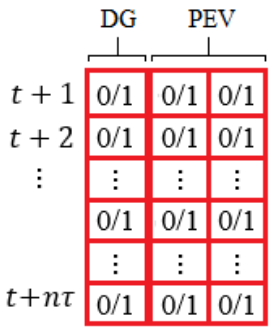

Figure 3.6: The structure of defined chromosome in the applied GA-LP.

In addition, the continuous variables of the problem optimized by the LP include the value of power of the DG (P^{DG}), the value of generated or consumed power of the battery of PEV (P^{PEV}), the value of transacted power with the DISCO through the grid (P^{Grid}), and the value of transacted powers with the connected SHs ($P^{N}_{h'}, \forall h \in H'$) at every time step of the optimization time horizon (for five-minute and one-hour time steps, separately), as can be seen in equation (3.7).

$$\begin{Bmatrix} P^{DG}_{h,t} & \cdots & P^{DG}_{h,t+n_\tau} \\ P^{PEV}_{h,t} & \cdots & P^{PEV}_{h,t+n_\tau} \\ P^{Grid}_{h,t} & \cdots & P^{Grid}_{h,t+n_\tau} \\ P^{N}_{h,t,1} & \cdots & P^{N}_{h,t+n_\tau,1} \\ \vdots & \cdots & \vdots \\ P^{N}_{h,t,n_{h'}} & \cdots & P^{N}_{h,t+n_\tau,n_{h'}} \end{Bmatrix},$$

$$\forall h \in H, H' = \{1, \dots, n_{h'}\}, t \in \{t_1, t_2\}, \forall t_1 \in T_1, \forall t_2 \in T_2 \qquad (3.7)$$

In the following, the steps for applying the GA-LP in the energy scheduling problem of a SH are presented and described.

- *Step 1: Obtaining the primary data*

Parameters for applying GA-LP: These parameters include the mutation probability of the genes (θ^{Mut}) and the size of the population (n_c) as the number of the chromosomes.

Parameters of the SH under study: The values of all the parameters of the SH and value of the defined scenario for the solar irradiance (for five-minute scale (t_1) and one-hour time scale (t_2)) over the optimization time horizon (presented in equation (3.1)) are obtained.

Initial population: The chromosomes of the population (Figure 3.6) are initialized with random binary values ("0" or "1").

- *Step 2: Updating the population*

Applying crossover operator: Three crossover points are randomly selected for every pair chromosomes, and then crossover operator is applied on the two chromosomes to reproduce two new chromosomes as the offspring.

Applying mutation operator: This operator is applied on every gene of every chromosome of the population with the definite probability θ^{Mut}.

- *Step 3: Selecting new population*

Evaluating fitness of every chromosome: For every chromosome, the LP is executed and if all the constraints are satisfied, fitness (fit_c) of the chromosome (the inverse of value of the forward-looking objective function (F^{FL})) is measured.

Applying selection process: As can be seen in equation (3.8), new chromosomes are selected using the probabilistic fitness-based selection (PFBS) technique, where the fitter chromosomes are more likely to be chosen. Herein, r_c is a random number between [0,100] generated for the chromosome (c).

The value of selection probability of every chromosome (θ_c^{PFBS}) is determined using equation (3.9), which is proportional to the fitness of the chromosome. Herein, n_c is the number of chromosomes in the population and a_c is the acceptance indicator of a chromosome for the new population.

$$a_c = \begin{cases} 1 & \theta_c^{PFBS} > r_c \\ 0 & \theta_c^{PFBS} < r_c \end{cases} \tag{3.8}$$

$$\theta_c^{PFBS} = \frac{fit_c}{Max\{fit_1, \dots, fit_{nc}\}} \times 100 \tag{3.9}$$

- *Step 4: Checking termination criterion*

In this step, the convergence status of the optimization procedure is checked. Based on this, the values of improvements in the fitness of the chromosomes of the old and new populations are measured and if there are no significant improvements in them, the optimization process is finished, otherwise, the algorithm is continued from *Step 2*.

- *Step 5: Introducing the outcome*

The consequences include the optimal value of the discrete and continuous variables for every time step of the optimization time horizon.

3.2 Mathematical Formulation for Cooperative Distributed Energy Scheduling of Smart Homes

3.2.1 Objective Function of the Problem

The goal of every SH is minimizing the value of stochastic forward-looking objective function over the optimization time horizon ($\mathbb{F}^{FL}$) subject to the constraints presented in equations (3.18)-(3.28). As can be seen in equation (3.10), the value of stochastic forward-looking objective function is determined by summing the values of forward-looking objective functions (F^{FL}) weighted by the corresponding occurrence probability (Ω_s^{PV}). The forward-looking objective function has been presented in equation (3.3) for single-time scale MPC and in equation (3.4) for multi-time scale MPC.

The time step objective function (F) that includes different cost and income terms is presented in equation (3.11). These terms include fuel cost of the DG (C^{F_DG}), carbon emissions cost of the DG (C^{E_DG}), start up cost of the DG (C^{STU_DG}), shut down cost of the DG (C^{SHD_DG}), switching cost of the battery of the PEV (C^{SW_PEV}), cost or benefit due to power transactions with the local DISCO through the grid ($P^{Grid} \times \acute{\pi}^{DISCO}$), and cost or benefit because of power transactions with the connected SHs ($\sum P^N \times \pi^N$).

$$min\, \mathbb{F}_{h,t}^{FL} = min \sum_{s \in S} F_{h,t,s}^{FL} \times \Omega_s^{PV}, \forall h \in H, t \in \{t_1, t_2\}, \forall t_1 \in T_1, \forall t_2 \in T_2 \tag{3.10}$$

$$F_{h,t,s} = \left\{ \begin{array}{c} \left[C_{h,t}^{F\_DG}\right] + \left[C_{h,t}^{E\_DG}\right] + \left[\left(1 - x_{h,t-1}^{DG}\right) \times x_{h,t}^{DG} \times C_h^{STU\_DG}\right] \\ + \left[x_{h,t-1}^{DG} \times \left(1 - x_{h,t}^{DG}\right) \times C_h^{SHD\_DG}\right] + \left[\acute{x}_{h,t}^{PEV} \times C_h^{SW\_PEV}\right] \\ + \left[P_{h,t}^{Grid} \times \acute{\pi}_t^{DISCO}\right] + \left[\sum_{h' \in H'} P_{h,t,h'}^{N} \times \pi_{h,t,h'}^{N}\right] \end{array} \right\},$$

$$\forall h \in H, t \in \{t_1, t_2\}, \forall t_1 \in T_1, \forall t_2 \in T_2 \tag{3.11}$$

where,

$$\acute{x}_{h,t}^{PEV} = \begin{cases} 0 & x_{h,t-1}^{PEV} = x_{h,t}^{PEV} \\ 1 & x_{h,t-1}^{PEV} \neq x_{h,t}^{PEV} \end{cases}, \forall h \in H, t \in \{t_1, t_2\}, \forall t_1 \in T_1, \forall t_2 \in T_2 \quad (3.12)$$

$$\acute{\pi}_t^{DISCO} = \begin{cases} \pi_t^{DISCO} & P_t^{Grid} > 0 \\ \varphi \times \pi_t^{DISCO} & P_t^{Grid} < 0 \end{cases}, \forall h \in H, t \in \{t_1, t_2\}, \forall t_1 \in T_1, \forall t_2 \in T_2 \quad (3.13)$$

The switching of battery of the PEV ($\acute{x}^{PEV}$) is determined using equation (3.12). If the status of the battery in the current time step (x_t^{PEV}) is the same as the previous time step (x_{t-1}^{PEV}), the switching indicator is zero; otherwise, it is one.

In equation (3.13), φ is the coefficient applied by the local DISCO to determine the price of selling power to the DISCO by a SH based on the NEM plan [11]. In the NEM plan, every SH can deliver its extra power to the grid and sell it to the local DISCO at a lower price compared to the purchasing price from the local DISCO [11]. Herein, $P^{Grid} > 0$ means the SH purchases power from the local DISCO and $P^{Grid} < 0$ means the SH sells power to the local DISCO.

The price of the transacted energy between two SHs is assessed based on the marginal cost of the installed DG in the power exporter SH; however, if there is no DG in the power exporter SH, the price is determined based on the marginal cost of the installed DG in the power importer SH. Moreover, if every SH has a DG, the price of electricity transaction is determined based on the average value of the marginal costs of the DGs. The marginal cost of a DG can be determined using equation (3.14) [28], [71].

$$\pi_{h,t}^{N} = \frac{\partial\left(C_{h,t}^{F\_DG} + C_{h,t}^{E\_DG}\right)}{\partial P_{h,t}^{DG}}, \forall h \in H, t \in \{t_1, t_2\}, \forall t_1 \in T_1, \forall t_2 \in T_2 \quad (3.14)$$

The fuel cost function and carbon emissions function of every DG are quadratic polynomials presented in equations (3.15) and (3.16), respectively [28], [71]. Herein, are the set of z_1^F, z_2^F, z_3^F and z_1^E, z_2^E, z_3^E are the fuel cost coefficients and carbon emissions coefficients of the DG, respectively. Also, β^E is the value of penalty for carbon emissions.

$$C_{h,t}^{F\_DG} = x_{h,t}^{DG} \times \left(z_{1,h}^F \times \left(P_{h,t}^G \right)^2 + z_{2,h}^F \times \left(P_{h,t}^G \right) + z_{3,h}^F \right),$$

$$\forall h \in H, t \in \{t_1, t_2\}, \forall t_1 \in T_1, \forall t_2 \in T_2 \tag{3.15}$$

$$C_{h,t}^{E\_DG} = x_{h,t}^{DG} \times \beta^E \times \left(z_{1,h}^E \times \left(P_{h,t}^G \right)^2 + z_{2,h}^E \times \left(P_{h,t}^G \right) + z_{3,h}^E \right),$$

$$\forall h \in H, t \in \{t_1, t_2\}, \forall t_1 \in T_1, \forall t_2 \in T_2 \tag{3.16}$$

The value of switching cost of the battery of a PEV is determined based on the value of total cumulative ampere-hours throughput of the battery (ξ^{PEV}) in its life cycle and the value of the initial price of the battery (Pr^{PEV}). In fact, considering this cost term prevents the battery of the PEV from unnecessary switching that is harmful to its life span.

$$C_h^{SW\_PEV} = \frac{Pr_h^{PEV}}{\xi_h^{PEV}}, \forall h \in H \tag{3.17}$$

3.2.2 Constraints of the Problem

In the following, the constraints of problem that must be held in every SH and at every time step of the operation period (with any time scale, that is, five-minute or one-hour scales) are presented and described.

Supply-demand balance: The sum of power of the DG, the power of the PV panels, the power of the battery of the PEV, the transacted power with the connected SHs, and the transacted power with the local DISCO through the grid must be equal to demand of the load (P^L) for every SH and in each time step of the operation period (with any time scale, that is, five-minute or one-hour scales). Herein, the transacted power with the connected SHs is considered positive if the SH imports power and it is negative if the SH exports power.

$$\left(x_{h,t}^{DG} \times P_{h,t}^{DG}\right) + \left(x_{h,t}^{PEV} \times P_{h,t}^{PEV}\right) + P_{h,t,s}^{PV} + P_{h,t}^{Grid} + \sum_{h' \in H'} P_{h,t,h'}^{N} = P_{h,t}^{L}$$

$$\forall h \in H, t \in \{t_1, t_2\}, \forall t_1 \in T_1, \forall t_2 \in T_2, \forall s \in S \qquad (3.18)$$

The output power of the PV panels (P^{PV}) is a nonlinear function of the estimated solar irradiance (ρ), as can be seen in equation (3.19) [75]. Herein, ρ^{st} and ρ^{c} are the solar irradiation in the standard environment set as 1000 W/m^2 and certain solar irradiation point set as 150 W/m^2. Also, $\overline{P^{PV}}$ indicates the rated power of the PV panels. In addition, *s* indicates the number of defined scenario for the value of estimated solar irradiance presented in equation (3.2).

$$P_{h,t,s}^{PV} = \begin{cases} \overline{P_h^{PV}} \times \dfrac{\left(\rho_{h,t,s}\right)^2}{\rho^{st} \times \rho^{c}} & \rho_{h,t,s} \le \rho^{c} \\ \overline{P_h^{PV}} \times \dfrac{\rho_{h,t,s}}{\rho^{st}} & \rho_{h,t,s} > \rho^{c} \end{cases},$$

$$\forall h \in H, t \in \{t_1, t_2\}, \forall t_1 \in T_1, \forall t_2 \in T_2, \forall s \in S \qquad (3.19)$$

Power limits of the DG: The maximum power limit ($\overline{P^{DG}}$) and minimum power limit ($\underline{P^{DG}}$) of a DG are presented in equation (3.20). In other words, the DG cannot generate power beyond the limits.

$$x_{h,t}^{DG} \times \left(\underline{P_h^{DG}} \leq P_{h,t}^{DG} \leq \overline{P_h^{DG}}\right), \forall h \in H, t \in \{t_1, t_2\}, \forall t_1 \in T_1, \forall t_2 \in T_2 \qquad (3.20)$$

Minimum up/down time limits of the DG: The duration that the DG is continuously "on" (Δt^{DG_ON}) and "off" (Δt^{DG_OFF}) must be more than the rated minimum up time (MUT^{DG}) and minimum down time (MDT^{DG}), as can be seen in equations (3.21) and (3.22), respectively. In other words, the DG cannot be started up immediately after it has been shut down and vice versa. Also, the time interval that the DG is continuously "on" (or "off") is determined based on the time that has passed from the last start up time (or shut down time) of the DG.

$$\Delta t_h^{DG\_ON} \geq MUT_h^{DG}, \forall h \in H \qquad (3.21)$$

$$\Delta t_h^{DG\_OFF} \geq MDT_h^{DG}, \forall h \in H \qquad (3.22)$$

Power limits of the battery of PEV: The battery of the PEV can act as a load or generator by being charged or discharged, respectively; however, the value of power of the battery of PEV must be in the rated range, as can be seen in equation (3.23). Herein, $\overline{P^{PEV}}$ is the value of rated power of the battery of PEV.

$$x_{h,t}^{PEV} \times \left(-\overline{P_h^{PEV}} \leq P_{h,t}^{PEV} \leq \overline{P_h^{PEV}}\right), \forall h \in H, t \in \{t_1, t_2\}, \forall t_1 \in T_1, \forall t_2 \in T_2 \quad (3.23)$$

Depth of discharge (DOD) limit of the battery of PEV: In order to prolong the life time of the battery of PEV, the battery must not be discharged more than the allowable

DOD. Moreover, the battery has a definite capacity that cannot be charged more than that, as can be seen in equation (3.24).

$$DOD_h^{PEV} \leq SOC_{h,t}^{PEV} \leq 100, \forall h \in H, t \in \{t_1, t_2\}, \forall t_1 \in T_1, \forall t_2 \in T_2 \qquad (3.24)$$

Disconnection of the PEV from the SH: This constraint indicates that the PEV is being used by its driver and the PEV is no longer connected to the SH in this interval ($\Delta t_{Dep-Arr}$), as can be seen in equation (3.25). In other words, the SH does not have any energy storage, thus the status of the battery of PEV is zero at these time steps.

$$x_{h,t}^{PEV} = 0, \forall h \in H, t \in \{\Delta t_{Dep-Arr}\} \qquad (3.25)$$

Full charge constraint for the battery of PEV before departure: By holding the constraint presented in equation (3.26), the owner of the PEV is confident that the PEV will have full charge at the desirable time (t_{Dep}) and ready to be used. In other words, the occupant of the SH prefers to have full charge in the battery of PEV before driving it.

$$SOC_{h,t_{Dep}}^{PEV} = 100, \forall h \in H \qquad (3.26)$$

Maximum accessible power from a connected SH: The power that the SH can import from a connected SH (P^N) must be less than the available power of the connected SH (P^A) at every time step of the optimization period, as can be seen in equation (3.27).

$$P_{h,t,h'}^{N} \leq P_{h',t}^{A}, \forall h \in H, \forall h' \in H', t \in \{t_1, t_2\}, \forall t_1 \in T_1, \forall t_2 \in T_2 \qquad (3.27)$$

where,

$$P_{h',t}^{A} = \begin{cases} x_{h',t}^{DG} \times \left(\overline{P_{h'}^{DG}} - P_{h',t}^{DG}\right) + \overline{P_{h'}^{PEV}} - P_{h',t}^{PEV} & x_{h',t}^{PEV} = 1 \\ x_{h',t}^{DG} \times \left(\overline{P_{h'}^{DG}} - P_{h',t}^{DG}\right) & x_{h',t}^{PEV} \neq 1 \end{cases} \qquad (3.28)$$

Based on equation (3.28), if the battery of PEV of a connected SH is in discharging status ($x_{h',t}^{PEV} = 1$), the battery has available capacity about ($\overline{P_{h'}^{PEV}} - P_{h',t}^{PEV}$) to help the SH. Also, if the DG of a connected SH is in "on" status, the DG has available capacity about ($\overline{P_{h'}^{DG}} - P_{h',t}^{DG}$) to help the SH.

3.3 Simulation and Results for Cooperative Distributed Energy Scheduling of Smart Homes

All the simulations are done in MATLAB environment using the Intel Xeon Sever with 64 GB RAM. The number of chromosomes in the population (n_c) and the value of mutation probability of the genes (θ^{Mut}) in the applied GA are considered about 100 and 10%, respectively. The standard deviation of prediction errors related to solar irradiance is considered about 5% in all the simulations.

3.3.1 The Small System

3.3.1.1 Characteristics of the Small System

Figure 3.7 illustrates the configuration of the small system that include five SHs with different set of sources including PV panels installed on the roof of the SH, PEV, DG, and electrical distribution grid. In addition, every SH has connections to some of the other SHs. The technical data for different types of the DGs are presented in Table 3.1. Furthermore, the value of other parameters of the system and problem are presented in Table 3.2. The value of penalty for carbon emissions (β^E) is based on the value introduced by California Air Resources Board auction of greenhouse gas emissions [76].

In Table 3.2, Cap^{PEV} indicates the value of capacity of the battery of PEV. Also, t_{Arr} and t_{Dep} are the time that the PEV is connected/disconnected to/from the SH by the occupant, respectively. The electricity price proposed by the local DISCO at every time step (five minutes) of the operation period (one day) is shown in Figure 3.8.

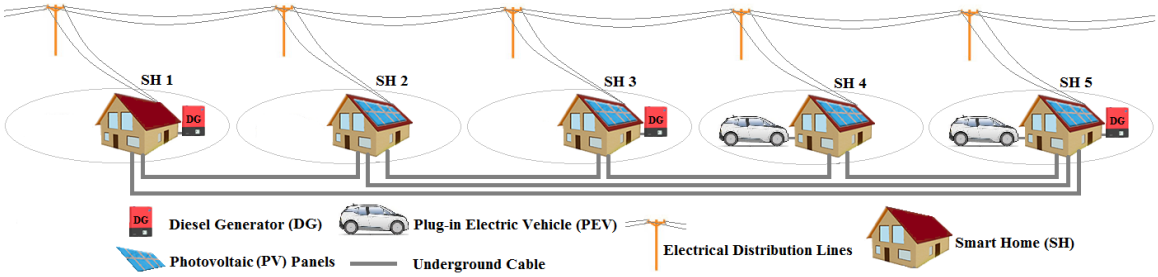

Figure 3.7: The configuration of small system.

Table 3.1: Technical data of different types of DGs.

Parameter	Type 1	Type 2	Type 3
z_1^F (¢/kWh^2)	0.00324	0.00243	0.00491
z_2^F (¢/kWh)	3.96	9.94	7.85
z_3^F (¢)	0	0	0
z_1^E (kg/kWh^2)	0.0007	0.0008	0.0008
z_2^E (kg/kWh)	0.39	0.94	0.61
z_3^E (kg)	0	0	0
$\underline{P^{DG}}$ (kW)	5	5	5
$\overline{P^{DG}}$ (kW)	20	10	15
MUT^{DG} (min)	10	10	10
MDT^{DG} (min)	10	10	10
C^{STU_DG} (¢)	100	100	100
C^{SHD_DG} (¢)	100	100	100

Table 3.2: The value of parameters of the system and problem.

n_t	288	$\overline{P_{Type\ 1}^{PEV}}$ (kW)	10	$SOC_{t_{Arr}}^{PEV}$ (%)	50
n_τ	12	$\overline{P_{Type\ 2}^{PEV}}$ (kW)	15	$\Delta t_{Dep-Arr}$	9-10 and 16-17
φ	0.5	$Cap_{Type\ 1}^{PEV}$ (kWh)	50	Pr^{PEV} (¢)	200,000
β^E (¢/kg)	1	$Cap_{Type\ 2}^{PEV}$ (kWh)	75	ξ^{PEV} (Ah)	10,000
$\overline{P_2^{PV}}$ (kW)	10	DOD^{PEV} (%)	20	θ^{Mut} (%)	5
$\overline{P_3^{PV}}$ (kW)	10	$SOC_{t_{Dep}}^{PEV}$ (%)	100	n_c	50

Table 3.3 presents the load demand pattern, the power pattern of the PV panels, the type of DG, and the type of PEV for every SH. The load demand patterns of SHs 1-5 are shown in Figures 3.9, 3.11, 3.13, 3.15, and 3.17, respectively. In addition, the power patterns of the PV panels related to SH 2-5 are illustrated in 3.11, 3.13, 3.15, and 3.17, respectively. Moreover, SH 4 and SH 5 have PEV of type 1 and type 2, respectively.

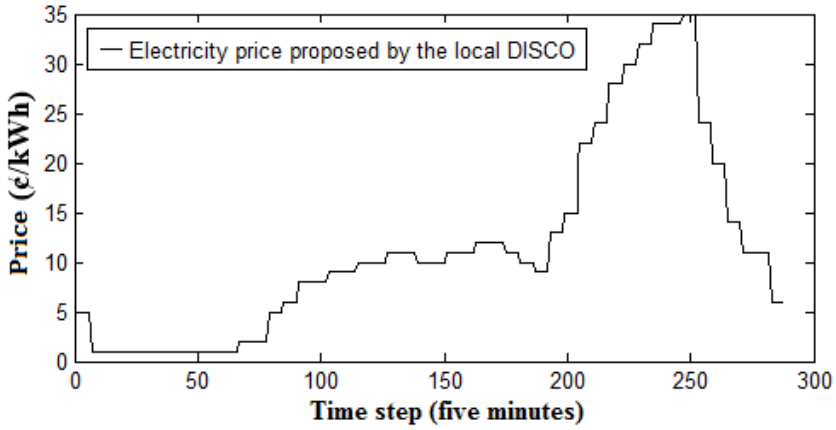

Figure 3.8: The electricity price proposed by the local DISCO at every time step of the operation period.

Table 3.3: The different sources of every SH with different pattern and type.

SH	Load	PV	DG	PEV	Grid
1	Pattern 1	-	Type 1	-	Yes
2	Pattern 2	Pattern 1	-	-	Yes
3	Pattern 3	Pattern 2	Type 2	-	Yes
4	Pattern 4	Pattern 3	-	Type 1	Yes
5	Pattern 5	Pattern 4	Type 3	Type 2	Yes

3.3.1.2 Results

3.3.1.2.1 Without Energy Scheduling

Table 3.4 presents the operation cost of every individual SH and the set of SHs without scheduling the energy resources of the SHs. In this condition, the power of the PV panels are considered as the negative demand and then it is added to the load demand of every individual SH. In addition, at every time step, the extra power of every SH is directly delivered to the grid and sold to the local DISCO. As can be seen, the total operation cost of the set of SHs is about $66.01/day.

3.3.1.2.2 Non-Cooperative Energy Scheduling

The daily operation cost of every individual SH (SHs 1-5) and the set of SHs with non-cooperative energy scheduling is given in Table 3.4. The energy scheduling of the set of SHs by applying five-minute scale, one-hour scale, and multi-time scale stochastic MPC approaches result in about 33.9%, 46.7%, and 47.3% cost reductions, respectively. The reason for superiority of the multi-time scale stochastic MPC is the ability of this approach for having vast vision for the optimization time horizon and precise resolution for the problem variables.

Table 3.4: The operation cost of every SH and the system ($/day) without energy scheduling and with non-cooperative and cooperative distributed energy scheduling.

-	SH	Time scale of MPC		
		Five-minute	One-hour	Multi
Without energy scheduling	SH 1	10.21		
	SH 2	11.47		
	SH 3	14.54		
	SH 4	13.38		
	SH 5	16.38		
	Total	66.01		
Non-cooperative energy scheduling	SH 1	-3.54	-3.46	-3.54
	SH 2	11.47	11.47	11.47
	SH 3	13.76	13.98	13.76
	SH 4	13.38	9.17	9.17
	SH 5	8.52	4.00	3.91
	Total	43.59	35.16	34.77
Cooperative distributed energy scheduling	SH 1	-4.66	-5.01	-5.31
	SH 2	9.52	7.20	7.20
	SH 3	10.20	8.54	8.54
	SH 4	10.55	5.11	5.11
	SH 5	5.21	2.67	2.33
	Total	30.82	18.51	17.87

3.3.1.2.3 Cooperative Distributed Energy Scheduling

3.3.1.2.3.1 Applying Five-Minute Scale Stochastic MPC

The daily operation cost of the set of SHs and every individual SH and the optimal schedule of the energy resources of the SHs in the cooperative distributed energy scheduling applying five-minute scale MPC are presented in Table 3.4 and Figures 3.9-3.18, respectively. As can be seen, the total operation cost of the set of SHs is decreased to about $30.82/day. In fact, cooperation of the SHs contribute to 29.2% cost saving

compared to non-cooperative energy scheduling. Moreover, the operation cost of every SH is reduced and SH 1 not only eliminates its operation cost, but also it makes income.

The demand pattern and power of the DG of SH 1 at every time step of the operation period are illustrated in Figure 3.9. As can be seen, the DG is shut down at 7th time step and the needed electricity is purchased from the local DISCO between the 7th-78th time steps of the operation period. For the rest of the operation period, SH 1 starts up its DG, supplies its demand, and exports its extra power to the connected SHs and the local DISCO, as can be seen in Figures 4.9 and 4.10.

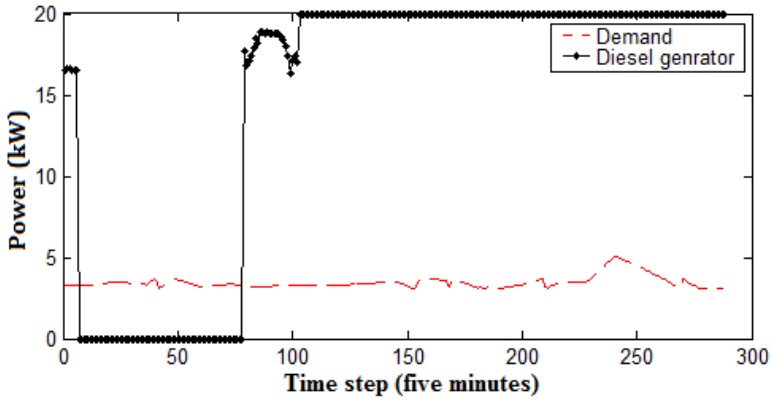

Figure 3.9: The demand level and optimal power pattern of the DG in SH 1 in cooperative distributed energy scheduling applying five-minute scale stochastic MPC.

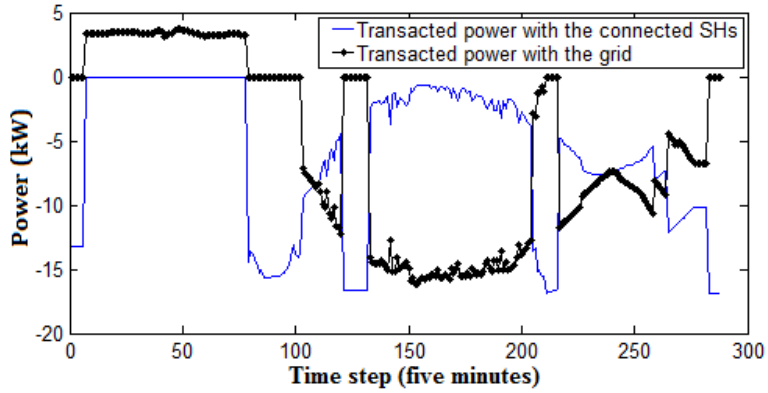

Figure 3.10: The optimal transacted powers between SH 1 and the connected SHs and local DISCO in cooperative distributed energy scheduling applying five-minute scale stochastic MPC.

The demand pattern and power pattern of the PV panels of SH 2 are shown in Figure 3.11. In addition, the transacted power between SH 2 and the other connected SHs and the local DISCO are shown in Figure 3.12. As can be seen, SH 2 purchases its needed power from the local DISCO just between 7^{th}-78^{th} time steps and in the other time steps, it purchases most of the demanded electricity from the connected SHs. In addition, SH 2 never sales electrical energy to the connected SHs or the local DISCO.

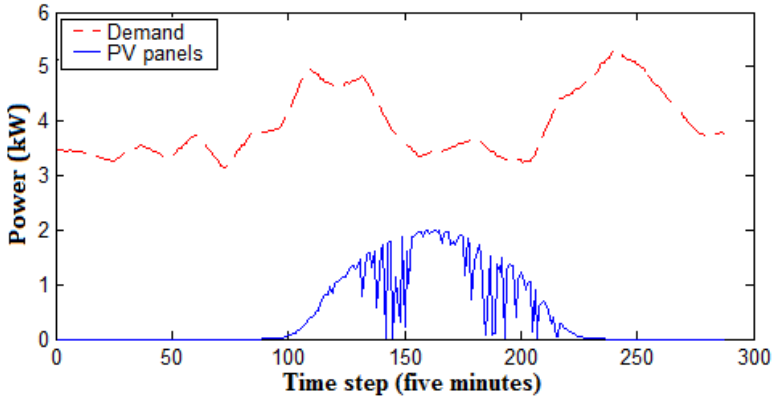

Figure 3.11: The demand level and power pattern of the PV panels in SH 2 in cooperative distributed energy scheduling applying five-minute scale stochastic MPC.

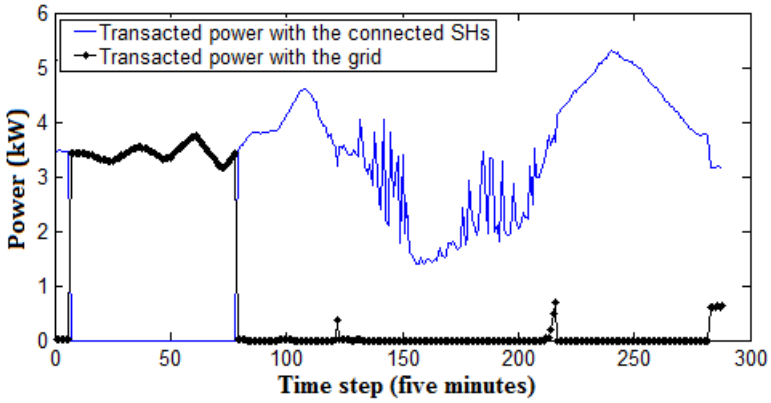

Figure 3.12: The optimal transacted powers between SH 2 and the connected SHs and local DISCO in cooperative distributed energy scheduling applying five-minute scale stochastic MPC.

The demand pattern, power pattern of the PV panels, and the generation level of DG of SH 3 are shown in Figure 3.13. As can be seen, the DG is turned "off" and "on" several times over the operation period, since this DG is the most expensive and pollutant DG, as can be realized from Table 3.1. In addition, the transacted power of the SH 3 with the local DISCO and the connected SHs are demonstrated in Figure 3.14.

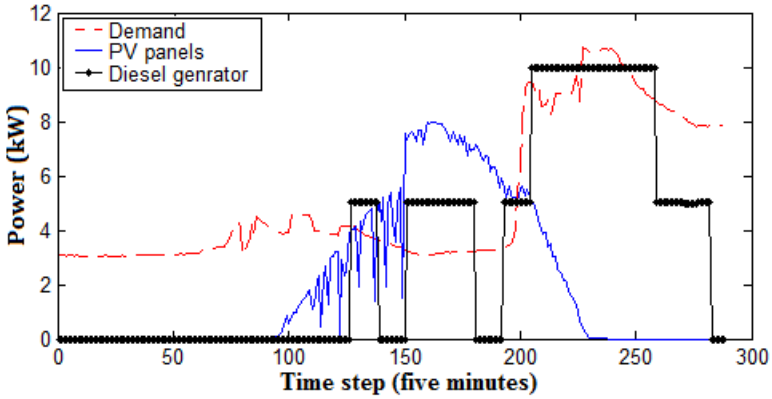

Figure 3.13: The demand level, power pattern of the PV panels, and optimal power pattern of the DG in SH 3 in cooperative distributed energy scheduling applying five-minute scale stochastic MPC.

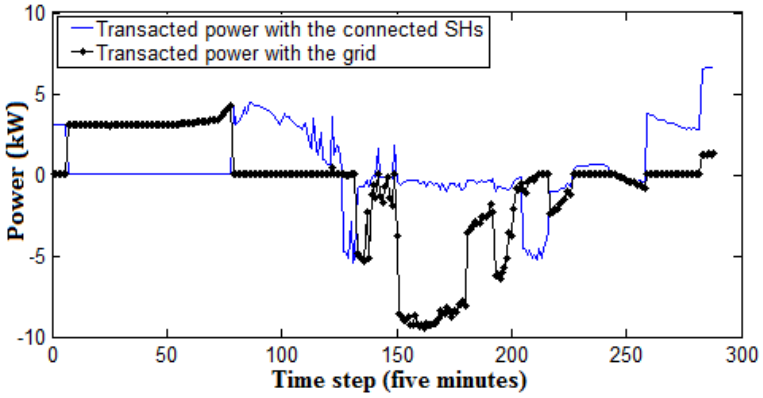

Figure 3.14: The optimal transacted powers between SH 3 and the connected SHs and local DISCO in cooperative distributed energy scheduling applying five-minute scale stochastic MPC.

The demand pattern, power patterns of the PV panels and the battery of the PEV related to SH 4 are shown in Figure 3.15. As can be seen, the battery of the PEV is charged between 121th-132th and 205th-216th time steps because the PEV has lost energy after it has been used by the driver. Moreover, the battery of PEV does not have any charging and discharging pattern. Furthermore, the transacted power between SH 4 the other connected SHs and the local DISCO are demonstrated in Figure 3.16.

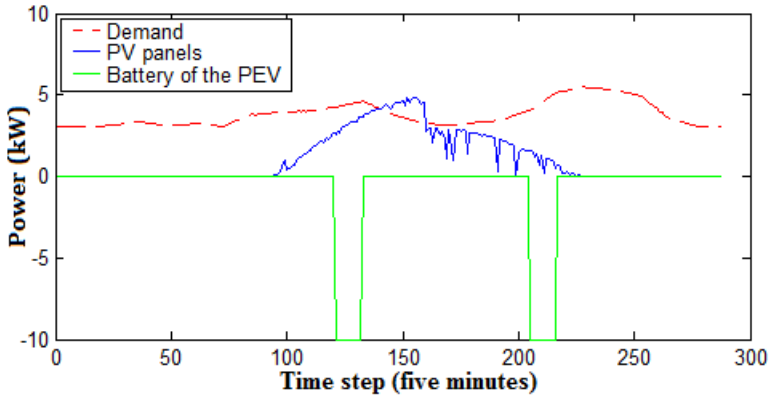

Figure 3.15: The demand level, power pattern of the PV panels, and optimal power pattern of the battery of the PEV in SH 4 in cooperative distributed energy scheduling applying five-minute scale stochastic MPC.

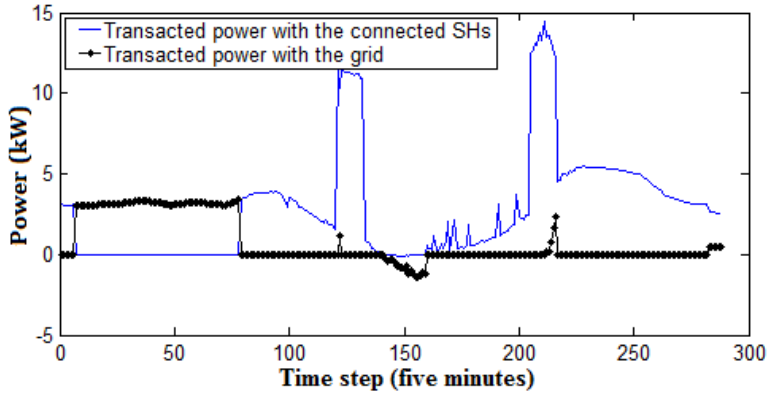

Figure 3.16: The optimal transacted powers between SH 4 and the connected SHs and local DISCO in cooperative distributed energy scheduling applying five-minute scale stochastic MPC.

The demand pattern, power pattern of the PV panels, power of the DG, and power of the battery of PEV related to the SH 5 are shown in Figure 3.17. As can be seen, SH 5 starts up its DG in 103th time step and keeps it "on" until 282th time step; however, in some periods, sets the power of the DG at minimum power limit and avoids shutting it down. In addition, the battery of the PEV in SH 5 has the same charging patterns as SH 4. Moreover, the transacted power of the SH 5 with the connected SHs and the local DISCO are illustrated in Figure 3.18.

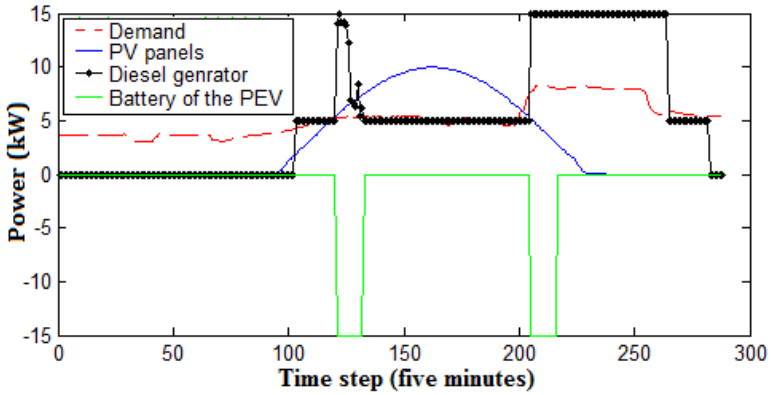

Figure 3.17: The demand level, power pattern of the PV panels, and optimal power patterns of the DG and the battery of the PEV in SH 5 in cooperative distributed energy scheduling applying five-minute scale stochastic MPC.

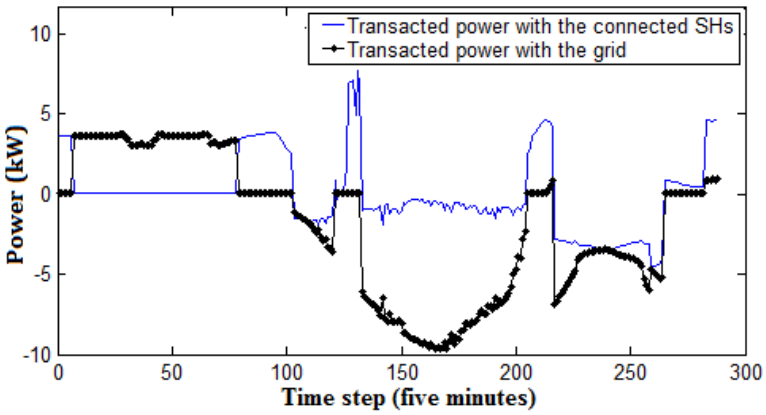

Figure 3.18: The optimal transacted powers between SH 5 and the connected SHs and local DISCO in cooperative distributed energy scheduling applying five-minute scale stochastic MPC.

3.3.1.2.3.2 Applying One-Hour Scale Stochastic MPC

The daily operation cost of the set of SHs and every individual SH for one-hour scale stochastic MPC can be seen in Table 3.4. Herein, the total operation cost of the set of SHs is about $18.51 that has 47.3% reduction compared to the result of the non-cooperative energy scheduling.

By applying one-hour scale stochastic MPC in the cooperative distributed energy scheduling problem of the set of SHs, the performance of battery of each PEV is improved. Figures 4.19 and 4.20 illustrate the optimal charging and discharging patterns of batteries of the PEVs in SH 4 and SH 5.

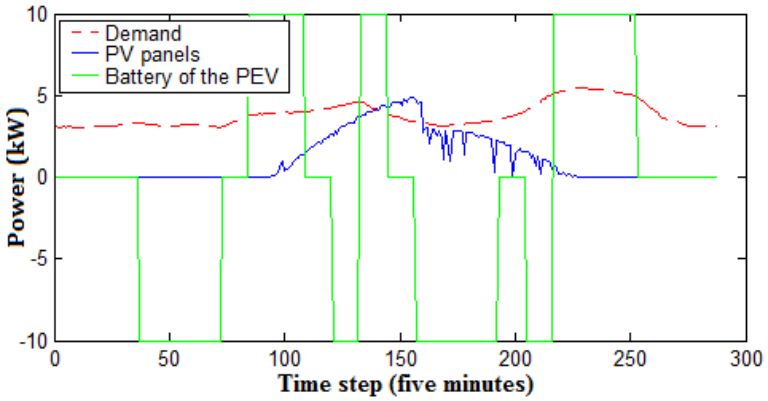

Figure 3.19: The demand level, power pattern of the PV panels, and optimal power patterns of the battery of PEV in SH 4 in cooperative distributed energy scheduling applying one-hour scale stochastic MPC.

3.3.1.2.3.3 Applying Multi-Time Scale Stochastic MPC

The daily operation cost of the set of SHs and every individual SH for multi-time scale stochastic MPC are presented in Table 3.4. As can be seen, the total operation cost

of the set of SHs is $17.87 that has about 48.6% reduction compared to the result of non-cooperative energy scheduling.

Figure 3.21 shows the demand level, the power pattern of the PV panels, and the optimal power pattern of the DG and the battery of the PEV in SH 5. As can be seen, the DG is able to program its generation in the small scales (five minute) between 121th-132th time step, and also the battery of the PEV is capable of having vast vision (12 hours) for the optimization time horizon to have optimal charging/discharging pattern.

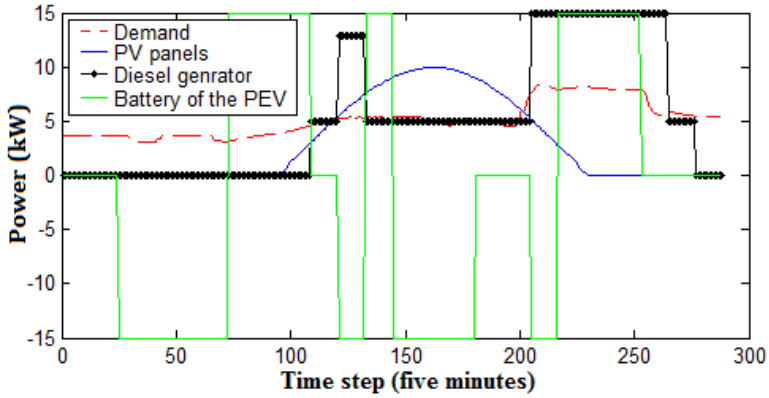

Figure 3.20: The demand level, power pattern of the PV panels, and optimal power patterns of the DG and the battery of the PEV in SH 5 in cooperative distributed energy scheduling applying one-hour scale stochastic MPC.

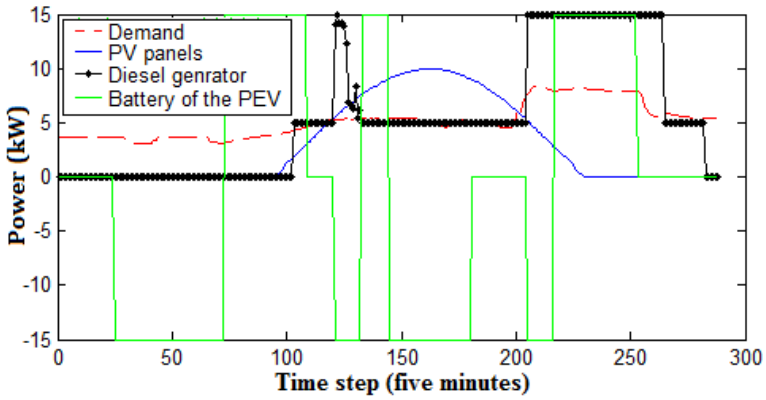

Figure 3.21: The demand level, the power pattern of the PV panels, and the optimal power pattern of the DG and the battery of PEV in SH 5 in cooperative distributed energy scheduling applying multi-time scale stochastic MPC.

3.3.2 The Big System

In this case study, cooperative distributed energy scheduling problem for a relatively large set of SHs (50 SHs) is investigated and the results are compared with the outcomes of simulation of the problem related to the small set of SHs (5 SHs).

3.3.2.1 Characteristics of the Big System

Figure 3.22 shows the configuration of the big system that includes 50 SHs with different set of sources. As can be seen, every SH has electrical connections to some of the neighboring SHs. In addition, different sources of every SH with different type and power pattern are indicated in Table 3.5.

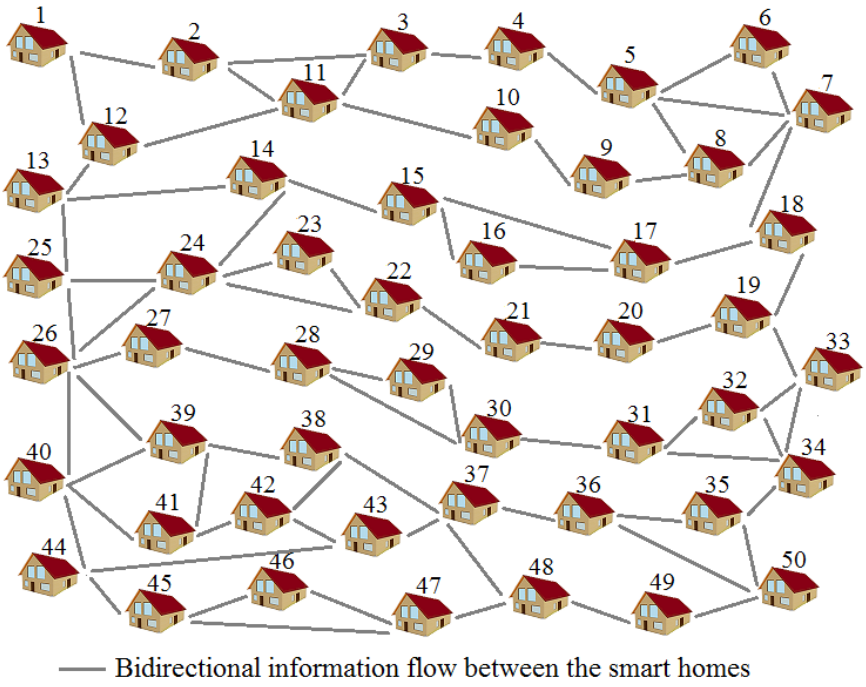

Figure 3.22: The configuration of big system.

Table 3.5: Different sources of every SH with different pattern and type.

SHs	Load	PV	DG	PEV	Grid
1,7,13,33,38	Pattern 1	Pattern 4	Type 1	Type 2	Yes
14,21,29,43,48	Pattern 2	Pattern 1	-	-	Yes
2,8,22,34,39	Pattern 3	Pattern 2	Type 2	-	Yes
15,23,30,40,44	Pattern 4	Pattern 3	-	Type 1	Yes
9,16,24,35,45	Pattern 5	-	Type 1	-	Yes
3,4,17,25,31	Pattern 1	Pattern 4	Type 2	Type 2	Yes
10,18,26,41,46	Pattern 2	Pattern 3	-	Type 1	Yes
5,11,27,36,49	Pattern 3	Pattern 1	Type 3	-	Yes
12,19,32,42,47	Pattern 4	-	-	-	Yes
6,20,28,37,50	Pattern 5	Pattern 2	Type 3	-	Yes

3.3.2.2 Results

Table 3.6 presents the value of total daily operation cost of the problem without energy scheduling, with non-cooperative energy scheduling, and with cooperative distributed energy scheduling. As can be seen, applying the multi-time scale stochastic MPC in the problems has better result compared to the single-time scale stochastic MPC with five-minute or one-hour scale. Also, cooperative distributed energy scheduling problem with multi-time scale stochastic MPC has the most cost reduction.

Figure 3.23 shows the operation cost of every SH ($/day) without energy scheduling and with cooperative distributed energy scheduling applying multi-time scale stochastic MPC. As can be seen, every SH is benefitted due to cooperation in the energy scheduling problem; however, the value of cost reduction for the SHs are not equal, since every SH has different sources of energy and various set of connections to other SHs.

Table 3.6: The operation cost of every SH and the system ($/day) without energy scheduling and with non-cooperative and cooperative distributed energy scheduling.

-	Time scale of MPC	Total operation cost ($/day)
Without energy scheduling	-	652.10
Non-cooperative energy scheduling	Five-minute	423.91
	One-hour	272.37
	Multi	263.53
Cooperative distributed energy scheduling	Five-minute	288.38
	One-hour	154.79
	Multi	144.87

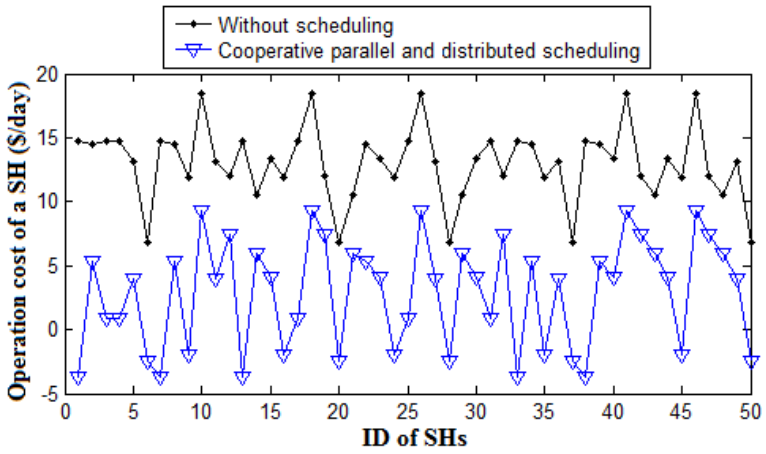

Figure 3.23: The operation cost of every SH ($/day) without energy scheduling and with cooperative distributed energy scheduling applying multi-time scale stochastic MPC.

Table 3.7 presents the percentage of cost reduction in the cooperative distributed energy scheduling of the set of SHs compared to the result of problem without energy scheduling for both small and big systems. As can be seen, the cooperation of SHs in the energy scheduling problem in the big system has more potential for cost reduction compared to the small system.

Table 3.7: The value of cost reduction (%) in the cooperative distributed energy scheduling compared to the result of problem without energy scheduling for small system and big system.

Time scale of MPC	Small system	Big system
Five-minute	53.3%	55.7%
One-hour	71.9%	76.2%
Multi	72.9%	77.7%

3.4 Conclusion of Problem I

In the first problem of dissertation, the single-time scale and multi-time scale stochastic MPC as the adaptive and dynamic optimization technique were applied in the cooperative distributed energy scheduling problem of the set of SHs with different sources of energy. Herein, the stochastic and MPC techniques addressed the uncertainty and variability issues of the power of photovoltaic (PV) panels, respectively.

After simulating the problem, it was observed that cooperation of SHs with one another in the distributed energy scheduling problem result in considerable cost saving in the small and big case studies. In fact, the reason for this achievement is related to the cooperation of SHs for sharing their energy sources including DG, PV panels, and the battery of PEV. Furthermore, it was proven that cooperation of more SHs in the energy scheduling problem has more potential for cost reduction.

In addition, due to considering the small and large time scales (five-minute and one-hour scales) in the multi-time scale MPC, the DG could adjust its output power level within more precise time step (five-minute), and also the battery of the PEV was able to

determine the optimal charging and discharging patterns due to having vast optimization time horizon (12 hours) over the operation period (one day).

As the extended and future work of this study, it is suggested to consider the effects of inaccessibility of the SHs to the electrical distribution network and disconnection of SHs with one another in the cooperative distributed energy scheduling problem.

CHAPTER FOUR

PROBLEM II: PRICE-CONTROLLED ENERGY MANAGEMENT OF SMART HOMES

4.1 Proposed Technique for Price-Controlled Energy Management of Smart Homes

4.1.1 Proposed Technique for Solving Generation Scheduling and unit commitment (UC) Problems of a GENCO

4.1.1.1 Price-Controlled Energy Management

For every scheme of price-controlled energy management (modifying the electricity price at peak using ρ^{EM}, as can be seen in equation (4.1)) introduced by the generation company (GENCO), the smart homes (SHs) react and optimally re-schedule their energy resources. Then, the energy scheduling and UC problems of the GENCO are optimally solved. The energy management of SHs is done for every possible value of ρ^{EM}, and finally the optimal scheme of energy management (optimal value of ρ^{EM}) is determined based on the maximum value of profit of the GENCO over the operation period (one day). Herein, ρ^{EM}, as the variable of price-controlled energy management scheme, can take zero, positive, and negative values.

$$\widetilde{\pi_t} = \begin{cases} \pi_t + \rho^{EM} & t \in peak\ period \\ \pi_t & t \notin peak\ period \end{cases} \tag{4.1}$$

Algorithm I presents the pseudo code for finding the optimal scheme of energy management of SHs by the GENCO.

Algorithm I: The pseudo code for finding the optimal scheme of energy management of SHs.

1: Set the value of $\rho^{EM} = \rho^{EM}_{MIN}$.

2: $\rho^{EM} = \rho^{EM} + 1$.

3: Update the electricity price ($\tilde{\pi}$) using equation (4.1).

4: SHs react and re-schedule their energy resources and change their electricity transaction with the GENCO to minimize their daily operation costs *//Presented in Section 4.1.2.*

5: Update demand of SHs (D^{SHs}), and consequently demand of system ($D^{SHs} + D^{PASS}$).

6: Solve the generation scheduling and UC optimization problems of the GENCO to maximize its daily profit using GA. *//Presented in Sections 4.1.1.2 and 4.1.1.3.*

7: Go to Step 2, if $\rho^{EM} < \rho^{EM}_{MAX}$

8: Determine optimal value of ρ^{EM} based on the maximum daily profit of GENCO.

4.1.1.2 Optimization Technique for UC Problem of the GENCO

The UC problem is as an optimization problem that determines the statuses of generation units to minimize the overall cost of system considering the operational constraints of generation units and the system. Herein, GA is applied to solve the UC problem of the GENCO. The objective function of the GENCO is maximizing its daily profit that includes income from selling electricity to the customers and cost terms due to fuel cost, emission cost, and start up and shut down costs of generation units. Therefore, the GENCO needs to design an optimal price-controlled energy management scheme (optimal scheme of electricity price) to maximize its electricity selling income, and also to optimally schedule its generation units to minimize their operation costs.

Herein, a chromosome in GA is the representative of statuses of the generation units at every hour of the operation period (one day), as can be seen in Figure 4.1. Herein, "1" means "on" and "0" means "off" for each generation unit (G1-G6). The daily profit

of GENCO is defined as the fitness of every chromosome, and then the GA tries to maximize the fitness of chromosomes.

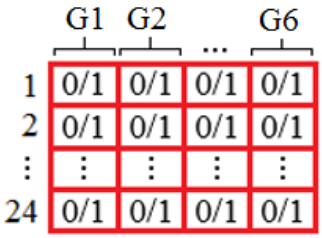

Figure 4.1: The structure of chromosome in the applied GA for UC problem of the GENCO.

In the following, the steps for applying the GA in the UC problem of the GENCO are presented and described. The problem inputs are the hourly demand level of system (sum of hourly demand of passive end users and the updated hourly demand of SHs due to their reaction with respect to the energy management scheme shown in Figures 4.11-4.13) and all the technical data of the generation units and problem presented in Table 4.3. Also, the outputs include the optimal generation level of each generation unit at every hour of a day that maximize the daily profit of GENCO.

- *Step 1: Obtaining the primary data*

Parameters for applying GA: These parameters include the mutation probability of the genes (θ^{Mut}) and the size of the population (n_c) as the number of the chromosomes.

Parameters of the system under study: The values of all the parameters of the generation system and problem are obtained (Table 4.3, Figures 4.11-4.13). Also, the value of variable of energy management (ρ^{EM}) is selected.

Updating demand level of the end users: The demand level of system including sum of demand pattern of passive customers and the updated demand pattern of active customers (SHs) is determined.

Initial population: The chromosomes of the population (Figure 4.1) are initialized with random binary values ("0" or "1").

- *Step 2: Updating the population*

Applying crossover operator: The crossover operator is applied on every two chromosomes to reproduce two new chromosomes as the offspring.

Applying mutation operator: The mutation operator is applied on every gene of every chromosome of the population with the definite probability θ^{Mut}.

- *Step 3: Selecting new population*

Evaluating fitness of every chromosome: For every chromosome, the generation scheduling problem of the GENCO is solved using Lambda-Iteration Economic Dispatch algorithm (presented in Section 4.1.1.3) [77] and if all the constraints of problem and system presented in equations (4.21)-(4.28) are satisfied, the fitness (fit_c) of chromosome (the total daily profit of GENCO) is calculated.

Applying selection process: The chromosomes are selected using the probabilistic fitness-based selection (PFBS) technique, where the fitter chromosomes are more likely to be chosen. Herein, r_c is a random number between [0,100] generated for the chromosome (c).

$$a_c = \begin{cases} 1 & \theta_c^{PFBS} > r_c \\ 0 & \theta_c^{PFBS} < r_c \end{cases} \tag{4.2}$$

The value of selection probability of every chromosome (θ_c^{PFBS}) is determined using equation (4.3), which is proportional to the fitness of the chromosome. Herein, n_c is the number of chromosomes in the population and a_c is the acceptance indicator of a chromosome for the new population.

$$\theta_c^{PFBS} = \frac{fit_c}{Max\{fit_1, \dots, fit_{nc}\}} \times 100 \qquad (4.3)$$

- *Step 4: Checking termination criterion*

In this step, the convergence status of the optimization procedure is checked. Based on this, the values of improvements in the fitness of the chromosomes of the old and new populations are computed and if there are no significant improvements in them, the optimization process is finished, otherwise, the algorithm is continued from *Step 2*.

- *Step 5: Introducing the outcome*

The consequences include the maximum value of daily profit of GENCO, the optimal commitment status and optimal generation level of units at every hour in the day.

4.1.1.3 Optimization Technique for Generation Scheduling Problem of the GENCO Using Lambda-Iteration Economic Dispatch Method

Herein, the status of generation units (determined by the GA in Section 4.1.1.2) and the demand level of system and all the technical data of generation units (Table 4.3, Figures 4.11-4.13) are the input of problem. Moreover, the outputs include the optimal generation level of each generation unit at every hour of a day.

When the statuses of generation units are determined by the GA, Lambda-Iteration Economic Dispatch method [77] is applied to solve the generation scheduling problem of the GENCO. The Lambda-Iteration Economic Dispatch includes finding the real power generation for each generation unit to minimize the total cost of the generation system subject to the equality constraint (supply-demand balance constraint) and inequality constraints (upper and lower power limits of every generation units) [77]. Herein, P , $Cost^F$, and $Cost^E$ are the power level, fuel cost, and emission cost of a generation unit, respectively. Also, D is the total demand of system. In addition, g and Ng are the indices of a generation unit and total number of units of the GENCO, respectively.

$$min\left\{\sum_{g=1}^{Ng} Cost_{g,t}^{F} + Cost_{g,t}^{E}\right\} \tag{4.4}$$

Subject to:

$$\sum_{g=1}^{Ng} P_{g,t} = D_t \tag{4.5}$$

The Lambda-Iteration Economic Dispatch method considers the equality constraint and solves the generation scheduling problem iteratively using the Lagrangian multipliers, as can be seen in equations (4.6)-(4.8). The marginal generation cost of system (λ) is the change in the total cost that arises when the amount of electricity produced is incremented by one power unit (1MW). Herein, λ is a variable and its optimal value results in the minimum cost of problem.

$$L_t = \sum_{g=1}^{Ng} \left(Cost_{g,t}^{F} + Cost_{g,t}^{E}\right) + \lambda \times \left(D_t - \sum_{g=1}^{Ng} P_{g,t}\right) \tag{4.6}$$

$$\frac{\partial L_t}{\partial P_{g,t}} = 0, \forall g \tag{4.7}$$

$$\frac{\partial L_t}{\partial \lambda} = 0, \forall g \tag{4.8}$$

Solving equations (4.6)-(4.8) result in equations (4.9)-(4.10).

$$\sum_{g=1}^{Ng} P_{g,t} = D_t \tag{4.9}$$

$$\frac{\partial\left(Cost_{g,t}^{F} + Cost_{g,t}^{E}\right)}{\partial P_{g,t}} = \lambda, \forall g \tag{4.10}$$

The generation units have minimum and maximum limits on their generation level that must be considered in the generation scheduling problem. Herein, the Kuhn-Tucker conditions (presented in equation (4.11)) complete the Lagrangian multipliers by adding the inequality constraints (minimum and maximum generation limits of every unit) as the additional terms, as can be seen in equation (4.11) [77].

$$\begin{cases} \dfrac{\partial\left(Cost_{g,t}^{F} + Cost_{g,t}^{E}\right)}{\partial P_{g,t}} \leq \lambda & P_{g,t} = P_g^{max} \\ \dfrac{\partial\left(Cost_{g,t}^{F} + Cost_{g,t}^{E}\right)}{\partial P_{g,t}} = \lambda & P_g^{min} \leq P_{g,t} \leq P_g^{max} \\ \dfrac{\partial\left(Cost_{g,t}^{F} + Cost_{g,t}^{E}\right)}{\partial P_{g,t}} \geq \lambda & P_{g,t} = P_g^{min} \end{cases} \tag{4.11}$$

By solving equations (presented in equations (4.9)-(4.10)) and inequality equations (presented in equation (4.11)), the Lambda-Iteration Economic Dispatch method outputs the optimal generation level of each generation unit.

4.1.2 Proposed Technique for Solving Energy Scheduling Problem of a SH

In the following, different parts of the proposed technique for solving energy scheduling problem of a SH is presented.

4.1.2.1 Scenario-Based Stochastic Optimization

In this study, in order to address the uncertainty and variability concerned with the power of photovoltaic (PV) panels, a scenario-based stochastic optimization approach is applied. Herein, a large number of effective and diverse scenarios are comprehensively defined for addressing the predictions uncertainties.

Forecasting value of uncertain states: The power of PV panels depends on the value of solar irradiance that it absorbs. However, solar irradiance has a large degree of variability and uncertainty. Herein, based on the historical values of solar irradiances, the value of solar irradiances (ρ) over the optimization time horizon (for every five-minute step of the next two hours (n_τ is 24)) are predicted using the neural network available in MATLAB. The historical data of the solar irradiances are the real solar irradiances recorded in Clemson, SC 29634, USA in July 2014. About 70% of the data is used for training the neural network and 30% of the data is used for validation and testing. The set of predicted solar irradiances ($\tilde{\rho}$) are presented in equation (4.12). Herein, 288 five-minute steps indicate one day as the operation period.

$$\{\tilde{\rho}_{t+1}, \dots, \tilde{\rho}_{t+n_\tau}\}, n_\tau = 24, t \in T, T = \{1, \cdots, 288\} \quad (4.12)$$

Modeling uncertainties of forecasted data: Figure 4.2 illustrates the predicted and measured solar irradiances for the current time step (t, with a 5-minute time duration) and past time steps $(1, 2, \cdots, t-1)$, and also the predicted solar irradiances for every time step of the optimization time horizon $(t+1, \cdots, t+n_\tau)$. The previously forecasted solar irradiances ($\tilde{\rho}$) are compared with the real solar irradiances (measured data) and the values of the error of the predictions are calculated. Next, the mean value of the prediction errors (μ^{Er}) is calculated. The values of μ^{Er} is updated in the next predictions in the optimization procedure of the problem over the operation period $(1, 2, \cdots, t, \cdots, 288)$.

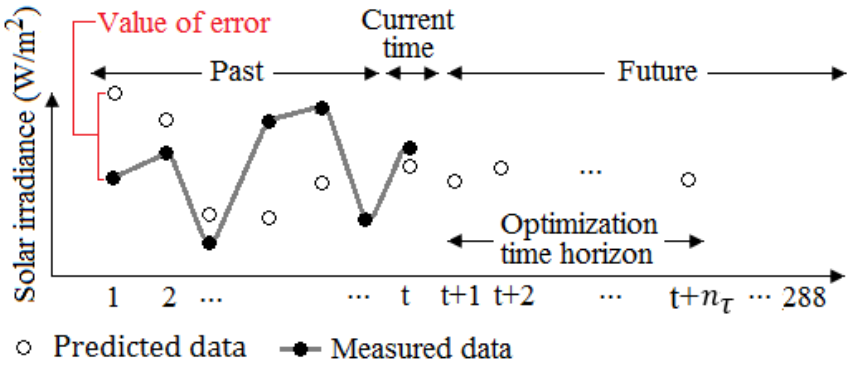

Figure 4.2: The predicted data, measured data, and value of the prediction error.

The important factor in defining the scenarios is comprehensively considering the most probable values for the estimated solar irradiances over the optimization time horizon. In other words, the defined scenarios should consider almost all the possibilities for the estimated values of uncertain state of the problem, and also they should have diversity (no similarity). Herein, the estimated values of solar irradiance are considered to be about under, equal to, and above its predicted values ($\tilde{\rho}_t + \mu^{Er}$, $\tilde{\rho}_t$ or $\tilde{\rho}_t - \mu^{Er}$), as the

most logical values. In addition, it is considered that the estimated values can be changed over the time steps of optimization time horizon. Based on this, 10 diverse scenarios ($s \in S$, $S = \{1, \dots, n_s\}$, n_s=10) are defined for the estimated solar irradiances with equal occurrence probabilities (Ω^{PV}), that is, each 10%. Figure 4.3 shows the defined scenarios for the uncertain state of the problem (solar irradiance) at every time step (every five minutes) over the optimization time horizon (next two hours). In this figure, the codes "1", "2", and "3" represent $\tilde{\rho}_t + \mu^{Er}$, $\tilde{\rho}_t$ and $\tilde{\rho}_t - \mu^{Er}$, respectively.

In fact, at every time step (t), the problem is solved 10 times and every time, one of the scenarios is applied for the value of solar irradiances, and finally the operation cost of SH is calculated as the expected value of operation costs of the 10 scenarios.

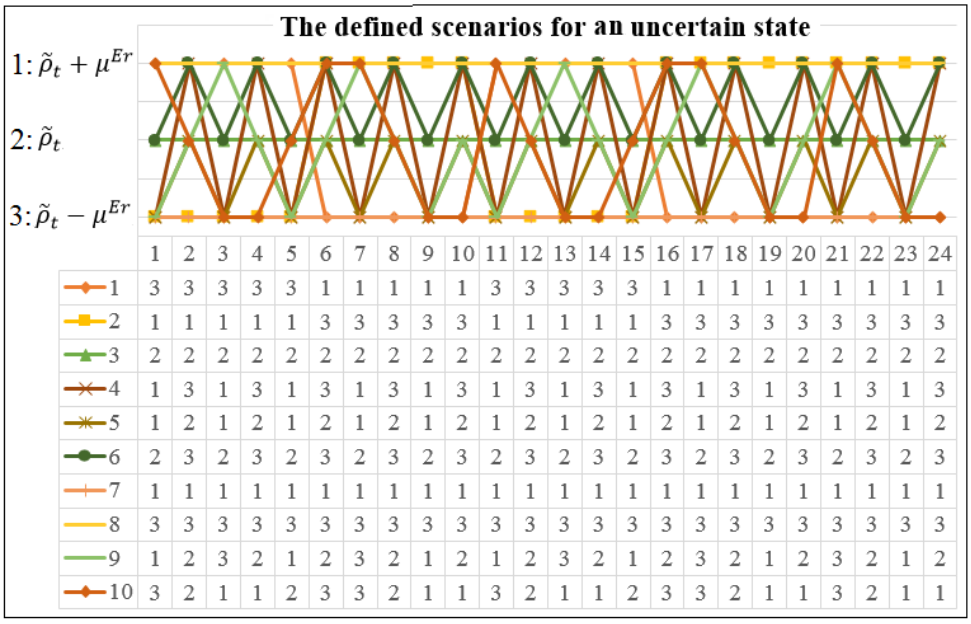

	1	2	3	4	5	6	7	8	9	10	11	12	13	14	15	16	17	18	19	20	21	22	23	24
1	3	3	3	3	3	1	1	1	1	1	3	3	3	3	3	1	1	1	1	1	1	1	1	1
2	1	1	1	1	1	3	3	3	3	3	1	1	1	1	1	3	3	3	3	3	3	3	3	3
3	2	2	2	2	2	2	2	2	2	2	2	2	2	2	2	2	2	2	2	2	2	2	2	2
4	1	3	1	3	1	3	1	3	1	3	1	3	1	3	1	3	1	3	1	3	1	3	1	3
5	1	2	1	2	1	2	1	2	1	2	1	2	1	2	1	2	1	2	1	2	1	2	1	2
6	2	3	2	3	2	3	2	3	2	3	2	3	2	3	2	3	2	3	2	3	2	3	2	3
7	1	1	1	1	1	1	1	1	1	1	1	1	1	1	1	1	1	1	1	1	1	1	1	1
8	3	3	3	3	3	3	3	3	3	3	3	3	3	3	3	3	3	3	3	3	3	3	3	3
9	1	2	3	2	1	2	3	2	1	2	1	2	3	2	1	2	3	2	1	2	3	2	1	2
10	3	2	1	1	2	3	3	2	1	1	3	2	1	1	2	3	3	2	1	1	3	2	1	1

Figure 4.3: The defined scenarios for the uncertain state of the problem (solar irradiance) at every time step (every five minutes) over the optimization time horizon (next two hours).

4.1.2.2 Optimization Technique for Energy Scheduling of a SH

Herein, the demand level of SH and all the technical data of energy resources of SH (DG, battery, and PV panels) presented in Table 4.1 and Figures 4.6-4.10 are the input of problem and the outputs include the optimal generation level of energy resources and optimal electricity transaction of SH with GENCO.

The energy scheduling problem of the SH is a mixed-integer nonlinear programming (MINLP) problem. The discrete variables of the problem and the continuous variables of the problem are presented in equations (4.13)-(4.14), respectively. Herein, x^{DG}, x^{B} are the status of diesel generator (DG) and battery and P^{DG}, P^{B}, P^{Grid} are the power of DG, power of battery, and power transaction between the SH and GENCO are. The values of "0" and "1" for x^{DG} mean "off" and "on", respectively. Also, the values of "-1", "0", and "1" for x^{B} mean charging, idle, and discharging, respectively.

$$\begin{Bmatrix} x_t^{DG} & \cdots & x_{t+n_\tau}^{DG} \\ x_t^{B} & \cdots & x_{t+n_\tau}^{B} \end{Bmatrix} \tag{4.13}$$

$$\begin{Bmatrix} P_t^{DG} & \cdots & P_{t+n_\tau}^{DG} \\ P_t^{B} & \cdots & P_{t+n_\tau}^{B} \\ P_t^{Grid} & \cdots & P_{t+n_\tau}^{Grid} \end{Bmatrix} \tag{4.14}$$

In this study, similar to the optimization technique presented in the first problem of dissertation, GA-LP technique as the combination of GA and LP is applied to solve the energy scheduling problem of the SH. Based on this, the dimensions of the defined

chromosome in the applied GA are $n_\tau \times 3$, as can be seen in Figure 4.4. Herein, one bit (gene) for indicating status of the DG ("0" for "off" and "1" for "on") and two bits for indicating the status of the battery ("00" and "10" for idle, "01" for discharging, and "11" for charging) are considered. The procedure for applying the GA in the energy scheduling problem of a SH has been presented in Section 3.1.4.

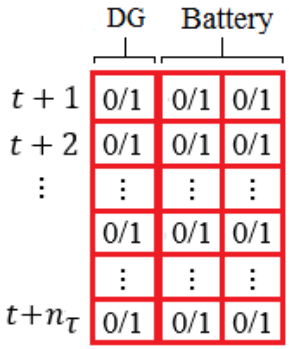

Figure 4.4: The structure of defined chromosome in the applied GA.

4.2 Mathematical Formulation for Price-Controlled Energy Management of Smart Homes

In this section, the mathematical formulations for UC problem of a GENCO and energy scheduling problem of a SH are presented.

4.2.1 Mathematical Formulation for UC Problem of a GENCO

4.2.1.1 Objective Function of a GENCO

The objective function of the GENCO over the operation period (one day) is presented in equation (4.15). As can be seen, it includes income due to selling electricity to the customers, the fuel cost of generation units, the greenhouse gas emissions cost of

generation units, the start-up cost of de-committed units, and the shut-down cost of committed units.

$$OF = max \sum_{t=1}^{Nt} \left[Income_t^{SELL} - \sum_{g=1}^{Ng} \begin{bmatrix} Cost_{g,t}^{F} + Cost_{g,t}^{E} \\ +Cost_{g,t}^{STU} + Cost_{g,t}^{SHD} \end{bmatrix} \right] \quad (4.15)$$

4.2.1.2 Income and Cost Terms of GENCO

In the following, the income and cost terms of the objective function are described.

Income of GENCO due to selling electricity: The income term is related to the selling electrical energy to all the end users. Thus, the income term depends on the values of demand of passive customers (D_t^{PASS}), demand of SHs (D_t^{SHs}), and the price of electricity at every hour of a day. The value of $\widetilde{\pi_t}$, as the updated value of electricity price at every hour of the day, has been defined in equation (4.1).

$$Income_t^{SELL} = \sum_{t=1}^{Nt} [D_t^{PASS} + D_t^{SHs}] \times \widetilde{\pi_t} \quad (4.16)$$

Fuel cost of generation units: The fuel cost of every generation unit ($Cost^F$) is a quadratic polynomial of power unit (P). In other words, the generation unit consumes more fuel per power unit when its power is in the upper level of power compared to the value of consumed fuel per power unit in the lower level. The α_1^F, α_2^F, and α_3^F are fuel cost coefficients of the generation unit and g is index of a generation unit.

$$Cost_{g,t}^{F} = \alpha_{1,g}^{F} \times \left(P_{g,t}\right)^2 + \alpha_{2,g}^{F} \times \left(P_{g,t}\right) + \alpha_{3,g}^{F} \quad (4.17)$$

Greenhouse gas emissions cost of generation units: The greenhouse gas emissions cost of every generation unit is a quadratic polynomial of power unit (P). α_1^E, α_2^E, and α_3^E are emission coefficients of the generation unit and β^E is emission cost factor.

$$Cost_{g,t}^E = \beta^E \times \left(\alpha_{1,g}^E \times \left(P_{g,t}\right)^2 + \alpha_{2,g}^E \times \left(P_{g,t}\right) + \alpha_{3,g}^E\right) \quad (4.18)$$

Start-up cost and shut down cost of generation units: The start-up cost of a de-committed unit ($Cost^{STU}$) and shut-down cost of a committed unit ($Cost^{SHD}$) at every hour of the operation period are presented in equations (4.19)-(4.20), respectively. In other words, starting a generation unit up or shutting a generation unit down is not free and imposes costs about C^{STU} and C^{SHD}, repsectively. Herein, x^G indicates the status of generation unit, where "1" and "0" mean "on" and "off", respectively.

$$Cost_{g,t}^{STU} = C_g^{STU} \times \left(1 - x_{g,t-1}^G\right) \times x_{g,t}^G \quad (4.19)$$

$$Cost_{g,t}^{SHD} = C_g^{SHD} \times x_{g,t-1}^G \times \left(1 - x_{g,t}^G\right) \quad (4.20)$$

4.2.1.3 Constraints of System in Operation Problem

In the following, the system and generation units' constraints are presented and explained.

System power balance constraint: The power-demand balance constraint of the system that must be held in every time step of the operation period is presented in equation (4.21).

$$\sum_{g=1}^{Ng} P_{g,t} \times x_{g,t}^G = D_t^{PASS} + D_t^{SHs} \quad (4.21)$$

System minimum generation constraint: The constraint of minimum power of the system generated by the "on" units for every hour of the operation period is presented in equation (4.22). In other words, the units, which are "on", must be able to supply the minimum demand level of the system.

$$\sum_{g=1}^{Ng} P_g^{min} \times x_{g,t}^G \leq D_t^{PASS} + D_t^{SHs} \tag{4.22}$$

System maximum generation constraint considering spinning reserve: The maximum generation of the power system considering spinning reserve level (SR) provided by the "on" units for every hour of the operation period is presented in equation (4.23). In other words, the units, which are "on", must be able to supply the maximum demand level of the system considering the required spinning reserve of the system.

$$\sum_{g=1}^{Ng} P_g^{max} \times x_{g,t}^G \geq D_t^{PASS} + D_t^{SHs} + SR_t \tag{4.23}$$

Generation units' power constraint: The maximum and minimum power constraints of every generation unit at every hour of the operation period is presented in equation (4.24). In other words, the generation unit cannot generate power beyond the upper and lower limits.

$$P_g^{min} \leq P_{g,t} \leq P_g^{max} \tag{4.24}$$

Generation units' ramp-up rate and ramp-down rate constraints: The ramp-up rate (RUR) and ramp-down rate (RDR) constraints of every generation unit at every hour of the operation period are presented in equations (4.25)-(4.26), respectively. In other

words, the generation unit is able to increase and decrease its generation level about the definite rates.

$$\left(P_{g,t+1} - P_{g,t}\right) \leq RUR_g \tag{4.25}$$

$$\left(P_{g,t} - P_{g,t+1}\right) \leq RDR_g \tag{4.26}$$

Generation units' minimum "off time" and minimum "on time" constraints: The minimum "off time" (MDT) and minimum "on time" (MUT) constraints of every generation unit at every hour of the operation period are presented in equations (4.27)-(4.28), respectively. In other words, the generation unit cannot be turned on sooner than the minimum off time interval after it has been turned off ($OFFT$). Also, the generation unit cannot be turned off sooner than the minimum on time duration after it has been turned on (ONT).

$$OFFT_{g,t} \geq MDT_g \tag{4.27}$$

$$ONT_{g,t} \geq MUT_g \tag{4.28}$$

4.2.2 Mathematical Formulation for Energy Scheduling of a SH

4.2.2.1 Objective Function of a SH

As can be seen in equation (4.29), the objective function (OF) of a SH is minimizing operation cost terms in every scenario ($s \in S$) weighted by the corresponding occurrence probability (Ω^{PV}) over the optimization time horizon (next two hours). In other words, the optimization problem is solved for every scenario of power (solar irradiance) of PV panels (presented in equation (4.12) and Figure 4.3) and then the value

of cost terms are multiplied with the value of probability of scenario. The cost terms include fuel cost of DG (C^{F_DG}), emission cost of DG (C^{E_DG}), start up cost of DG (C^{STU_DG}), shut down cost of DG (C^{SHD_DG}), switching cost of battery (C^{SW_B}), and the value of income or cost due to electricity transaction with GENCO ($P^{Grid} \times \acute{\pi}$).

$$OF = min\left\{\sum_{s\in S} \Omega_{t,s}^{PV} \times \sum_{t=1}^{n_\tau} \left\{\begin{matrix} \left[C_{t,s}^{F\_DG}\right] + \left[C_{t,s}^{E\_DG}\right] \\ +\left[\left(1 - x_{t-1,s}^{DG}\right) \times x_{t,s}^{DG} \times C^{STU\_DG}\right] \\ +\left[x_{t-1,s}^{DG} \times \left(1 - x_{t,s}^{DG}\right) \times C^{SHD\_DG}\right] \\ +\left[\acute{x}_{t,s}^{B} \times C^{SW\_B}\right] + \left[P_{t,s}^{Grid} \times \acute{\pi}_{t,s}\right] \end{matrix}\right\}\right\} \quad (4.29)$$

The mathematical definition of $\acute{x}_{t,s}^{B}$, $\acute{\pi}_{t,s}$, $C_{t,s}^{F\_DG}$, $C_{t,s}^{E\_DG}$, and C^{SW_B} have been presented in (2.12)-(2.17), respectively. In addition, the constraints of problem including supply-demand balance, power limits of the DG, minimum up/down time limits of the DG, power limits of the battery, depth of discharge (DOD), and state of charge (SOC) limits of the battery have been presented in (2.18)-(2.24), respectively.

4.3 Simulation and Results for Price-Controlled Energy Management of Smart Homes

All the simulations are conducted in the MATLAB environment using the Intel Xeon Sever with 64 GB RAM. The number of chromosomes in the population (n_c) and the value of mutation probability of the genes (θ^{Mut}) in the applied GA are considered about 100 and 10%, respectively.

4.3.1 Energy Scheduling Problem of the SHs

4.3.1.1 Characteristics of the SHs

Figure 4.5 illustrates the structure of a SH that includes PV panels installed on the roof of SH, an energy storage like a battery, DG, and access to the electrical distribution

grid. The technical data of 3 types of SHs are presented in Table 4.1. The value of penalty for carbon emissions (β^E) in Table 4.1 is based on the introduced value by California Air Resources Board auction of greenhouse gas emissions [76]. Also, Cap^B indicates the value of capacity of the battery.

Figure 4.6 shows given demand level of SHs (type 1-3). Moreover, the forecasted power pattern for the PV panels of the SHs (type 1-3) at every five-minute step of the operation period (one day) are shown in Figures 4.7-4.9, respectively. As can be seen, the amount of generated power of PV panels is zero in some period of time due to nightfall.

The mean value of prediction errors (μ^{Er}) related to the solar irradiances is considered about 10%. In addition, Figure 4.10 illustrates the initial electricity price (i.e., 10% more than marginal cost as the defined value of profit for the GENCO) proposed by the GENCO at every time step (five minutes) of the operation period (before energy management). Considering the demand level of passive end users presented in Figure 4.11, the marginal cost of system are determined by solving the generation scheduling and UC problems of GENCO before energy management of SHs. In fact, the updated electricity price (due to implementing energy management) is determined based on the initial electricity price (presented in Figure 4.10) and equation (4.1).

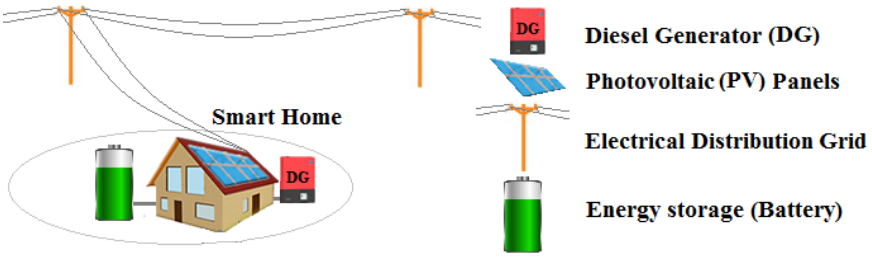

Figure 4.5: The structure a SH that includes different energy resources.

Table 4.1: The technical data of SHs with different types of sources.

-	Parameter	Unit	Type 1	Type 2	Type 3
DG	z_1^F	¢/kWh^2	0.324	0.491	0.843
	z_2^F	¢/kWh	41.66	40.85	46.04
	z_3^F	¢	0	0	0
	z_1^E	kg/kWh^2	0.07	0.08	0.09
	z_2^E	kg/kWh	1.39	1.61	1.94
	z_3^E	kg	0	0	0
	$\underline{P^{DG}}$	kW	15	10	5
	$\overline{P^{DG}}$	kW	40	30	20
	MUT^{DG}	Minute	10	10	10
	MDT^{DG}	Minute	10	10	10
	C^{STU_DG}	$	1	1	1
	C^{SHD_DG}	$	1	1	1
	β^E	¢/kg	1		
Battery	$\overline{P^B}$	kWh	10		
	Cap^B	kWh	200		
	DOD^B	%	20		
	Pr^B	$	20,000		
	ξ^B	Ah	100,000		
PV panels	$\overline{P^{PV}}$	kW	10		
Access to grid	P^{Grid}	kW	Yes		
	φ	-	0.8		
Number of SHs			5000	5000	5000

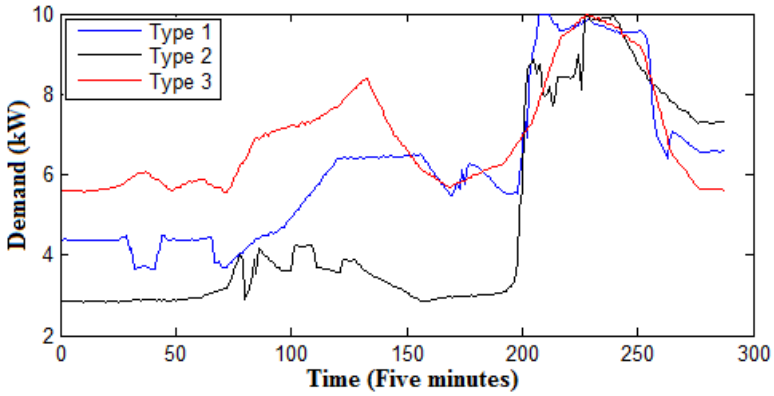

Figure 4.6: Demand level (kW) of SHs with type 1-3 at every five-minute step of the operation period (one day).

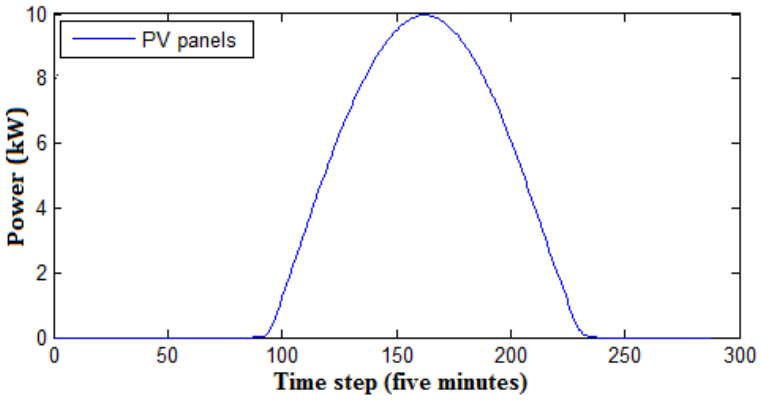

Figure 4.7: The forecasted power pattern for the PV panels (type 1) in a purely sunny day at every five-minute step of the operation period (one day).

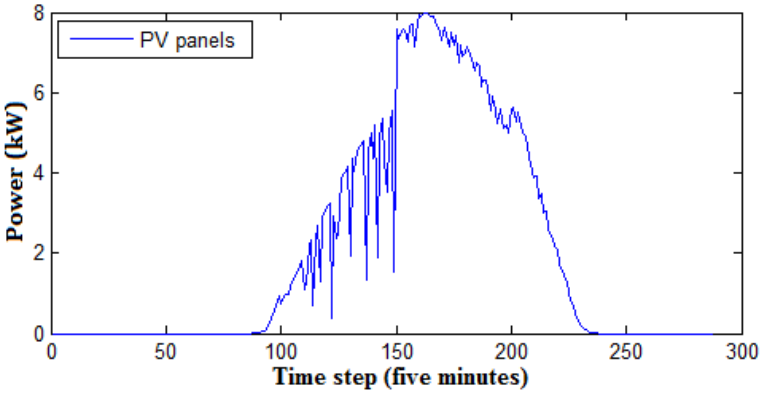

Figure 4.8: The forecasted power pattern for the PV panels (type 2) in a cloudy day at every five-minute step of the operation period (one day).

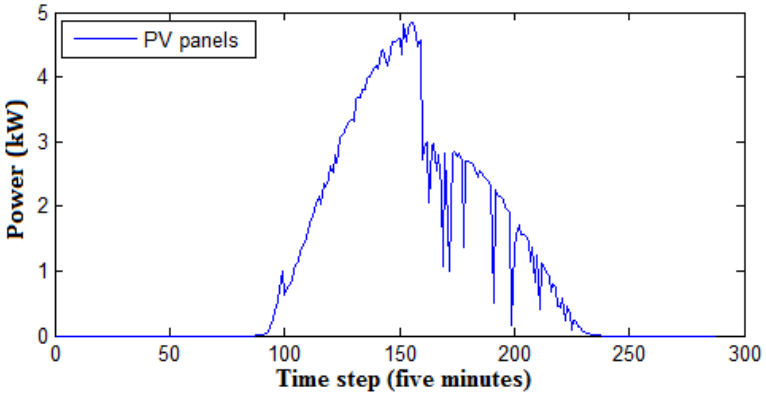

Figure 4.9: The forecasted power pattern for the PV panels (type 3) in a cloudy day at every five-minute step of the operation period (one day).

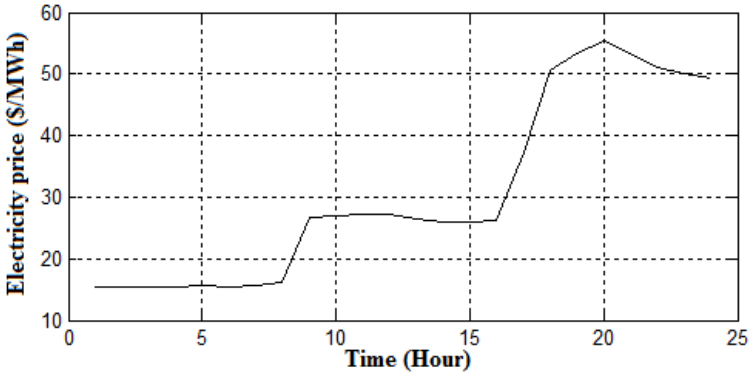

Figure 4.10: Initial electricity price proposed by the GENCO at every hour of the operation period (one day), before energy management.

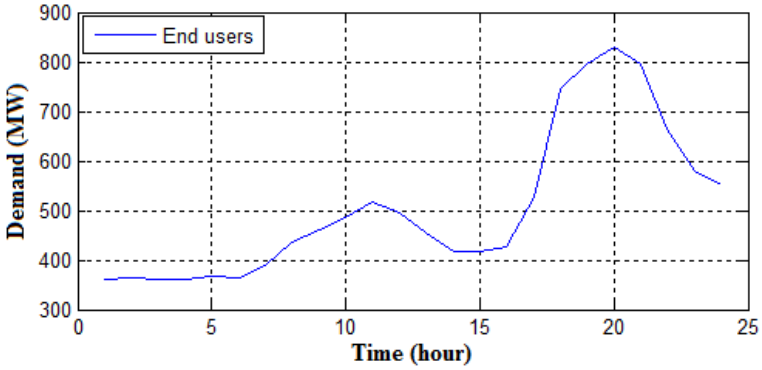

Figure 4.11: Hourly demand level of end users (MW).

4.3.1.2 Results

Table 4.2 presents the daily operation cost of SHs before price-controlled energy management. In addition, Figures 4.12 and 4.13 illustrate the optimal schedule of energy sources before energy management of SHs for SH (type 1) and SH (type 3), respectively. As can be seen, the DGs are started up and shut down and batteries are switched into charging/discharging modes throughout the operation period; however, the DG of SH (type 1) is applied more than the DG of SH (type 2), since the DG of SH 1 generates electricity in lower cost. Also, as can be seen in Table 4.2, the SH (type 1) and the SH (type 3) has the least and the most daily operation costs, respectively. The optimal

schedule of energy resources of SHs after optimal energy management scheme will be shown in Figures 4.16 and 4.17.

Table 4.2: Daily operation cost ($) of SHs before energy management.

	SH (Type 1)	SH (Type 2)	SH (Type 3)
Operation cost ($/day)	17.07	14.23	29.11

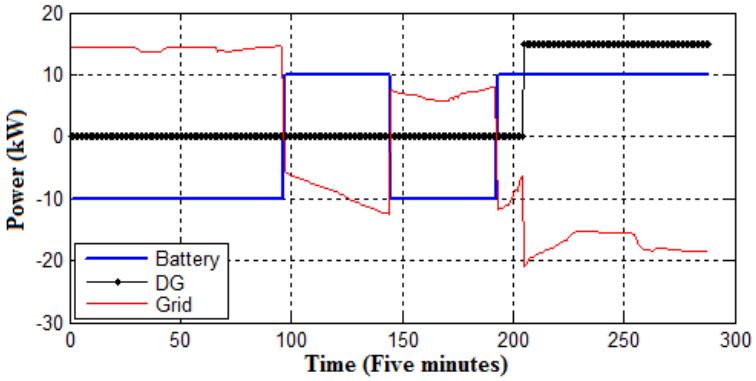

Figure 4.12: Demand level and the optimally scheduled power of DG and battery at every five-minute step of the operation period (one day) for a SH with type 1 (before EM).

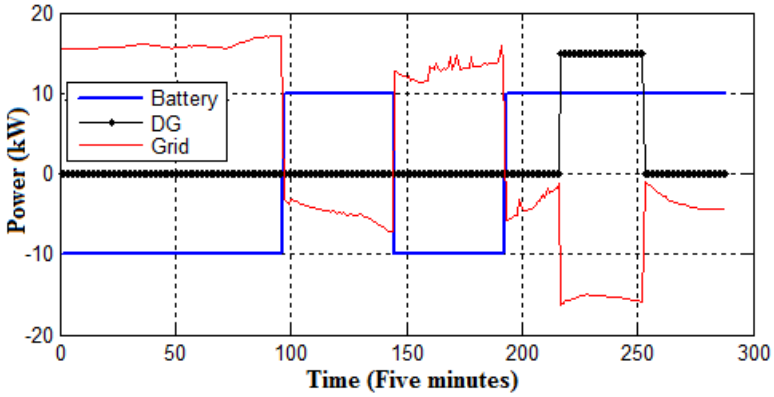

Figure 4.13: Demand level and the optimally scheduled power of DG and battery at every five-minute step of the operation period (one day) for a SH with type 3 (before EM).

4.3.2 Generation Scheduling and UC Problems of the GENCO

4.3.2.1 Characteristics of the Generation System

The technical characteristics of generation units including the fuel cost coefficient of generation units, the emission coefficient of generation units, the power limits of units, the minimum up/down time of units, the ramp up rate and ramp down rate of units, the start-up cost and shut down cost of units, and the initial status of units are presented in Table 4.3. Positive and negative numbers for the status of units mean "on" and "off", respectively.

Moreover, the minimum value of spinning reserve at every hour of a day is assumed to be 10% of demand at the same hour. Furthermore, the value of penalty for greenhouse gas emissions is assumed about $10 per ton based on the California Air Resources Board auction of greenhouse gas emissions [76]. The number of chromosomes of GA (for indicating the status of generation units over the operation period) in the population (n_c) and the value of mutation probability of genes (θ^{Mut}) are considered to be 100 and 10%, respectively.

4.3.2.2 Results

4.3.2.2.1 Without Energy Management

Table 4.4 presents the generation level of units at every hour of the operation period (one day) before energy management. As can be seen, generators G1-G5 as the least expensive generation units are operated all the day, while G6 as the most expensive and pollutant generation unit is utilized just in a short period of time. In this condition, the daily profit of GENCO is determined about $6,684.

Table 4.3: Technical characteristics of the generation units.

Generation unit	G1	G2	G3	G4	G5	G6
α_1^F (\$/MWh^2)	0.00048	0.00031	0.00200	0.00211	0.00398	0.00712
α_2^F (\$/MWh)	16.19	17.26	16.60	16.50	19.70	22.26
α_3^F (\$)	1000	970	700	680	450	370
α_1^E (Ton/MWh^2)	0.0005	0.0005	0.0005	0.0005	0.0010	0.0020
α_2^E (Ton/MWh)	0.4050	0.4320	0.4150	0.4120	0.4930	0.5560
α_3^E (Ton)	0.3000	0.4250	0.4500	0.7000	0.7250	0.9250
P^{min} (MW)	75	75	15	15	15	10
P^{max} (MW)	200	200	120	100	100	80
MUT (h)	5	5	5	5	5	3
MDT (h)	-5	-5	-5	-5	-5	-3
RUR (MW/h)	125	125	120	75	50	10
RDR (MW/h)	125	125	120	75	50	10
C^{STU} (\$)	4500	5000	550	560	900	170
C^{SHD} (\$)	4500	5000	550	560	900	170
Initial status	+24	+24	+24	+24	+24	-7

Table 4.4: The generation level of units (MW) before energy management.

Hour	G1	G2	G3	G4	G5	G6
1	200	143	120	100	15	0
2	200	144	120	100	15	0
3	200	143	120	100	15	0
4	200	142	120	100	15	0
5	200	150	120	100	15	0
6	200	145	120	100	15	0
7	200	176	120	100	15	0
8	200	200	120	100	33	10
9	158	75	51	69	15	10
10	160	75	52	70	15	10
11	169	75	59	77	15	0
12	152	75	46	64	15	0
13	200	150	120	100	15	0
14	200	104	120	100	15	0
15	200	112	120	100	15	0
16	200	132	120	100	15	0
17	172	75	62	79	15	0
18	200	101	120	100	15	0
19	200	110	120	100	15	0
20	200	169	120	100	15	0
21	200	126	120	100	15	0
22	200	75	94	100	15	0

23	164	75	56	73	15	0
24	200	103	15	15	15	0

4.3.2.2.2 With Optimal Energy Management

After optimal price-controlled energy management of responsive end users (SHs), it is realized that the optimal scheme of energy management is considering -3 $/MWh for the value of ρ^{EM}, as can be seen in Figure 4.14. In other words, the electricity prices should be decreased at peak period instead of being increased. In this condition (implementation of optimal scheme of price-controlled energy management), the daily profit of GENCO is calculated about $14,243/day, which has 113% increase compared to before energy management. In fact, although the electricity is sold at the lower prices at peak period, the overall profit of GENCO is increased due to selling more electrical energy to the active end users (SHs).

The generation level of units at every hour of the operation period after optimal energy management scheme ($\rho^{EM} = -3$ $/MWh) are presented in Table 4.5. As can be seen, the generation level of all the units are increased and even the most expensive and pollutant unit (G6) is started up and applied in some hours of the peak period. The reason is related to decreasing the utilization of DGs of SHs (as can be seen in Figure 4.15) and increasing electricity purchase from the GENCO due lower price proposed by the GENCO. The demand level of passive end users (with constant demand pattern) and active end users (SHs) before and after optimal energy management, and also the total demand of system before and after optimal energy management at every hour of the operation period (one day) are shown in Figure 4.15. The demand of SHs and the total

demand of system before and after energy management are overlapped between hours 1-17. By looking at Figures 4.16 and 4.17, it is realized that SH (type 1) decreases the utilization of its DG and SH (type 3) shuts down its DG in the whole operation period.

Table 4.6 presents the daily operation cost ($) of SHs with different types and daily profit of GENCO ($) before and after optimal energy management. As can be seen, the daily operation costs of all types of SHs are decreased and daily profit of GENCO is increased after optimal scheme of energy management. In other words, the social welfare of the complex system (consisting of GENCO and SHs) is increased after optimal energy management scheme.

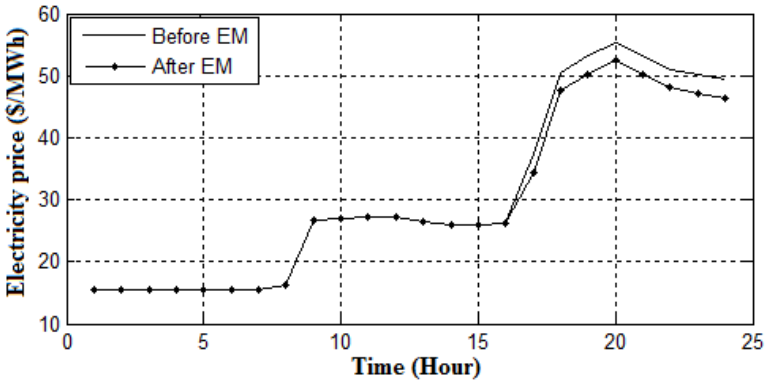

Figure 4.14: Electricity price proposed by the GENCO before and after optimal energy management at every hour of the operation period (one day).

Table 4.5: The generation level of units (MW) after optimal energy management.

Hour	G1	G2	G3	G4	G5	G6
1	200	143	120	100	15	0
2	200	144	120	100	15	0
3	200	143	120	100	15	0
4	200	142	120	100	15	0
5	200	150	120	100	15	0
6	200	145	120	100	15	0
7	200	176	120	100	15	0
8	200	200	120	100	33	10

9	158	75	51	69	15	10
10	160	75	52	70	15	10
11	169	75	59	77	15	0
12	152	75	46	64	15	0
13	200	150	120	100	15	0
14	200	104	120	100	15	0
15	200	112	120	100	15	0
16	200	132	120	100	15	0
17	172	75	62	79	15	0
18	200	200	120	100	56	10
19	200	175	120	100	15	10
20	200	200	120	100	49	10
21	200	200	120	100	16	0
22	200	199	120	100	15	0
23	200	98	120	100	15	0
24	200	184	15	85	15	0

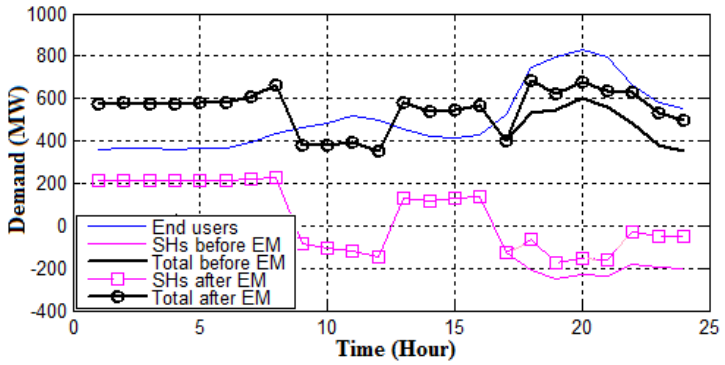

Figure 4.15: Demand of passive end users, demand of active end users (SHs) before and after optimal energy management, and total demand of system before and after optimal energy management in MW at every hour of the operation period (one day).

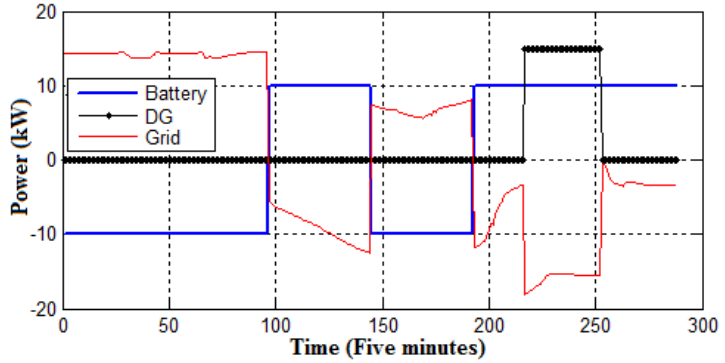

Figure 4.16: Demand level and the optimally scheduled power of DG and battery at every five-minute step of the operation period (one day) for a SH with type 1 (after optimal EM).

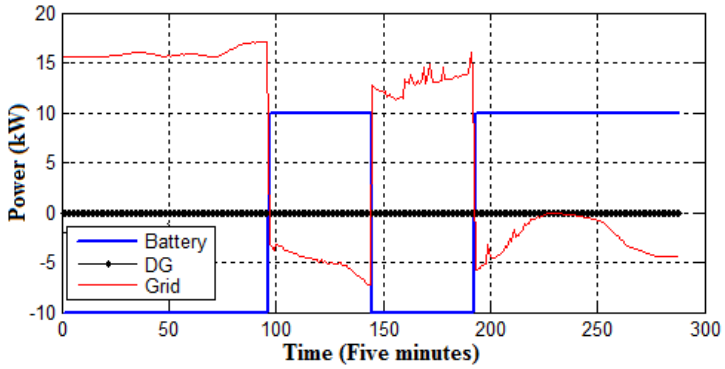

Figure 4.17: Demand level and the optimally scheduled power of DG and battery at every five-minute step of the operation period (one day) for a SH with type 3 (after optimal EM).

Table 4.6: The daily operation cost ($) of SHs with different types and daily profit of GENCO ($) before and after optimal energy management.

	Before EM	After optimal EM
Operation cost of SH (Type 1) in $/day	17.07	14.53
Operation cost of SH (Type 2) in $/day	14.23	12.17
Operation cost of SH (Type 3) in $/day	29.11	23.31
Operation profit of GENCO in $/day	6684	14243

The sensitivity plot of daily profit of GENCO with respect to the value of ρ^{EM} ($/MWh) is shown in Figure 4.18. As can be seen, -3 $/MWh is the optimal value for ρ^{EM}. In other words, the electricity should be sold to the customers in a less price at peak period based on equation (4.1). As can be seen, the curve is a nonlinear function of ρ^{EM}. In other words, the relation between the daily profit of GENCO and the price-controlled energy management scheme is not direct and determining the optimal scheme is not possible without investigating it. Therefore, the optimal value of ρ^{EM} must be probed, since a predetermined scheme of energy management is not efficient and a random

energy management scheme might bring about detriment for the GENCO, as can be seen in Figure 4.8 for $\rho^{EM} \leq -7$ and $\rho^{EM} \geq 8$.

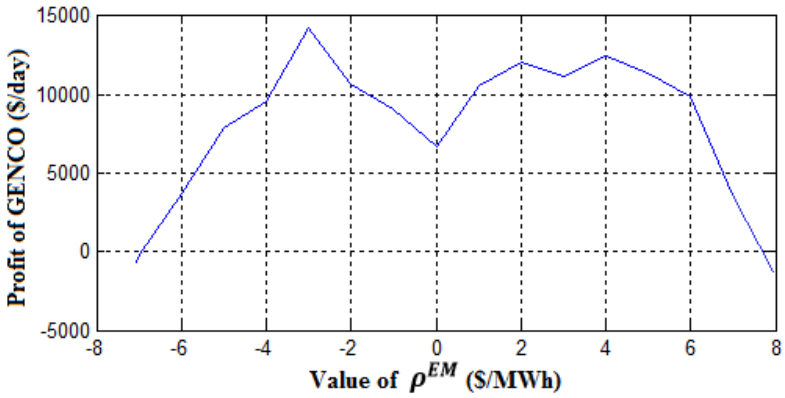

Figure 4.18: Value of profit of the GENCO with respect to value of ρ^{EM} ($/MWh).

4.4 Conclusion of Problem II

In this study, price-controlled energy management of responsive customers (SHs) was investigated in the generation scheduling and UC problems of a GENCO to maximize the daily profit of GENCO. Due to electricity price changes, each SH reacted and re-scheduled its own energy resources to minimize its daily operation cost applying a scenario-based stochastic optimization approach. In addition, the generation scheduling and UC problems of GENCO were solved using Lambda-Iteration Economic Dispatch and GA, respectively.

The simulation results demonstrated that optimal price-controlled energy management of the responsive end users (SHs) in the generation scheduling and UC problem is noticeably advantageous for the GENCO and even for the SHs, since it can increase the profit of GENCO and decrease the operation cost of every type of SH.

In order to maximize the daily profit of GENCO, it was proven that the value of profit is a nonlinear function of ρ^{EM} (variable of energy management scheme). In other words, the relation between the daily profit of GENCO and the price-controlled energy management scheme is not predictable, thus a default scheme of energy management will not lead to the favorable results and the optimal scheme must be investigated.

It was intriguing to find out that in order to maximize the daily profit of GENCO, the electricity price at peak period must be decreased to motivate the SHs to purchase more electrical energy from the GENCO. In fact, although the electricity is sold in a lower price at peak period, the overall profit of GENCO is increased due to selling more electrical energy to the SHs.

As the extended and future work of this study, it is recommended to model the reaction of other types of end users (in addition to SHs) based on the price elasticity of demand and their social welfare.

CHAPTER FIVE

PROBLEM III: TRAFFIC AND GRID-BASED PARKING LOT ALLOCATION AND CHARGING MANAGEMENT OF PEVS

5.1 Proposed Technique for Traffic and Grid-Based Parking Lot Allocation and Charging Management of PEVs

5.1.1 Modeling Driving Patterns of the plug-in electric vehicles (PEVs) Fleet

Figure 5.1 illustrates a synthetic power system that includes a generation company (GENCO), some transmission feeders (TFs), distribution companies (DISCOs), and distribution feeders (DFs). Herein, the GENCO includes 10 generation units, every TF supplies two DISCOs, and each DISCO has two DFs. DF 1 has 28 distribution buses (substations) and each of them has real latitude and longitude with real geographic data of Washington D.C., U.S.

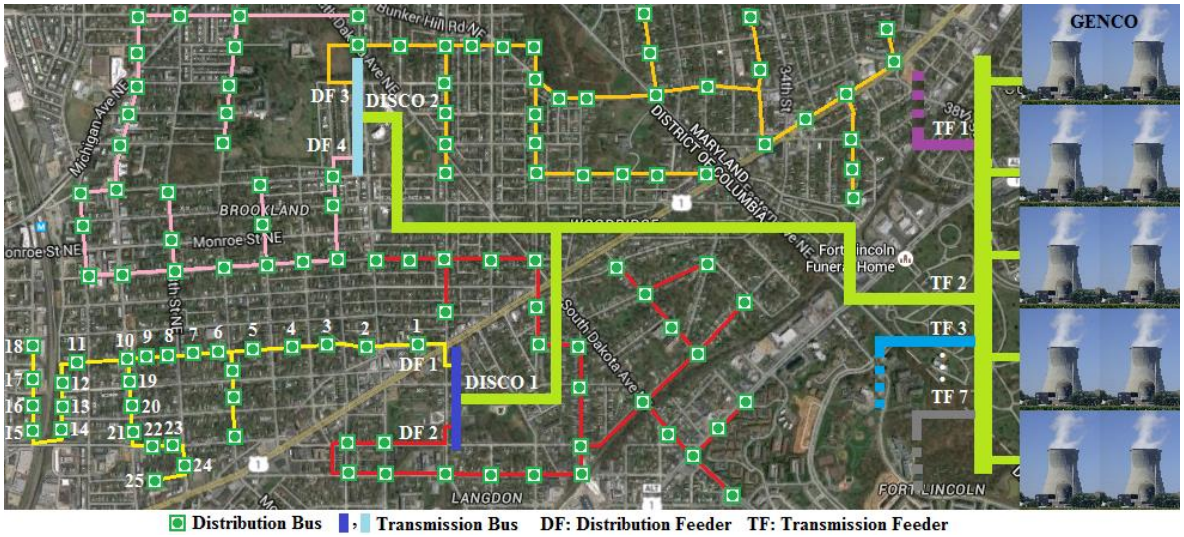

Figure 5.1: The power system under study that includes a GENCO (with 10 generation units), some transmission feeders (TFs), DISCOs, and distribution feeders (DFs). Every

TF supplies two DISCOs, every DISCO has two DFs, and every DF has several distribution buses.

In order to determine the daily driving pattern (i.e., route) of a PEV, the hourly position data (latitude and longitude) of the PEV can be specified using global positioning system (GPS). Herein, in order to simulate the problem, the hourly position and speed of vehicles are randomly generated by the computer considering the real geographic borders of each DF (based on the real latitude and longitude of points in Washington D.C. using Google Map) and the minimum and maximum traffic velocity limits in the residential area in Washington D.C. (32-80 km/h [78]). The defined area for each DF covers a square zone based on the nearest and farthest buses of the feeder.

Figure 5.2 illustrates the hourly position of six PEVs (as the six driving patterns) around the buses of DF 1, which is randomly generated by the computer considering the geographic borders of feeder and the minimum and maximum velocity limits of vehicles in the residential area in Washington D.C. In this study, every PEV is considered as the representative of 100 PEVs. In other words, 600 PEVs are moving around DF 1.

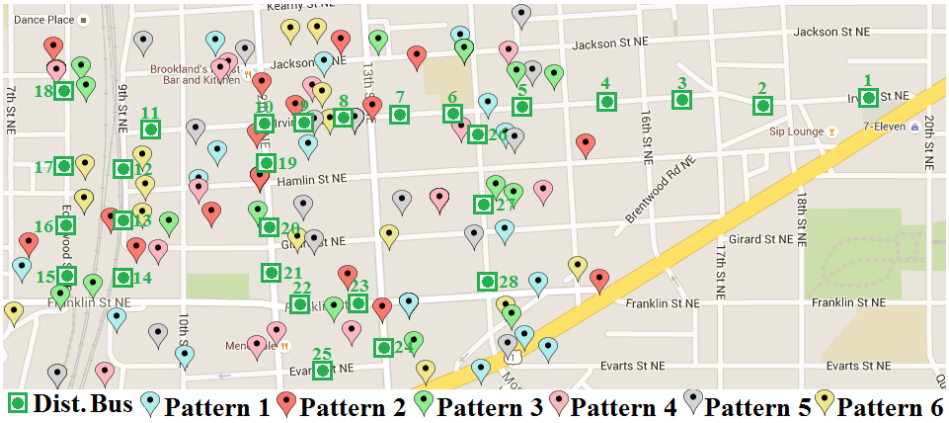

Figure 5.2: The hourly position data (longitude and latitude) of PEVs fleet (Patterns 1-6) around DF 1.

Figure 5.3 shows the hourly space-time driving patterns of the PEVs around DF 1 (Patterns 1-6) in a day. As can be seen, at some hours the day (hours 1-7 and 23-24), the PEVs do not move in the space as time goes on, since the PEVs have been parked. Moreover, every driving pattern has different average daily distance from each bus of electrical distribution system. In other words, two PEVs from different driving patterns will not have identical reaction to the value of incentive due to their different average daily distances from a candidate parking lot.

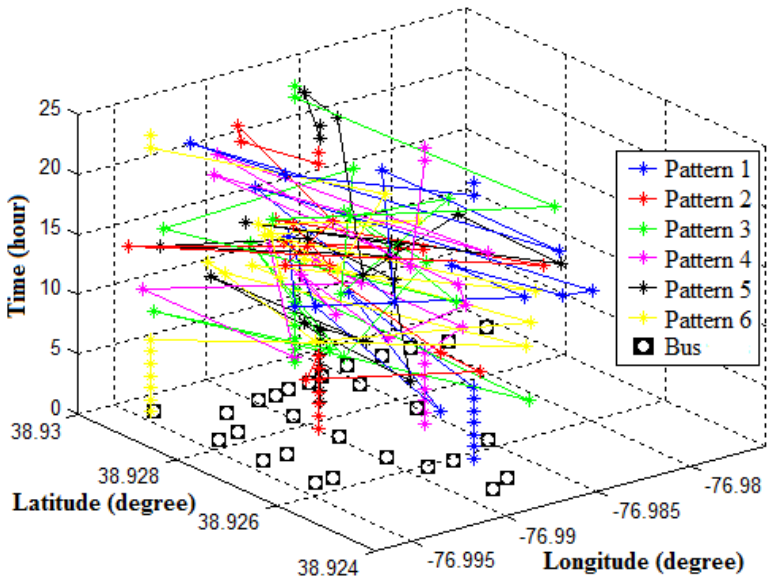

Figure 5.3: The hourly space-time driving patterns of the PEVs fleet around DF 1 (Patterns 1-6) in a day.

Using the above mentioned approach for other feeders of the power system, the total number of vehicles in the whole territory of power system is calculated about 16,800 because:

$$6(\text{Driving patterns}) \times 100(\text{Number of PEVs per driving pattern})$$
$$\times 4(\text{Number of DFs of a TF}) \times 7(\text{Number of TFs in system}) = 16{,}800$$

Now, by knowing the driving pattern of the e^{th} PEV, the amount of average daily distance of the PEV from the b^{th} bus of the feeder ($\overline{\beta_{e,b}}$) can be calculated using the hourly position data (at every t) of the PEV ($x_{e,t}^{PEV}, y_{e,t}^{PEV}$) and the bus ($x_b^B, y_b^B$), as can be seen in equation (5.1). Every bus of the feeder ($\forall b \in \{1, \dots, Nb\}$) is considered as a candidate for installing a parking lot. The value of $\overline{\beta_{e,b}}$ (along with the value of incentive) will be applied for determining the percentage of drivers that charge their PEVs through the parking lot (ξ) installed in the b^{th} bus of the feeder. Smaller value of $\overline{\beta_{e,b}}$ will result in higher value of ξ, since drivers normally prefer to park in a nearby parking lot.

$$\overline{\beta_{e,b}} = \frac{1}{24} \times \sum_{t=1}^{24} \sqrt{\left(x_{e,t}^{PEV} - x_b^B\right)^2 + \left(y_{e,t}^{PEV} - y_b^B\right)^2},$$
$$\forall e \in \{1, \dots, N_{Tot}^{PEVs}\}, \forall b \in \{1, \dots, Nb\} \quad (5.1)$$

Herein, N_{Tot}^{PEVs} (600 PEVS) is the total number of PEVs existing around the feeder and Nb is the total number of buses of the feeder.

By knowing the driving pattern of the PEV, the state of charge (SOC) of the PEV can be approximated, since the SOC of a PEV has a direct relation with the amount of distance that it travels in a day. The value of SOC of the PEV is used to determine the amount of power and energy demands of the installed parking lot in bus. The value of SOC of a PEV at every hour of a day (t) can be determined using equation (5.2). Herein, kWh_{km} is the amount of energy (kWh) that the PEV needs to travel about 1 km and C_e^{PEV} is the capacity of battery of PEV.

$$SOC_{e,t}^{PEV} = 100 \times \left(1 - kWh_{km} \times \sum_{t=1}^{t} \sqrt{\left(x_{e,t}^{PEV} - x_{e,t-1}^{PEV}\right)^2 + \left(y_{e,t}^{PEV} - y_{e,t-1}^{PEV}\right)^2} \times \frac{1}{C_e^{PEV}}\right),$$

$$\forall e \in \{1, \dots, N_{Tot}^{PEVs}\}, \forall t \in \{1, \dots, 24\} \quad (5.2)$$

5.1.2 Modeling Behavior of Drivers as a Function of Incentive and Distance

The percentage of drivers that charge their PEVs through the suggested parking lot as the function of discount on charging fee (γ in percent) for power function with exponent 0.3 and 3, logarithmic function, linear function, and exponential function are presented in Table 5.1 and Figure 5.4 [63]. As can be seen, almost all the surface of figure is covered with the presented functions. In other words, approximately all the possibilities for the reaction of drivers are considered for the reaction of the PEVs' drivers respect to the value of incentive. As can be seen, the drivers of PEVs do not charge their vehicles through the parking lot if there is no incentive, and also considering 100% discount on charging fee of the PEVs motivate all the drivers to charge their vehicle through the parking lot.

Table 5.1: The percentage of drivers that charge their PEVs through the parking lot as the mathematical functions of discount on charging fee (%) [63].

Mathematical model	Percentage of drivers that charge their PEVs through the parking lot
Power model	$\xi_{Pow} = 100 \times \left(\frac{\gamma}{100}\right)^n, n\epsilon\{0.3,3\}$
Linear model	$\xi_{Lin} = \gamma$
Logarithmic model	$\xi_{Log} = 100 \times ln\left(\frac{\gamma}{100} \times (exp(1) - 1) + 1\right)$
Exponential model	$\xi_{Exp} = 100 \times exp\left(M \times \left(\frac{\gamma}{100} - 1\right)\right), M \gg 1$

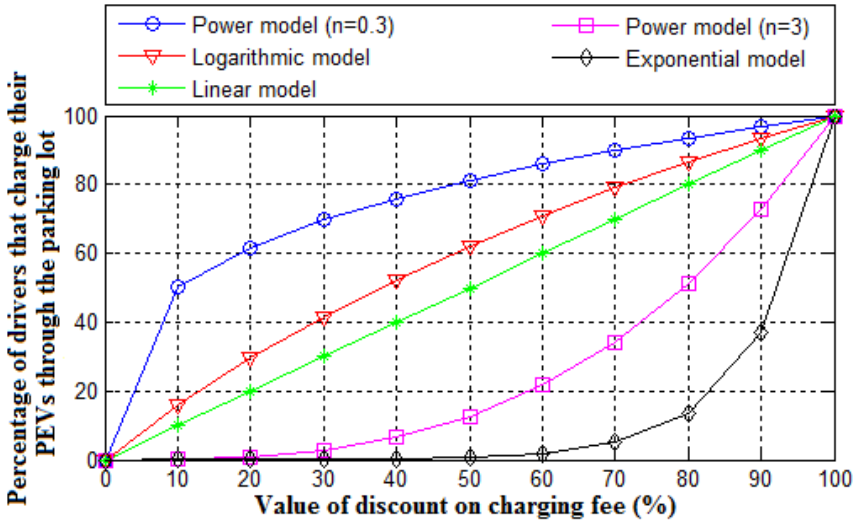

Figure 5.4: The percentage of drivers that charge their PEVs through the parking lot as the mathematical functions of discount on charging fee (%) [63].

In this study, the behavior of PEVs' drivers is modeled based on two parameters ($\overline{\beta}, \gamma$). In fact, in addition to the value of discount on charging fee (γ), the average daily driving distance of the PEVs from the location of parking lot ($\overline{\beta}$) is considered. Herein, a linear function is assumed between ξ (percentage of drivers that charge their PEVs through the parking lot) and $\overline{\beta}$, as can be seen in Table 5.2. The a_1 and a_2 are the constant values needed for modeling linear reaction of drivers with respect to their average daily distance form parking lot. Herein, considering linear reaction for the PEVs drivers with respect to their average daily distance from the parking lot seems to be the most logical modeling; however, other modeling can be studied in in the future work.

Table 5.2: The percentage of drivers that charge their PEVs through the parking lot as the mathematical functions of discount on charging fee (%) and distance from the parking lot (meter).

Mathematical model	Percentage of drivers that charge their PEVs through the parking lot
Power model	$\xi_{Pow} = \left(a_1 \times \overline{\beta} + a_2\right) \times 100 \times \left(\frac{\gamma}{100}\right)^n, n\epsilon\{0.3,3\}$
Linear model	$\xi_{Lin} = \left(a_1 \times \overline{\beta} + a_2\right) \times \gamma$
Logarithmic model	$\xi_{Log} = \left(a_1 \times \overline{\beta} + a_2\right) \times 100 \times ln\left(\frac{\gamma}{100} \times (exp(1) - 1) + 1\right)$
Exponential model	$\xi_{Exp} = \left(a_1 \times \overline{\beta} + a_2\right) \times 100 \times exp\left(M \times \left(\frac{\gamma}{100} - 1\right)\right), M \gg 1$

By considering these two parameters ($\overline{\beta}, \gamma$), the two-dimensional plots presented in Figure 5.4 are changed into three-dimensional spatial surfaces, as can be seen in Figures 5.5-5.6 (for $a_1 = -1/1200, a_2 = 1$). These figures illustrate the percentage of drivers that charge their PEVs through the parking lot. In all of these figures, the behavioral model of drivers (percentage of drivers that charge their PEVs through the parking lot) has linear relation with the amount of average daily distance of the drivers from the parking lot (meter), and Power relation (with exponent 0.3), Logarithmic relation, Linear relation, Power relation (with exponent 3), and Exponential relation with the value of discount on charging fee (%), respectively.

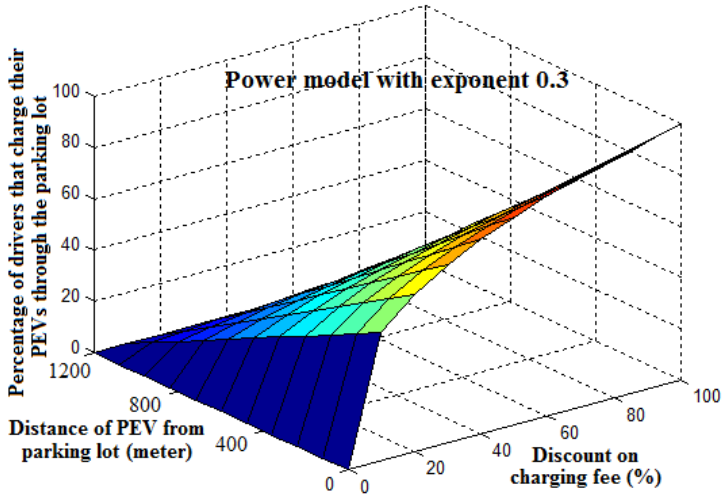

Figure 5.5: The percentage of drivers that charge their PEVs through the parking lot as Power function (exponent is 0.3) of discount on charging fee (%) and Linear function of average daily distance from the parking lot (meter).

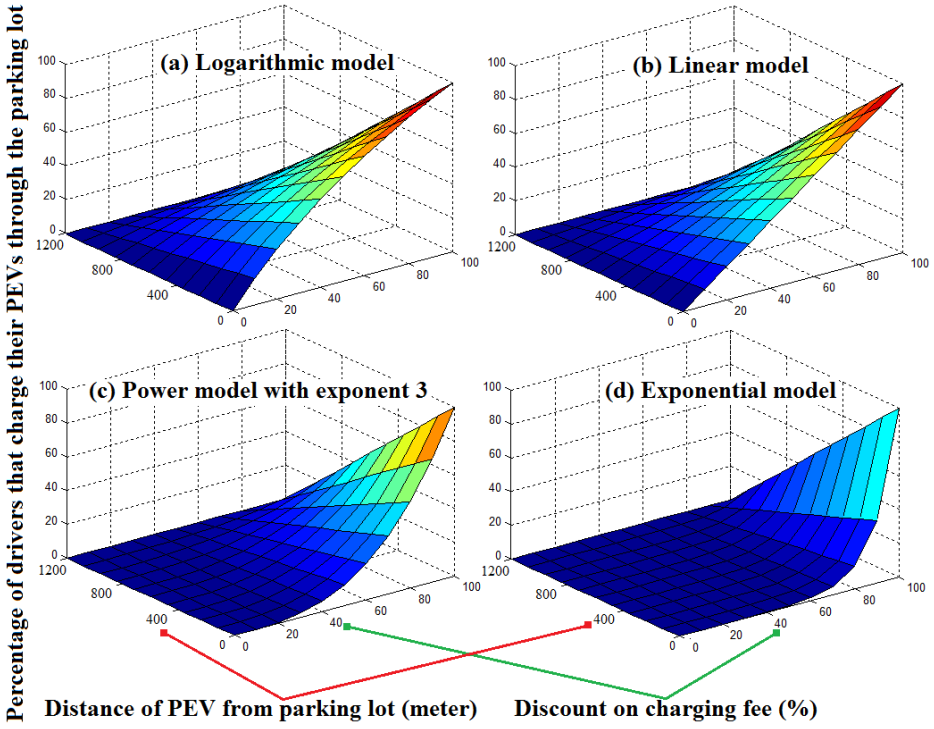

Figure 5.6: The percentage of drivers that charge their PEVs through the parking lot as (a) Logarithmic, (b) Linear (c), Power (with exponent 3), and (d) Exponential functions of discount on charging fee (%) and Linear function of average daily distance from the parking lot (meter).

The number of PEVs that charge their vehicles through the parking lot (N_{Model}^{PEVs}), as the size of the parking lot, is determined using equation (5.3) that depends on the value of incentive (γ), the average daily distance of PEVs from the location of parking lot ($\overline{\beta}$), and the total number of PEVs around the feeder (N_{Tot}^{PEVs}). Moreover, the hourly demand of parking lot (D_t^{PL}) in Mega Watt (MW) is approximated applying equation (5.4).

$$N_{Model}^{PEVs} = \xi_{Model} \times N_{Tot}^{PEVs} \tag{5.3}$$

$$D_t^{PL} = \sum_{e=1}^{N_{Model}^{PEVs}} \left(1 - \frac{SOC_{e,t}^{PEV}}{100}\right) \times \frac{C_e^{PEV}}{1000} \tag{5.4}$$

5.1.3 Optimization Technique

In this section, the optimization techniques for solving the planning problem of a DISCO (Section 5.1.3.1) and the operation problem of the GENCO (Section 5.1.3.2) are presented.

5.1.3.1 Optimization Technique for Solving the Planning problem of a DISCO

In this study, quantum computation concept is applied in the SA to design the quantum-inspired SA (QSA) algorithm and solve the optimization problem [79], which is a mixed-integer nonlinear programming (MINLP) problem. Other optimization algorithms could be used for this problem; however, quantum parallelism, as the superiority of the quantum computation, which originates from the uncertainty of quantum states, is the advantage compared to the other algorithms [80].

A classical bit can be either 0 or 1, while in quantum computation, a quantum bit (Q-bit) is a linear superposition of both states (0 and 1), which simultaneously lies in both states [81], as can be seen in equation (5.5). However, when a Q-bit is observed, it collapses to one determined state (0 or 1) with a certain probability. The superposition of the states is also presented in other forms such as $\alpha \begin{pmatrix} 1 \\ 0 \end{pmatrix} + \beta \begin{pmatrix} 0 \\ 1 \end{pmatrix}$ and $\alpha|\uparrow\rangle + \beta|\downarrow\rangle$.

$$|\psi\rangle = \alpha|0\rangle + \beta|1\rangle \tag{5.5}$$

Herein, $|0\rangle$ and $|1\rangle$ represent the state '0' and '1', respectively and α and β are generally complex numbers where $|\alpha|^2$ and $|\beta|^2$ represent the probability amplitudes that the Q-bit will be observed in the '0' state and '1' state, respectively with respect to equation (5.6). In this study, applying two dimensional quantum computation in the SA algorithm is enough, thus equation (5.6) can be simplified as $(\alpha)^2 + (\beta)^2 = 1$.

$$|\alpha|^2 + |\beta|^2 = 1 \tag{5.6}$$

The Q-bit matrix of the problem variables ($\mathbb{Q}$ matrix) includes the Q-bits related to the location of parking lots and the value of incentive (discount on charging fee for the PEVs), as can be seen in equation (5.7). Herein, the number of drivers that charge their PEVs through the parking lot and the demand of parking lot are determined based on the value of considered incentive and the average daily distance of PEVs from the parking lot using equations (5.3) and (5.4), respectively. As can be seen in equation (5.7), every bus of the feeder ($\forall b \in \{1, \dots, Nb\}$) is considered as a candidate for installing a parking lot. In other words, every bus of the feeder can have a parking lot. Therefore, the b^{th} bus has a parking lot with the probability amplitude about $(\beta_b^{PL})^2$ or this bus does not have a parking lot with the probability amplitude about $(\alpha_b^{PL})^2$, based on equation (5.6)

In addition, the value of incentive is changed from 0% (or 0) to 100% (or 10) with the 10% (or 1) steps. Thus, the minimum number of needed Q-bits for indicating the value of incentive is 4, since $2^3<10<2^4$. In other words, for indicating the numbers 0, 1, …, and 10 (proportional to 0%, 10%, …, and 100%), at least 4 binary variables are needed. It is noteworthy to mention that $(\alpha_1^{INC})^2$ and $(\beta_1^{INC})^2$ are the probability amplitudes that the binary variable is '0' and '1', respectively. Based on this, 0% discount and 100% discount can be indicated by the states $|0000\rangle$ and $|1010\rangle$ that have probability amplitude about $(\alpha_1^{INC})^2 \times (\alpha_2^{INC})^2 \times (\alpha_3^{INC})^2 \times (\alpha_4^{INC})^2$ and $(\beta_1^{INC})^2 \times (\alpha_2^{INC})^2 \times (\beta_3^{INC})^2 \times (\alpha_4^{INC})^2$, respectively.

$$\mathbb{Q} = \left[\begin{pmatrix}\alpha_1^{PL}\\ \beta_1^{PL}\end{pmatrix} \quad \cdots \quad \begin{pmatrix}\alpha_b^{PL}\\ \beta_b^{PL}\end{pmatrix} \quad \cdots \quad \begin{pmatrix}\alpha_{Nb}^{PL}\\ \beta_{Nb}^{PL}\end{pmatrix}\middle|\begin{pmatrix}\alpha_1^{INC}\\ \beta_1^{INC}\end{pmatrix} \quad \cdots \quad \begin{pmatrix}\alpha_4^{INC}\\ \beta_4^{INC}\end{pmatrix}\right] \qquad (5.7)$$

Herein, the value of objective function of problem is defined as the value of internal energy of the molten metal (ε) and then it is used to try to minimize the amount of this energy. Based on the concept of SA, in the cooling process of molten metal, the temperature of molten metal is gradually decreased to minimize the internal energy of molten metal [79].

In the following, different steps for applying QSA algorithm in the problem are presented and described.

- ***Step 1:*** *Obtaining the primary data*

Setting the controlling parameters of the QSA algorithm: These parameters include the initial temperature of the molten metal (θ_0), coefficient for gradually decreasing temperature of the molten metal (z), the total number of trials for producing

new solution at every temperature (Nk), and the parameters of the interim heating function (ω_1 and ω_2).

Obtaining the parameters of the grid and problem: The values of all the parameters of grid and problem are obtained. These parameters are presented in Tables 5.3-5.5 and Figures 5.9-5.10.

Initializing Q-bits: Initial value of the $\mathbb{Q}$ matrix is quantified as follows:

$$\alpha_{i,\theta,k}^{j} = \frac{\sqrt{2}}{2}, \beta_{i,\theta,k}^{j} = \frac{\sqrt{2}}{2}, \forall i \in \{1, \dots, Nb+4\}, \forall j \in \{PL, INC\} \quad (5.8)$$

As can be seen, equal values are considered for the initial values of Q-bits. In other words, a Q-bit has equal probability (50% due to $(\alpha_b^{PL})^2 = 0.5$ and $(\beta_b^{PL})^2 = 0.5$) for being observed in '0' state or '1' state in the initial stage. Herein, θ is the temperature of the molten, and k is the index of trial for generating new solution.

- ***Step 2:*** *Generating an acceptable solution*

Interim heating: Based on the quantum concept, observation means determining the exact value (0 or 1) of a Q-bit based on the probability of being 0 and 1. Since the observation method cannot generate a diverse solution (between 0 and 1) when the current Q-bits solution stays in the determined states, an interim heating process are applied to impose disturbance on the Q-bits before their observation [79]. The value of $\alpha_{i,\theta,k}^{j}$ and $\beta_{i,\theta,k}^{j}$ are updated based on equation (5.9) at every stage (k) of every temperature θ .

$$\begin{pmatrix} \alpha_{i,\theta,k}^{j} \\ \beta_{i,\theta,k}^{j} \end{pmatrix} = \begin{pmatrix} \sqrt{\left(\alpha_{i,\theta,k}^{j}\right)^2 + \mu_\theta \times \left(\frac{1}{2} - \left(\alpha_{i,\theta,k}^{j}\right)^2\right)} \\ \sqrt{\left(\beta_{i,\theta,k}^{j}\right)^2 + \mu_\theta \times \left(\frac{1}{2} - \left(\beta_{i,\theta,k}^{j}\right)^2\right)} \end{pmatrix},$$

$$\forall i \in \{1, \dots, Nb+4\}, \forall j \in \{PL, INC\} \tag{5.9}$$

Herein, a sigmoid heating function (μ_θ) is defined, which is presented in equation (5.10) [79]. Since the value of the sigmoid heating function is big (near to one) at high temperature (θ) and small (near to zero) at low temperature, $\alpha_{i,\theta,k}^{j}$ and $\beta_{i,\theta,k}^{j}$ change their values dramatically at the initial stages, but slightly in the final stages. Therefore, the observed Q-bits have small relationship with the current Q-bits state in initial stages and have great relationship in final stages. This characteristic of the heating process results in global searching in initial stages and local searching in final stages.

$$\mu_\theta = \frac{1}{1 + e^{-\omega_1 \times \left(\frac{\theta}{\theta_0} - \omega_2\right)}} \tag{5.10}$$

Observing the Q-bits: The Q-bits observation is done for every Q-bit separately by comparing the probability amplitude of being '0' state (or '1' state) with a random variable (denoted by r).

$$O_{i,\theta,k}^{j} = \begin{cases} 0 & \left(\alpha_{i,\theta,k}^{j}\right)^2 \geq r_{i,\theta,k}^{j} \\ 1 & \left(\alpha_{i,\theta,k}^{j}\right)^2 < r_{i,\theta,k}^{j} \end{cases}, \forall i \in \{1, \dots, Nb+4\}, \forall j \in \{PL, INC\} \tag{5.11}$$

Now, the value of every Q-bits is determined. In other words, the locations of parking lots and value of incentive are certain. Then, the number of drivers that charge their vehicles through the parking lots (N_{Model}^{PEVs}) can be determined using equation (5.3) and Table 5.2 and the value of demand of every parking lot can be calculated using equation (5.4).

Checking the problem constraints: All the constraints of the problem resented in Section 5.2.1.3 are checked and if they are satisfied, the algorithm goes on; otherwise, the process is repeated form ***Step 2.***

Updating the value of internal energy of molten metal: Herein, the value of internal energy of the molten metal related to the observed Q-bits ($\varepsilon_{\theta,k}^{O}$) is measured and the previous value of internal energy of the molten metal ($\varepsilon_{\theta,k-1}$) is updated.

$$\varepsilon_{\theta,k} = \begin{cases} \varepsilon_{\theta,k}^{O} & \varepsilon_{\theta,k}^{O} \leq \varepsilon_{\theta,k-1} \\ \Omega_{\theta,k} & \varepsilon_{\theta,k}^{O} > \varepsilon_{\theta,k-1} \end{cases} \tag{5.12}$$

Where, value of Ω_k is calculated using equation (5.13) [79].

$$\Omega_{\theta,k} = \varepsilon_{\theta,k-1} \times \left(\cos\left(f_{\theta,k}^{BOLTZ} \times \frac{\pi}{2}\right)\right)^2 + \varepsilon_{\theta,k}^{O} \times \left(\sin\left(f_{\theta,k}^{BOLTZ} \times \frac{\pi}{2}\right)\right)^2 \tag{5.13}$$

Also, $f_{\theta,k}^{BOLTZ}$, as the Boltzmann function, is given in equation (5.14).

$$f_{\theta,k}^{BOLTZ} = e^{\frac{\varepsilon_{\theta,k} - \varepsilon_{\theta,k}^{O}}{\theta_k}} \tag{5.14}$$

Updating the Q-bits: In SA algorithm, every bit has the same probability to be changed into '0' or '1' state, while in QSA algorithm, every Q-bit has a different probability of being observed in '0' or '1' state, thus every Q-bits has different activity level. Herein, the new Q-bits are generated using equation (5.15). Based on this, the current Q-bits rotates onto the observed Q-bits whenever $\varepsilon_{\theta,k}^{O} \leq \varepsilon_{\theta,k-1}$ and the current Q-bits rotates towards the observed Q-bits about $\Delta\varphi_{i,\theta,k}$ whenever $\varepsilon_{\theta,k}^{O} > \varepsilon_{\theta,k-1}$. Figure 5.7 graphically shows the Q-bits updating mechanism using the rotation gate ($Rot_{i,\theta,k}$).

$$\begin{pmatrix} \alpha_{i,\theta,k+1}^{j} \\ \beta_{i,\theta,k+1}^{j} \end{pmatrix} = \begin{cases} \begin{pmatrix} 1 - O_{i,\theta,k}^{j} \\ O_{i,\theta,k}^{j} \end{pmatrix} & \varepsilon_{\theta,k}^{O} \leq \varepsilon_{\theta,k-1} \\ Rot_{i,\theta,k} \times \begin{pmatrix} \acute{\alpha}_{i,\theta,k}^{j} \\ \acute{\beta}_{i,\theta,k}^{j} \end{pmatrix} & \varepsilon_{\theta,k}^{O} > \varepsilon_{\theta,k-1} \end{cases},$$

$$\forall i \in \{1, \dots, Nb + 4\}, \forall j \in \{PL, INC\} \tag{5.15}$$

Where,

$$Rot_{i,\theta,k}^{j} = \begin{pmatrix} \cos\left(\Delta\varphi_{i,\theta,k}^{j}\right) & -\sin\left(\Delta\varphi_{i,\theta,k}^{j}\right) \\ \sin\left(\Delta\varphi_{i,\theta,k}^{j}\right) & \cos\left(\Delta\varphi_{i,\theta,k}^{j}\right) \end{pmatrix} \tag{5.16}$$

$$\Delta\varphi_{i,\theta,k}^{j} = f_{\theta,k}^{BOLTZ} \times \left(\frac{\pi}{2} \times O_{i,\theta,k}^{j} - \varphi_{i,\theta,k}^{j}\right) \tag{5.17}$$

$$\varphi_{i,\theta,k}^{j} = \text{Arctan}\left(\frac{\beta_{i,\theta,k}^{j}}{\alpha_{i,\theta,k}^{j}}\right) \tag{5.18}$$

- ***Step 3:*** *Checking the number of iteration for the current temperature*

If the number of trials at current temperature (θ) is not equal to the predefined value (Nk), the process is repeated form ***Step 2***; otherwise, the temperature of the molten metal is decreased by the factor z, where $0 < z < 1$.

- ***Step 4:*** *Concluding*

Checking temperature of the molten metal: Temperature of the molten metal is measured and if the molten metal is frozen ($\theta \approx 0$), the optimization process is finished, otherwise, the process is repeated form ***Step 2***.

Introducing outcomes: The consequences include the optimal value of the $\mathbb{Q}$ matrix, as the optimal value of the problem variables including the optimal location of parking lots and the optimal value of incentive.

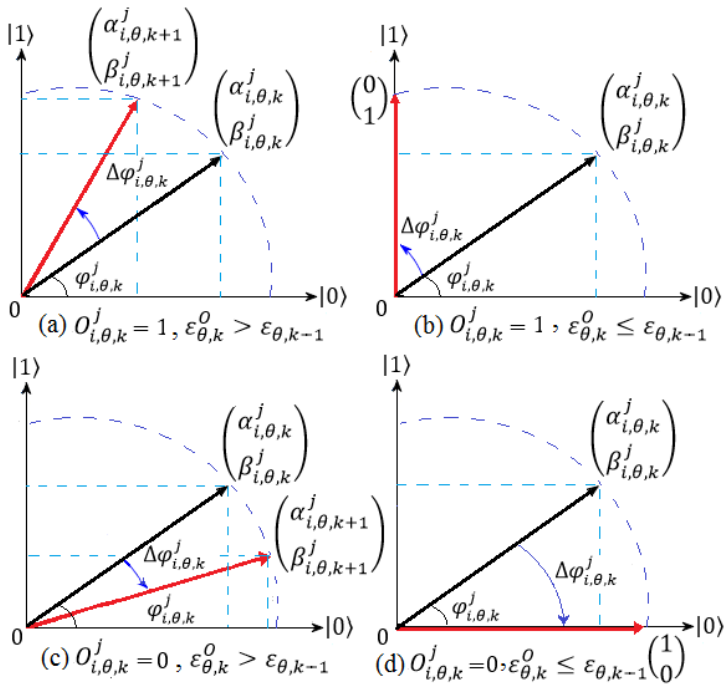

Figure 5.7: The updating scheme of Q-bits. (a): Rotating towards $|1\rangle$, (b): Rotating onto $|1\rangle$, (c): Rotating towards $|0\rangle$, (d): Rotating onto $|0\rangle$.

Algorithm I presents the pseudo code for finding the optimal locations of parking lots in a DF and the optimal value of incentive in the planning problem of a DISCO.

Algorithm I: The pseudo code for finding the optimal scheme of planning problem of a DISCO.

While (optimal solution is not achieved based on QSA criteria)

{

1. Generate Q-bits for the locations of parking lots and the value of incentive (γ).
2. Calculate $\overline{\beta}$ using equation (5.1).
3. Determine ξ_{Model} (percentage of drivers that charge their PEVs through the parking lot using Table 5.2).
4. Determine the number of drivers that charge their PEVs through the parking lots (N^{PEVs}_{Model}) and demand of each parking lot (D^{PL}_t) using equations (5.3) and (5.4), respectively.
5. Calculate the total cost of planning problem of DISCO using equation (5.21)

}

6: Introduce the optimal locations of parking lots in a DF and optimal value of γ based on the minimum cost of planning problem of DISCO.

5.1.3.2 Optimization Technique for Solving the Operation problem of a GENCO

Herein, GA is applied to solve the optimization problem of GENCO. The value of objective function (the total profit of GENCO over the operation period (one day)) is defined as the fitness of a chromosome, and then the GA tries to maximize the fitness of chromosomes. A chromosome (shown in Figure 5.8) represents the status of all the generation units at every hour of a day. This problem optimization is done for every possible value of incentive (credit which is equal to the percentage of charging fee of PEVs) with a 10% step increase, that is, 0%, 10%, …, 100%. Then, the optimal value of incentive is determined based on the maximum value of GENCO's profit over the operation period (one day). Algorithm II presents the pseudo code for finding the optimal scheme of charging management (optimal value of credit for drivers) of PEVs parked in the parking lots in the operation problem of GENCO.

Algorithm II: The pseudo code for finding the optimal scheme of charging management by the GENCO.

1: Set $\gamma = 0$. // *The value of credit which is equal to the percentage of charging fee.*

2: Solve the optimization problem to maximize the daily profit of GENCO.

Use GA to determine the status of generation units. *//Presented in Section 5.1.3.2.*

Use Lambda-Iteration method to determine generation level of units. *//Presented in Section 4.1.1.3.*

Calculate the daily profit of GENCO.

3: $\gamma = \gamma + 10$.

4: Determine the number of drivers that let the GENCO to decide about the charging time of their PEVs (parked in the parking lots allocated by the DISCOs) based on Table 5.2 and equation (5.3).

5: Go to Step 2, if $\gamma \leq 100$.

6: Determine the optimal value of γ based on the maximum daily profit of GENCO.

In the following, the steps for applying the GA in the optimization problem of GENCO are presented and described. The value of inputs and outputs of problem are mentioned in Step 1 and Step 5, respectively.

- *Step 1: Obtaining the primary data*

Parameters for applying GA: These parameters include the mutation probability of the genes (θ^{Mut}) and the size of the population (number of chromosomes) (n_c) as the number of the chromosomes.

Parameters of the system under study: The values of all the parameters of the system and problem are obtained. These parameters are presented in Table 5.9, and Figure 5.13. Also, the value of incentive (γ as value of credit which is equal to the percentage of charging fee) is chosen.

Updating participation percentage of PEVs' drivers: The participation percentage of drivers (and consequently the number of drivers) that let the GENCO to decide on the charging time of their PEVs through the installed parking lot are determined using Table 5.2 and equation (5.3). Then the revised demand of the system is identified.

Initial population: The chromosomes of population (Figure 5.8) are initialized with random binary values ("0" or "1").

- *Step 2: Updating the population*

Applying crossover operator: The crossover operator is applied on every two chromosomes to reproduce two new chromosomes as the offspring.

Applying mutation operator: The mutation is applied on every gene of every chromosome of the population with the definite probability θ^{Mut}.

- *Step 3: Selecting new population*

Evaluating fitness of every chromosome: For every chromosome, the optimal generation scheduling problem of GENCO (presented in Section 4.1.1.3) is solved using the Lambda-Iteration Economic Dispatch method [77] and if all the constraints are satisfied, fitness (fit_c) of the chromosome is calculated.

Applying selection process: The new chromosomes are selected using the probabilistic fitness-based selection (PFBS) technique, where the fitter chromosomes are more likely to be chosen. Herein, r_c is a random number between [0,100] generated for the chromosome (c).

$$a_c = \begin{cases} 1 & \theta_c^{PFBS} > r_c \\ 0 & \theta_c^{PFBS} < r_c \end{cases} \tag{5.19}$$

The value of selection probability of every chromosome (θ_c^{PFBS}) is determined using equation (5.20), which is proportional to the fitness of the chromosome. Herein, n_c is the number of chromosomes in the population and a_c is the acceptance indicator of a chromosome for the new population.

$$\theta_c^{PFBS} = \frac{fit_c}{Max\{fit_1, \dots, fit_{nc}\}} \times 100 \tag{5.20}$$

- *Step 4: Checking termination criterion*

In this step, the convergence status of the optimization procedure is checked. Based on this, the values of improvements in the fitness of the chromosomes of the old and new populations are computed and if there are no significant improvements in them, the optimization process is finished, otherwise, the algorithm is continued from *Step 2*.

- *Step 5: Introducing the outcome*

The consequences include the maximum value of GENCO's profit over the operation period (one day), the generation level of units, and the revised demand of system.

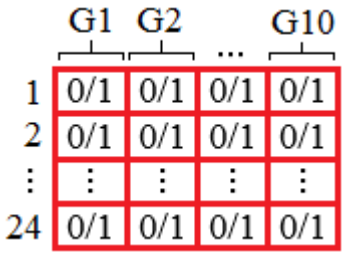

Figure 5.8: The structure of chromosome in the applied GA.

5.2 Mathematical Formulation for Traffic and Grid-Based Parking Lot Allocation and Charging Management of PEVs

In this section, the mathematical formulations for planning problem of a DISCO (Section 5.2.1) and operation problem of a GENCO (Section 5.2.2) are presented, respectively.

The goal of a DISCO is minimizing total cost of the planning problem over the planning time horizon (30 years). Herein, the inputs of planning problem of a DSICO include all the technical and economic parameters of problem and all the technical data of the electrical distribution network (Tables 5.3-5.5, Figures 5.9-5.10), and also the outputs of problem include the optimal location of parking lots and the optimal value of incentive.

The aim of a GENCO is maximizing its profit over the operation period (one day). Herein, the inputs of problem include the demand level of system and all the technical data of generation units (Table 5.9, and Figure 5.13), and also the outputs include the

optimal status and generation level of each generation unit and the optimal value of incentive.

The percentage of drivers that charge their PEVs through the parking lot, indicated by ξ_{Model} (Table 5.2), or the number of drivers that charge their PEVs through the parking lot, indicated by N_{Model}^{PEVs} (equation (5.3)), and demand of parking lot D_t^{PL} (equation (5.4)) directly affect the cost terms in the planning problem of a DISCO. The relationship between the above mentioned parameters and the cost terms will be presented in the problem formulation in Section 5.2.1. The values the above mentioned parameters are determined using average daily distance of PEVs from the parking lot ($\overline{\beta}$) and the value of incentive (discount on charging fee (γ) proposed by the DISCO) presented in Sections 5.1.1 and 5.1.2.

The location of installed parking lots by the DISCOs (known $\overline{\beta}$ for the optimal location of parking lots) and the calculated values of D^{PL} (the value of charging demand of PEVs that is under control of GENCO) and ξ_{Model} (percentage of drivers that is under control of GENCO) or N_{Model}^{PEVs} (the number of PEVs that is under control of GENCO) affect the daily profit of GENCO. The relation between the above mentioned parameters and income and cost terms of GENCO will be explained in the problem formulation in Section 5.2.2. The values of ξ_{Model}, N_{Model}^{PEVs}, and D^{PL} for the GENCO are determined just by the value of incentive (extra credits (γ)) in Sections 5.1.1 and 5.1.2 because the location of parking lots (that affects the value of $\overline{\beta}$) have already been determined by the DISCOs.

5.2.1 Formulating the Planning Problem of a DISCO

5.2.1.1 Objective Function of a DISCO

The objective function of planning problem of a DISCO is minimizing total cost of the problem over the planning period (Ny) by installing the parking lots in the optimal locations of the feeders. Herein, the driving patterns of the PEVs' drivers and their behavioral model respect to the value of incentive (discount on charging fee) and the distance from the parking lot are considered in the planning problem. In addition, several economic and technical factors including yearly inflation and interest rates, hourly and daily variations of the load demand, yearly load growth rate of the feeder, and yearly growth rate of the PEVs' application are taken into consideration.

The cost terms of the objective function include total investment cost for installing the parking lots in the optimal locations ($Cost^{INV}$), present worth value of maintenance cost of the installed parking lots over the operation period ($\widetilde{Cost_{Ny}^{MAINT}}$), present worth value of cost of discount on charging fee of the PEVs over the operation period ($\widetilde{Cost_{Ny}^{INC}}$), present worth value of energy loss cost of the feeder over the operation period ($\widetilde{Cost_{Ny}^{EL}}$), and present worth value of expected energy not supplied cost of the feeder over the operation period ($\widetilde{Cost_{Ny}^{EENS}}$), as can be seen in (5).

$$OF_{Ny}^{DISCO} = min\left\{Cost^{INV} + \widetilde{Cost_{Ny}^{MAINT}} + \widetilde{Cost_{Ny}^{INC}} + \widetilde{Cost_{Ny}^{EL}} + \widetilde{Cost_{Ny}^{EENS}}\right\} \quad (5.21)$$

The percentage of drivers that charge their PEVs through the parking lot, indicated by ξ_{Model}, or the number of drivers that charge their PEVs through the parking lot, indicated by N_{Model}^{PEVs} directly affect Investment cost, Maintenance cost, Incentive cost

and indirectly affect energy loss cost and expected energy not supplied cost, as can be seen in equations (5.22)-(5.32), respectively. In fact, ξ_{Model} is changed by the value of incentive (γ) and average daily distance of PEVs from the parking lot ($\overline{\beta}$), as can be seen in Table 5.2. In other words, the value of incentive (in the optimization process of the problem in Section 5.1.3), as one of the variables of the problem, changes the total number of drivers that charge their vehicles through the parking lots (N_{Model}^{PEVs}), and consequently the overall cost of planning problem is modified. In the following, the cost terms of objective function of DISCO are presented and described.

5.2.1.2 Cost Terms of the Planning Problem

Investment cost: The total investment cost for purchasing and installing the equipment of parking lots ($Cost^{INV}$) in the optimal locations of the feeder is presented in (6). Herein, C^{INV} is the amount of investment for equipping the parking lot for one PEV.

$$Cost^{INV} = C^{INV} \times N_{Model}^{PEVs} \tag{5.22}$$

Maintenance cost: The value of maintenance cost of the installed parking lot in the y^{th} year ($Cost_y^{MAINT}$) and the present worth value of maintenance cost of the parking lot over the operation period ($\widetilde{Cost_{Ny}^{MAINT}}$) are given in equations (5.23) and (5.24), respectively. Herein, C^{MAINT} is the amount of yearly maintenance cost of the parking lot for one PEV and IFR and ITR are inflation and interest rates, respectively. Also, Ny is the number of years in the planning period (30 years).

$$Cost_y^{MAINT} = C^{MAINT} \times N_{Model}^{PEVs} \tag{5.23}$$

$$\widetilde{Cost_{Ny}^{MAINT}} = \sum_{y=1}^{Ny} Cost_y^{MAINT} \times \left(\frac{1+\frac{IFR}{100}}{1+\frac{ITR}{100}}\right)^y \quad (5.24)$$

Incentive cost: The value of the cost of discount on charging fee of the PEVs in the y^{th} year ($Cost_y^{INC}$), and also the present worth value of cost of discount on charging fee of the PEVs over the operation period ($\widetilde{Cost_{Ny}^{INC}}$) are presented in equations (5.25) and (5.26), respectively. Herein, γ and π^E are the percentage of discount on charging fee and the price of electricity in Cents per kWh, respectively. Also, the value of D^{PL} has been presented in equation (5.4). Herein, t, d, and π^E are index of time in hour, index of day, and the value of charging price.

$$Cost_y^{INC} = \sum_{d=1}^{365}\sum_{t=1}^{24} D_t^{PL} \times \frac{\gamma}{100} \times \pi^E \times 10 \quad (5.25)$$

$$\widetilde{Cost_{Ny}^{INC}} = \sum_{y=1}^{Ny} Cost_y^{INC} \times \left(\frac{1+\frac{IFR}{100}}{1+\frac{ITR}{100}}\right)^y \quad (5.26)$$

Energy loss cost: The value of energy loss of feeder over the planning horizon (EL_{Ny}) is presented in equation (5.27). Moreover, the energy loss cost of the feeder in the y^{th} year ($Cost_y^{EL}$) and the present worth value of energy loss cost of the feeder over the operation period ($\widetilde{Cost_{Ny}^{EL}}$) are given in equations (5.28) and (5.29), respectively. Herein, R is the value of resistance of the branch of feeder, $|I|$ is the magnitude of current flowing through the branch, and MVA^{BASE} is the value of base power in per unit system (p.u.). Also, Nbr is the total number of branches of feeder.

$$EL_{Ny} = \sum_{y=1}^{Ny} \sum_{d=1}^{365} \sum_{t=1}^{24} \sum_{br=1}^{Nbr} R_{br} \times \left|I_{y,d,t,br}\right|^2 \times MVA^{BASE} \quad (5.27)$$

$$Cost_y^{EL} = \sum_{d=1}^{365} \sum_{t=1}^{24} \sum_{br=1}^{Nbr} R_{br} \times \left|I_{y,d,t,br}\right|^2 \times MVA^{BASE} \times \pi^E \times 10 \quad (5.28)$$

$$\widetilde{Cost_{Ny}^{EL}} = \sum_{y=1}^{Ny} Cost_y^{EL} \times \left(\frac{1+\frac{IFR}{100}}{1+\frac{ITR}{100}}\right)^y \quad (5.29)$$

Expected energy not supplied cost: The value of expected energy not supplied of the feeder over the operation period ($EENS_{Ny}$) is determined using equation (5.30) [82-83]. As can be seen, this value, as the reliability index or risk level of the system, depends on the failure rate of the branches of the feeder (λ), failure locating duration (τ^{FL}), and failure repairing duration (τ^{FR}). Herein, LNS^{FL} is the value of load not supplied during locating the fault and LNS^{FR} is the value of load not supplied during repairing the fault.

The expected energy not supplied cost in the y^{th} year ($Cost_y^{EENS}$) and the present worth value of expected energy not supplied cost of the feeder over the operation period ($\widetilde{Cost_{Ny}^{EENS}}$) are presented in equations (5.31) and (5.32), respectively. Herein, π^{ENS} is the value of cost of energy not supplied of the customers in Cents per kWh. Also, b and Nb are the index of the bus and the total number of buses of the feeder, respectively.

$$EENS_{Ny} = \sum_{y=1}^{Ny} \sum_{br=1}^{Nbr} \lambda_{br} \times \left(\tau^{FL} \sum_{b=1}^{Nb} LNS_y^{FL} + \tau^{FR} \sum_{b=1}^{Nb} LNS_y^{FR}\right) \quad (5.30)$$

$$Cost_y^{EENS} = \sum_{br=1}^{Nbr} \lambda_{br} \times \left(\tau^{FL} \sum_{b=1}^{Nb} LNS_{y,b}^{FL} + \tau^{FR} \sum_{b=1}^{Nb} LNS_{y,b}^{FR}\right) \times \pi^{ENS} \times 10 \quad (5.31)$$

$$\widetilde{Cost_{Ny}^{EENS}} = \sum_{y=1}^{Ny} Cost_{y}^{EENS} \times \left(\frac{1+IFR}{1+ITR}\right)^{y} \quad (5.32)$$

5.2.1.3 Security Constraints of System in Planning Problem

Loading limit of the branches: The loading constraint of each branch, as its thermal limit, is presented in equation (5.33). As can be seen, the magnitude of apparent power flowing through the branch ($|MVA_{br}|$) must be less than the allowable magnitude of the apparent power of the branch ($|\overline{MVA}_{br}|$).

$$|MVA_{br}| \leq |\overline{MVA}_{br}|, \forall br \in \{1, \dots, Nbr\} \quad (5.33)$$

Voltage magnitude limits of the buses: The magnitude of voltage of each bus ($|V_b|$) must be within the allowable minimum and maximum limits. Herein, σ^V is the acceptable tolerance of voltage magnitude and $|\bar{V}_b|$ is the magnitude of rated voltage of bus.

$$(1-\sigma^V/100) \times |\bar{V}_b| \leq |V_b| \leq (1+\sigma^V/100) \times |\bar{V}_b|, \forall b \in \{1, \dots, Nb\} \quad (5.34)$$

5.2.2 Formulating the Operation Problem of a GENCO

5.2.2.1 Objective Function of a GENCO

The objective function of operation problem of the GENCO (maximizing daily profit of GENCO) over the operation period (one day) is presented in equation (5.35). As can be seen, it includes income term due to selling electricity to the end user customers and PEVs' drivers ($Income_t^{SELL}$), cost of discount on charging fee of the PEVs ($Cost_t^{INC}$), fuel cost of the generation units ($Cost_{g,t}^{F}$), greenhouse gas emissions cost of

the generation units ($Cost_{g,t}^{E}$), the start-up cost of de-committed units (the units that are in "off" status) $Cost_{g,t}^{STU}$, and the shut down cost of committed units $Cost_{g,t}^{SHD}$(i.e., the units that are in "on" status). Herein, g and Ng are index of generation unit and total number of generation units, respectively.

$$OF^{GENCO} = max \sum_{t=1}^{24} \left[\begin{array}{c} Income_t^{SELL} - Cost_t^{INC} \\ - \sum_{g=1}^{Ng} \left[Cost_{g,t}^{F} + Cost_{g,t}^{E} + Cost_{g,t}^{STU} + Cost_{g,t}^{SHD} \right] \end{array} \right] \quad (5.35)$$

5.2.2.2 Income and Cost Terms of the Operation Problem

In the following, the income and cost terms of objective function are described. As can be seen in equation (5.36), income term of GENCO ($Income_t^{SELL}$) includes the value of earning from electricity selling to the end user customers (D^{EU}) and PEVs (D^{PL}). Herein, π^{E} indicates electricity price.

$$Income_t^{SELL} = \sum_{t=1}^{24} [D_t^{EU} + D_t^{PL}] \times \pi^{E} \quad (5.36)$$

Incentive cost: The incentive cost ($Cost^{INC}$) imposed to the GENCO includes the value of credit (γ) offered to PEVs which is equal to the percentage of charging fee of the PEVs in all the parking lots. Herein, PL and NPL are indices of parking lot and total number of installed parking lots in the whole power system.

$$Cost_t^{INC} = \sum_{PL=1}^{NPL} D_t^{PL} \times \frac{\gamma}{100} \times \pi^{E} \times 10 \quad (5.37)$$

Fuel cost of generation units, greenhouse gas emissions cost of generation units, start-up cost and shut down cost of generation units have been presented in equations (4-17)-(4.20) in Section 4.2.1.2.

5.2.2.3 Constraints of System in Operation Problem

In the following, the system and generation units' constraints are presented and explained.

System power balance constraint: The power-demand balance constraint of the system (to ensure that demand is equal to supply) that must be held in every time step of the operation period is presented in equation (5.38). Herein, D_t^{EU} and D_t^{PL} are hourly demands of end users and PEVs fleet, respectively.

$$\sum_{g=1}^{Ng} P_{g,t} \times x_{g,t}^{G} = D_t^{EU} + D_t^{PL} \tag{5.38}$$

System minimum generation constraint: The constraint of minimum power of the system generated by "on" units for every hour of the operation period is presented in equation (5.39). In other words, the units, which are "on", must be able to supply the minimum demand level of the system.

$$\sum_{g=1}^{Ng} P_g^{min} \times x_{g,t}^{G} \leq D_t^{EU} + D_t^{PL} \tag{5.39}$$

System maximum generation constraint considering spinning reserve: The maximum generation of the power system considering spinning reserve level (SR) provided by the "on" units for every hour of the operation period is presented in equation

(5.40). In other words, the units, which are "on", must be able to supply the maximum demand level of the system considering the required spinning reserve of the system.

$$\sum_{g=1}^{Ng} P_g^{max} \times x_{g,t}^{G} \geq D_t^{EU} + D_t^{PL} + SR_t \qquad (5.40)$$

Generation units' power constraint, generation units' ramp-up rate and ramp-down rate constraints and generation units' minimum "off time" and minimum "on time" constraints have been presented in equations (4-24)-(4.28) in Section 4.2.1.2.

5.3 Simulation and Results for Traffic and Grid-Based Parking Lot Allocation and Charging Management of PEVs

The simulations are done in MATLAB environment using the Intel Xeon Sever with 64 GB RAM. The number of chromosomes in the population (n_c) and the value of mutation probability of the genes (θ^{Mut}) in the applied GA are considered about 100 and 10%, respectively.

5.3.1 Simulating the Planning Problem of a DISCO

5.3.1.1 Primary Data of the Grid and Problem

In this part, the optimal parking allocation problem is investigated on DF 1 (first feeder of DISCO 1 as shown in Figure 5.1) that includes 28 buses. The total number of PEVs around DF 1 is 600. The technical data of different types of PEVs including Nissan Leaf BEV, Chevy Volt 2012 PHV, and Toyota Prius 2012 PHV are presented in Table 5.3 [84]. In the simulation of planning problem of a DISCO, the type of PEVs is

considered to be Nissan Leaf BEV. However, in the sensitivity analyses (for value of profit of DISCO with respect to value of incentive, location of parking lot, driving pattern, and type of PEVs) in Section 5.3.1.3, other types will be studied. Table 5.4 presents the value of parameters of the planning problem. In addition, Figures 9 and 10 illustrate the hourly power demand of DF 1 throughout a day (p.u.) and the daily power demand of DF 1 throughout a year (p.u.), respectively. These two figures are generated based on the shape of typical demands in a system. As can be seen, the value of demands in Figures 9 and 10 are around 1 per unit (p.u.) because the value of hourly and daily real demands have been divided by the value of a specific demand level. Figures 5.9 and 5.10 are used to determine the value of demand in every hour of a day and in every day of a year.

Moreover, the values of parameters of DF 1 and demand of end users of DF 1 related to March 1st at 5 pm are given in Table 5.5 [67]. Demand level of DF 1 at every hour of a typical day can be determined by considering the ratio the target demand level and demand level at 5pm presented in Figure 5.9. In addition, demand level of DF 1 in other days of the first year of planning can be determined by comparing the target demand level and demand level on March 1st presented in Figure 5.10. The position of each bus of DF 1 (latitude and longitude) can be seen in Table 5.5.

Table 5.3: The technical data of the different types of PEVs [84].

-	Nissan Leaf BEV	Chevy Volt 2012 PHV	Toyota Prius 2012 PHV
Performance (kWh/km)	0.21	0.17	0.18
Battery capacity (kWh)	24	16	4.5
Charging voltage (V)	240	240	240

Table 5.4: The value of parameters of planning problem.

Parameter	Value	Unit	Symbol
Operation period	30	Year	Ny
Load growth rate	0.6	%/year	-
PEV application growth rate	5	%/year	-
Inflation rate	10	%/year	IFR
Interest rate	5	%/year	ITR
Investment cost for parking lot [84]	2200	$/PEV	C^{INV}
Maintenance cost for parking lot	1	%/year	C^{MAINT}
Electricity price [85]	10	Cent/kWh	π^{E}
Energy not supplied cost	50	Cent/kWh	π^{ENS}
Failure rate of a branch	3	Fault/year	λ
Locating duration of a fault place	1	Hour	τ^{FL}
Repairing duration of a defective branch	3	Hour	τ^{FR}
Acceptable voltage tolerance	5	%	σ^{V}
Base power in per unit system	10	MVA	MVA^{BASE}

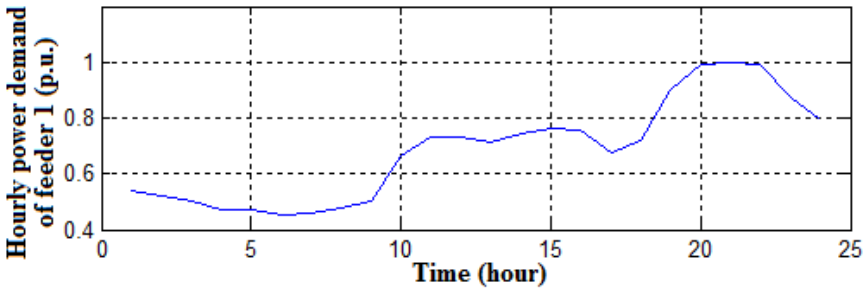

Figure 5.9: Hourly power demand of DF 1 (first feeder of DISCO 1) throughout a day (p.u.).

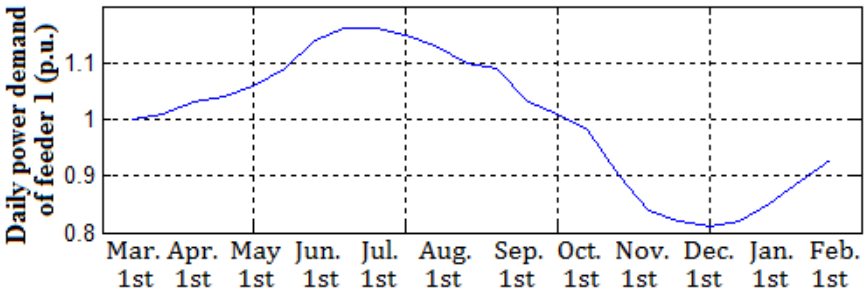

Figure 5.10: Daily power demand of DF 1 (first feeder of DISCO 1) throughout a year (p.u.).

Table 5.5: The value of technical parameters of DF 1 (first feeder of DISCO 1). The demand level of end users is related to March 1st at 5 pm [67].

First bus	End bus	Latitude of end bus	Longitude of end bus	Active demand (MW)	Reactive demand (MVAR)	Resistance (p.u.)	Reactance (p.u.)	Loading limit of branch (MVA)
1	1	38.9290	-76.9776	0.2	0.1	-	-	-
1	2	38.9289	-76.9799	0.2	0.1	0.0040	0.0020	41
2	3	38.9290	-76.9817	0.5	0.2	0.0075	0.0109	39
3	4	38.9290	-76.9832	0.5	0.2	0.0089	0.0081	36
4	5	38.9290	-76.9851	0.6	0.2	0.0096	0.0084	34
5	6	38.9289	-76.9867	0.6	0.2	0.0078	0.0098	28
6	7	38.9288	-76.9877	0.6	0.2	0.0081	0.0130	26
7	8	38.9288	-76.9888	0.6	0.2	0.0100	0.0102	24
8	9	38.9287	-76.9898	0.6	0.2	0.0099	0.0112	21
9	10	38.9287	-76.9907	0.7	0.3	0.0105	0.0112	19
10	11	38.9286	-76.9927	0.7	0.3	0.0085	0.0028	9
11	12	38.9280	-76.9937	0.7	0.3	0.0093	0.0054	8
12	13	38.9270	-76.9937	0.7	0.3	0.0080	0.0083	7
13	14	38.9260	-76.9939	0.5	0.2	0.0096	0.0100	6
14	15	38.9260	-76.9949	0.9	0.4	0.0118	0.0089	5
15	16	38.9270	-76.9950	0.9	0.4	0.0115	0.0097	4
16	17	38.9279	-76.9950	0.9	0.4	0.0071	0.0050	3
17	18	38.9292	-76.9950	0.9	0.4	0.0071	0.0050	2
10	19	38.9280	-76.9907	0.9	0.4	0.0070	0.0026	9
19	20	38.9271	-76.9906	0.9	0.4	0.0095	0.0031	8
20	21	38.9262	-76.9905	0.9	0.4	0.0109	0.0068	7
21	22	38.9256	-76.9899	1.0	0.4	0.0099	0.0058	5
22	23	38.9256	-76.9885	1.0	0.4	0.0126	0.0064	4
23	24	38.9247	-76.9880	1.0	0.4	0.0111	0.0029	3
24	25	38.9245	-76.9893	1.0	0.4	0.0110	0.0025	2
5	26	38.9284	-76.9860	0.9	0.4	0.0126	0.0064	4
26	27	38.9273	-76.9859	0.9	0.4	0.0111	0.0029	3
27	28	38.9259	-76.9858	0.9	0.4	0.0110	0.0025	2

5.3.1.2 Results

Before allocating parking lots to DF 1, the value of energy loss and energy not supplied of DF 1 over the planning period are about 2.9173 and 0.1349 Million MWh,

respectively. Without installing parking lots, PEVs are changed from their nearest buses between 10 am- 11 pm.

After solving the problem of traffic and grid-based parking lot allocation, it is observed that just one parking lot is allocated to DF 1 considering each of the PEVs behavioral model (power, logarithmic, linear, and exponential models for reaction of the PEVs' drivers respect to the value of incentive and linear model for distance of the PEVs from the parking lot). Table 5.6 presents the detailed results of the planning problem simulation. As can be seen, power model with exponent 0.3 and exponential model (and power model with exponent 3, as well) are the most and the least desirable behavioral models for the PEV fleet, since the total profit (the difference between the costs before and after the parking lot allocation) of the DISCO 1 are the most and the least, respectively. Regarding the power model (with exponent 0.3), by installing a parking lot with the size of 756 PEVs in bus 26 and considering 30% discount on the charging fee of PEVs, the energy loss and expected energy not supplied of DF 1 are decreased about 142,800 and 700 MWh over the operation period, respectively.

It should be noticed that although the exponential model (and power model with exponent 3, as well) has the least value of energy loss and expected energy not supplied (and accordingly the least value of cost of energy loss and cost of expected energy not supplied), these models are not the most favorable model because minimizing the total cost of the local DISCO is the objective function of the problem.

By investigating the results presented in Table 5.6, it is observed that the optimal value of discount on charging fee, the optimal location of parking lot, and the optimal

size of parking lot are not the same for every behavioral model of the PEVs fleet. In other words, a predetermined value of incentive and default size and location of the parking lot will not result in minimum cost for the local DISCO.

Table 5.6: The detailed results of optimal parking lot allocation on DF 1 (first feeder of DISCO 1) considering different behavioral models for the PEVs' drivers.

-	Without parking lot	Pow. (exponent is 0.3)	Log.	Lin.	Exp. or Pow. (exponent is 3)
Optimal discount (%)	0	30	70	90	100
Optimal bus for parking lot	-	26	3	3	2
Optimal size of parking lot (No. of PEVs)	0	756	542	617	686
Energy loss (Million MWh)	2.9173	2.7745	2.7772	2.7592	2.7432
Risk level (Million MWh)	0.1349	0.1342	0.1344	0.1343	0.1342
Investment cost (Million $)	0	1.6636	1.1928	1.3593	1.5104
Maintenance cost (Million $)	0	1.0612	0.7608	0.8670	0.9634
Cost of discount (Million $)	0	6.346	10.617	15.557	19.206
Energy loss cost (Million $)	620.26	589.91	590.48	586.66	583.26
Risk cost (Million $)	143.41	142.73	142.87	142.80	142.73
Maximum profit (Million $)	-	21.963	17.755	16.433	16.002

5.3.1.3 Sensitivity Analyses

5.3.1.3.1 Sensitivity Analysis for Value of Incentive

Herein, it is assumed that the parking lot has been placed in the optimal bus of the feeder for every model of the drivers' behavior, and then the total benefit of the local DISCO is investigated based on different value of incentive. Figure 5.11 shows the total profit of the local DISCO over the planning period (Million $) with respect to the value of discount on charging fee (%) for Power model with exponent 0.3 (optimal bus is 26), Logarithmic model (optimal bus is 3), Linear model (optimal bus is 3), Power model with

exponent 3 (optimal bus is 2), and Exponential model (optimal bus is 2) for the PEVs' drivers behavior. As can be seen, the presented data in Table 5.6 regarding the optimal value of discount on charging fee is approved by Figure 5.11.

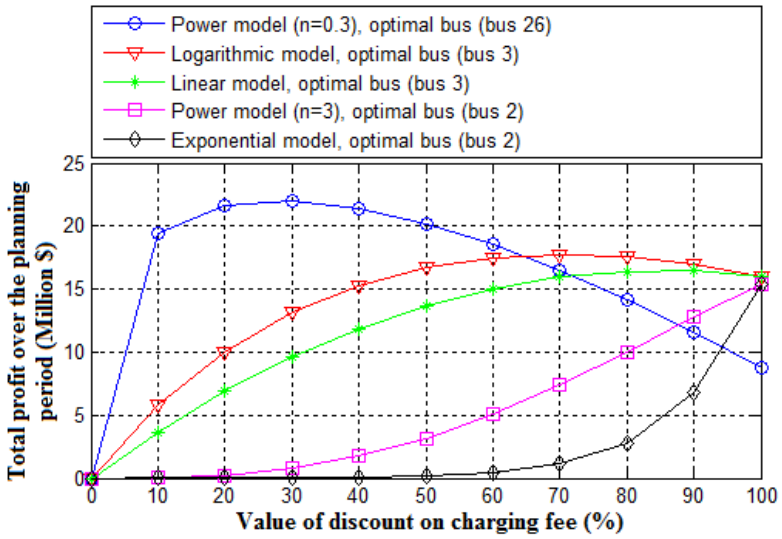

Figure 5.11: Total profit over the operation period (Million $) with respect to the value of discount on charging fee (%) due to installing the parking lot in the optimal bus of the feeder considering Power model with exponent 0.3 (optimal bus is 26), Logarithmic model (optimal bus is 3), Linear model (optimal bus is 3), Power model with exponent 3 (optimal bus is 2), and Exponential model (optimal bus is 2) for the PEVs behavior.

5.3.1.3.2 Sensitivity Analysis for Location of Parking Lot

In this part, it is assumed that the optimal value of incentive for every model of the drivers' behavior has been determined, and then the optimal bus of the feeder for installing one parking lot is probed. Figure 5.12 illustrates the total profit of the local DISCO over the planning period (Million $) with respect to the location of parking lot considering Power model with exponent 0.3 (with optimal discount equal to 30%), Logarithmic model (with optimal discount equal to 70%), Linear model (with optimal

discount equal to 90%), Power model with exponent 3 (with optimal discount equal to 100%), and Exponential model (with optimal discount equal to 100%) for the PEVs' drivers behavior. As can be seen, Figure 5.12 agrees with the presented data in Table 5.6 regarding the optimal location of the parking lot.

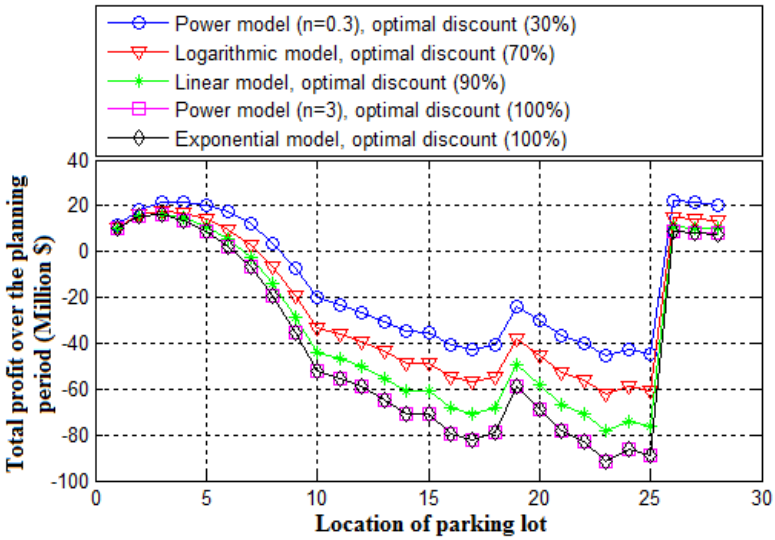

Figure 5.12: Total profit over the operation period (Million $) with respect to the location of parking lot considering Power model with exponent 0.3 (optimal discount is 30%), Logarithmic model (optimal discount is 70%), Linear model (optimal discount is 90%), Power model with exponent 3 (optimal discount is 100%), and Exponential model (optimal discount is 100%) for the PEVs behavior.

5.3.1.3.3 Sensitivity Analysis for Model of Driving Pattern

In this part, the optimal traffic and grid-based parking lot allocation problem is investigated considering different driving patterns for the PEVs and the results are compared with consequences of the problem for default driving pattern of the PEVs fleet, that is, 100 PEVs per each driving pattern (Patterns 1-6). Herein, power model (with exponent 0.3) is considered for the drivers' behavior. As can be seen in Table 5.7, the

value of optimal discount on charging fee, the optimal location of the parking lot, and maximum profit of the local DISCO are affected by the model of driving pattern of the PEVs fleet. This phenomenon indicates the necessity for realistically determining the driving pattern of the PEVs fleet in the traffic and grid-driven parking lot allocation problem.

Table 5.7: The results of optimal parking lot allocation considering different driving patterns for the PEVs (Drivers' behavior model is power with exponent 0.3).

Driving pattern of the PEVs	Optimal discount (%)	Optimal bus for parking lot	Maximum profit (Million $)
Default (100 PEVs for each pattern)	30	26	21.963
All PEVs have pattern 1	40	3	23.772
All PEVs have pattern 2	30	26	16.427
All PEVs have pattern 3	40	3	39.864
All PEVs have pattern 4	30	26	16.914
All PEVs have pattern 5	40	3	21.956
All PEVs have pattern 6	30	5	18.567

5.3.1.3.4 Sensitivity Analysis for Type of PEV

Herein, the optimal traffic and grid-based parking lot allocation problem is investigated for other types of the PEV, that is, *Chevy Volt 2012 PHV* and *Toyota Prius 2012 PHV* and the outcomes are compared with results of default type of the PEV (*Nissan Leaf BEV*). As can be seen in Table 5.8, different types of the PEVs fleet change some of the outcomes of problem. Thus, the type of PEVs fleet must be identified in the optimal parking lot allocation problem. The reason for achieving lower profit with *Chevy Volt 2012 PHV* and T*oyota Prius 2012 PHV* is related to their smaller battery capacity,

and also their better performance (lower value for kWh per km) compared to *Nissan Leaf BEV*. In other words, *Nissan Leaf BEV* has the biggest battery capacity and high value of kWh per km (more energy consumption), thus this vehicle has more daily energy demand, and thus parking lot placement for this type of PEV will result in more profit.

Table 5.8: The results of optimal parking lot allocation considering different type for the PEV (Drivers' behavior model is Linear).

Type of PEV	Optimal discount (%)	Optimal bus for parking lot	Maximum profit (Million $)
Default (Nissan Leaf BEV)	90	3	16.433
Chevy Volt 2012 PHV	80	3	11.470
Toyota Prius 2012 PHV	60	3	1.947

5.3.2 Simulating the Operation Problem of a GENCO

5.3.2.1 Characteristics of the Generation System

The technical characteristics of generation units including the fuel cost coefficient of generation units, the emission coefficient of generation units, the power limits of the units, the minimum up/down time of units, the ramp up rate and ramp down rate of units, the start-up cost and shut down cost of units, and the initial status of units are presented in Table 5.9. Positive and negative numbers for the status of units mean the time interval in hour that the unit is in "on" and "off" statuses, respectively.

The hourly demand pattern of the whole power system (shown in Figure 5.1) throughout a day (p.u.) and the daily demand pattern of the power system throughout a year (p.u.) are the same as presented in Figures 5.9 and 5.10, respectively. Moreover, the

minimum value of spinning reserve at every hour of a day is assumed to be about 10% of demand at the same hour. Furthermore, the value of penalty for greenhouse gas emissions is assumed about $10 per ton based on the California Air Resources Board auction of greenhouse gas emissions [76]. Figure 5.13 illustrates the hourly demand of end users, the hourly demand of PEV fleet, and the hourly demand of power system (shown in Figure 5.1). Total number of PEVs in the whole area (supplied by the GENCO) is 16,800 PEVs. The driving patterns of PEVs around every distribution feeder are the same as presented in Figures 5.2 and 5.3. Regarding the operation problem of GENCO, the type of PEVs is considered Nissan Leaf BEV; however, in the sensitivity analyses, other types will be studied. Herein, the value of electricity price for the end users' consumption or charging the PEVs is considered about $30.35/MWh, which is 10% more than the marginal cost of the generation system ($27.59/MWh). In other words, the GENCO profits about $2.76/MWh.

Table 5.9: The technical characteristics of generation units.

Generation unit	G1	G2	G3	G4	G5
α_1^F ($/MWh^2)	0.00048	0.00031	0.00200	0.00211	0.00398
α_2^F ($/MWh)	16.19	17.26	16.60	16.50	19.70
α_3^F ($)	1000	970	700	680	450
α_1^E (Ton/MWh^2)	0.0005	0.0005	0.0005	0.0005	0.0010
α_2^E (Ton/MWh)	0.4050	0.4320	0.4150	0.4120	0.4930
α_3^E (Ton)	0.3000	0.4250	0.4500	0.7000	0.7250
P^{min} (MW)	75	75	15	15	15
P^{max} (MW)	200	200	120	100	100
MUT (h)	5	5	5	5	5
MDT (h)	-5	-5	-5	-5	-5
RUR (MW/h)	110	110	80	80	80

RDR (MW/h)	110	110	80	80	80
C^{STU} ($)	4500	5000	550	560	900
C^{SHD} ($)	4500	5000	550	560	900
Initial status	+24	+24	+24	+24	+24
Generation unit	G6	G7	G8	G9	G10
α_1^F ($/MWh^2)	0.00712	0.00790	0.00813	0.00822	0.00873
α_2^F ($/MWh)	22.26	27.74	25.92	27.27	27.79
α_3^F ($)	370	480	660	665	670
α_1^E (Ton/MWh^2)	0.0020	0.0020	0.0024	0.0025	0.0025
α_2^E (Ton/MWh)	0.5560	1.0940	1.6480	1.6820	1.6950
α_3^E (Ton)	0.9250	1.2000	1.6500	1.6625	1.7750
P^{min} (MW)	10	10	10	10	10
P^{max} (MW)	80	50	25	20	20
MUT (h)	3	1	1	1	1
MDT (h)	-3	-1	-1	-1	-1
RUR (MW/h)	60	20	10	10	10
RDR (MW/h)	60	20	10	10	10
C^{STU} ($)	170	30	30	30	30
C^{SHD} ($)	170	30	30	30	30
Initial status	-1	-2	-2	-2	-2

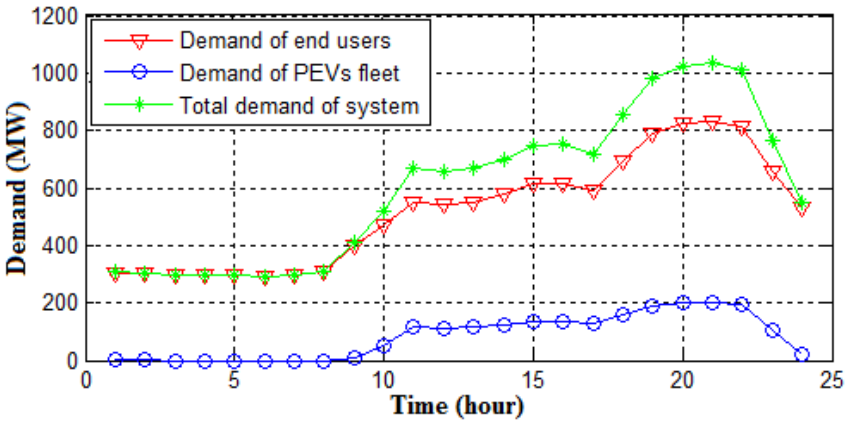

Figure 5.13: Hourly demand (MW) of end users, PEVs fleet, and system before charging management.

5.3.2.2 Results

The detailed simulation results of the GENCO's operation problem are presented in Table 5.10 that includes the total daily profit of GENCO without charging management and with optimal charging management of the PEVs fleet considering different behavioral model for the drivers. As can be seen, the GENCO has $38,101/day profit without charging management of the PEVs fleet. In addition, the charging management of PEVs parked in the parking lots with any behavioral model result in more profit for the GENCO, while the power model with exponent 0.3 leads to the most benefit for it. The results show the effectiveness of considering incentive (extra credit) for the PEVs' owners in the generation scheduling and unit commitment (UC) problems. Although considering incentive for the drivers imposes extra cost to the GENCO, its overall profit increases because of optimal charging management of PEVs due to deferring the most expensive generation units in the generation scheduling and UC problems. Moreover, as can be seen in Table 5.10, the value of incentive is not the same for every model. In other words, the predetermined value of incentive will not result in the maximum profit of the GENCO and knowing the behavioral model of drivers is an important factor.

Figure 5.14 illustrates the hourly demand (MW) of PEVs and system before and after charging management considering optimal incentive (10% discount on charging fee) and power model (exponent is 0.3) for the drivers' behavior. As can be seen, one part of PEVs' demand is shifted from the peak period to the valley period that affects the demand of system in the similar pattern.

Table 5.10: The detailed results of optimal charging of PEVs fleet considering different behavioral models for them.

-	Without charging management	With optimal charging management of PEVs fleet				
		Pow. (exponent is 0.3)	Log.	Lin.	Pow. (exponent is 3)	Exp.
Optimal discount (%)	0	10	20	30	50	50
Cost of discount ($/day)	0	3096	3649	5559	3860	208
Cost of UC ($/day)	381010	366340	369340	369210	372090	380050
Income of selling electricity ($/day)	419110	419110	419110	419110	419110	419110
Total profit ($/day)	38101	49679	46124	44343	39914	38851

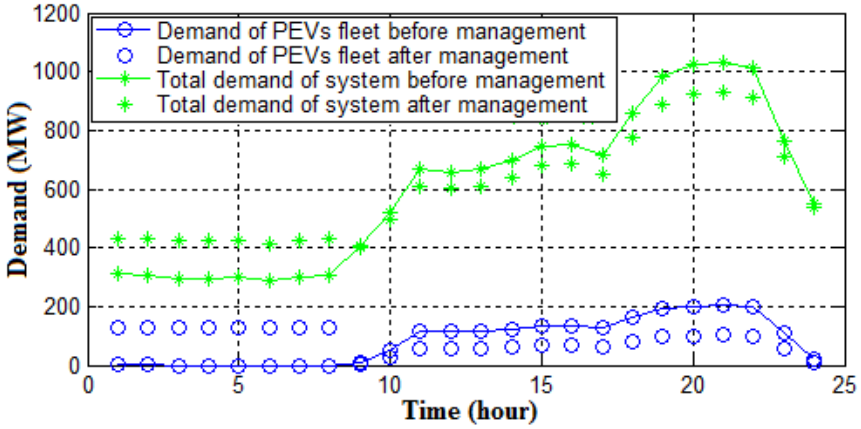

Figure 5.14: Hourly demand (MW) of the PEVs and system before and after charging management considering optimal incentive (10% discount on charging fee) and power model (exponent is 0.3) for the drivers' behavior.

The generation level of units at every hour of the operation period (one day) without charging management and with optimal charging management of the PEVs (parked in parking lots) considering power model (with exponent of 0.3) are presented in Table 5.11 and Table 5.12, respectively. As can be seen in Table 5.11, G6-G10 as the most expensive units are utilized just in the short period of the day. In addition, as can be

seen in Table 5.12, by optimal charging management of the PEVs parked in the parking lots, some of the most expensive units (G7-G10) are shut down, operation of one of them (G6) is decreased, and operation of the less expensive generation units (G1-G5) are increased in the valley period.

Table 5.11: The power level of generation units (MW) before optimal charging management of PEVs fleet.

Hour	G1	G2	G3	G4	G5	G6	G7	G8	G9	G10
1	133	75	32	50	15	0	0	0	0	0
2	133	75	32	49	15	0	0	0	0	0
3	130	75	29	47	15	0	0	0	0	0
4	130	75	29	47	15	0	0	0	0	0
5	132	75	30	48	15	0	0	0	0	0
6	127	75	27	45	15	0	0	0	0	0
7	132	75	30	48	15	0	0	0	0	0
8	134	75	33	50	15	0	0	0	0	0
9	171	75	61	78	15	0	0	0	0	0
10	198	75	82	100	15	0	0	0	0	0
11	200	118	120	100	15	0	0	0	0	0
12	200	111	120	100	15	0	0	0	0	0
13	200	118	120	100	15	0	0	0	0	0
14	200	143	120	100	15	0	0	0	0	0
15	200	179	120	100	15	0	0	0	0	0
16	200	182	120	100	15	0	0	0	0	0
17	200	155	120	100	15	0	0	0	0	0
18	200	200	120	100	66	10	0	0	0	0
19	200	200	120	100	100	53	10	10	0	0
20	200	200	120	100	100	65	10	10	10	10
21	200	200	120	100	100	72	10	10	10	10
22	200	200	120	100	100	56	10	10	10	10
23	200	200	120	100	29	10	0	0	0	0
24	200	95	120	100	15	0	0	0	0	0

Table 5.12: The power level of generation units (MW) after optimal charging management of PEVs fleet with power behavioral model (exponent is 0.3).

Hour	G1	G2	G3	G4	G5	G6	G7	G8	G9	G10
1	183	75	70	87	15	0	0	0	0	0
2	183	75	70	88	15	0	0	0	0	0
3	180	75	68	86	15	0	0	0	0	0
4	180	75	68	86	15	0	0	0	0	0
5	181	75	69	87	15	0	0	0	0	0
6	178	75	66	83	15	0	0	0	0	0
7	181	75	69	87	15	0	0	0	0	0
8	184	75	72	89	15	0	0	0	0	0
9	169	75	59	77	15	0	0	0	0	0
10	188	75	75	92	15	0	0	0	0	0
11	200	75	105	100	15	0	0	0	0	0
12	200	75	99	100	15	0	0	0	0	0
13	200	75	105	100	15	0	0	0	0	0
14	200	81	120	100	15	0	0	0	0	0
15	200	112	120	100	15	0	0	0	0	0
16	200	114	120	100	15	0	0	0	0	0
17	200	91	120	100	15	0	0	0	0	0
18	200	181	120	100	15	0	0	0	0	0
19	200	200	120	100	68	10	0	0	0	0
20	200	200	120	100	94	10	0	0	0	0
21	200	200	120	100	90	10	10	0	0	0
22	200	200	120	100	87	10	0	0	0	0
23	200	169	120	100	15	0	0	0	0	0
24	200	86	120	100	15	0	0	0	0	0

5.3.2.3 Sensitivity analyses

5.4.2.3.1 Sensitivity Analysis for GENCO's Profit with Respect to the Value of Incentive

Figure 5.15 shows the sensitivity of the GENCO's profit with respect to the value of discount on charging fee of the PEVs considering different behavioral models. As can be seen, there is a certain amount of discount on charging fee, as the optimal value of incentive, for each behavioral model of drivers. In other words, considering more or less incentive for the drivers will not increase the daily profit of the GENCO.

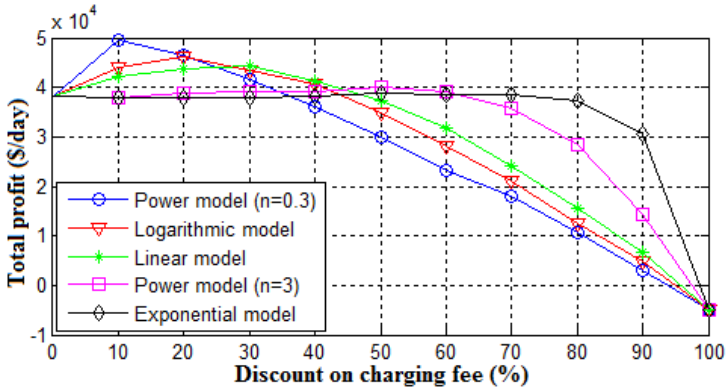

Figure 5.15: Total profit of GENCO ($/day) with respect to value of incentive for every behavioral model of PEVs fleet.

5.3.2.3.2 Sensitivity Analysis for GENCO's Profit with Respect to the Type of PEV

Figure 5.16 shows the sensitivity of GENCO's profit with respect to the type of PEVs. Herein, Figure 5.16 illustrates the value of increase in profit of GENCO ($/day) for every type of PEV considering different behavioral model for the drivers. As can be seen, Nissan Leaf has the most potential for increasing the profit of GENCO with any behavioral model of drivers. The reason of this reality is related to the larger battery capacity of Nissan Leaf compared to other types of PEVs, as can be realized from Table 5.3.

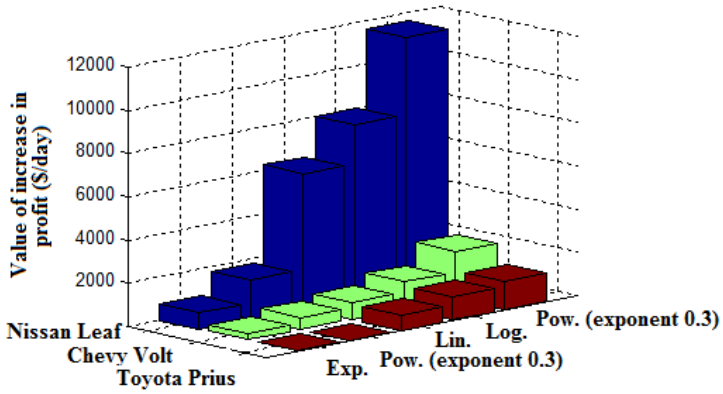

Figure 5.16: Value of increase in profit of GENCO ($/day) for every behavioral model of PEVs fleet considering different PEV type.

5.4 Conclusion of Problem III

In this study, traffic and grid-based parking lot allocation and charging management of PEVs fleet were investigated in the planning problem of a DISCO and operation problem of GENCO, respectively. Herein, the driving pattern and behavioral model of the drivers with respect to value of incentive and the average daily distance of PEVs from the parking lot were considered in both planning and operation problems.

In the planning problem, each DISCO allocated parking lots to the optimal location of electrical feeders to minimize the total cost of planning problem over the planning time horizon by minimizing the power loss and EENS of the feeders. In addition, in the operation problem, the GENCO optimally managed the charging time of PEVs parked in the parking lots to maximize its daily profit by deferring the more expensive and pollutant generation units.

Among the different behavioral models of the drivers, the power model (with exponent 0.3) and exponential model, as the interested and reluctant behavior model respected to the value of incentive, resulted in the most and the least favorable outcomes for the every DISCO and GENCO.

It was proven that the drivers' behavioral model, their driving patterns, and even the type of PEVs can remarkably affect the outcomes of both planning and operation problems. In other words, these factors affected the optimal sizes and locations of the parking lots in the planning problem of DISCO, optimal value of incentive in both planning and operation problems of DISCO and GENCO, and minimum cost of DISCO

and maximum profit of GENCO. Therefore, these factors must be modeled precisely in the traffic and grid-based parking lot allocation and charging management problems.

For the future studies, it is suggested to consider energy management of end users (along with charging management of PEVs) in the operation problem of GENCO and load model of end users (residential, commercial, and industrial customers) in the planning problem of DISCO.

CHAPTER SIX

CONCLUSION

Restructuring a traditional power system for establishing a smart grid has many benefits from social, economic, and environmental points of view that include improving the efficiency and reliability of the power system, decreasing average price of electricity, and minimizing carbon emissions. To build a smart grid, in this dissertation, three important problems including energy scheduling, energy management, and parking lot allocation and charging management of PEVs were investigated.

It was shown that application of SHs, instead of conventional buildings, are beneficial for the occupants from social, economic, and environmental viewpoints. In other words, SHs have a high capability for minimizing energy consumption cost and carbon emissions (by including renewable energy resources), and consequently for improving the social welfare of occupants. Herein, we proposed cooperative distributed energy scheduling that enables SHs to cooperate in energy transaction to minimize their daily operation cost. Also, we used a multi-time scale stochastic MPC as the adaptive and dynamic optimization technique to address the problem of uncertainty and variability issues of the power of PV panels. In fact, the cooperation of SHs for sharing their energy sources (DG, PV panels, and the battery of PEV) and considering the small and large time scales (five-minute and one-hour scales) in the multi-time scale MPC resulted in cost saving. In addition, we demonstrated that cooperation of more SHs in the energy scheduling problem has more potential for cost minimization.

In addition, it was demonstrated that price-controlled energy management, as one of the schemes of demand side management in a smart grid, is capable of increasing the social welfare of system by increasing the profit of GENCO and decreasing the operation cost of active and responsive end user customers (SHs). In this study, based on the energy price determined by GENCO, the energy scheduling problem of each SH was solved using scenario-based stochastic optimization to minimize the operation cost of the SH. Based on the demand from SHs resulted from the optimization solution, the unit commitment problem and generation scheduling problem of the GENCO were solved applying the Lambda-Iteration Economic Dispatch method and GA, respectively. In the unit commitment problem, GA determines the statuses of generation units at every hour of the day and in the generation scheduling problem, Lambda-Iteration Economic Dispatch method determines the generation level of units. The simulation results demonstrate that price-controlled energy management of the active and responsive end users (smart homes) in the generation scheduling problem is noticeably advantageous for the GENCO and even for the smart homes, since it can increase the profit of GENCO and decrease the operation cost of smart homes.

Moreover, it was proven that not only the risk of replacing internal combustion based vehicles with PEVs (causing congestion in feeders, resulting in overload in power distribution and generation systems) can be avoided but also it can bring about a considerable opportunity for the GENCO and DISCOs by optimal parking lot allocation and optimal management of charging time of PEVs in a smart grid infrastructure. In other words, replacing internal combustion based vehicles with PEVs is beneficial from social,

economic, and environmental viewpoints, since it can mitigate the carbon emissions and improve the system reliability. In this problem, each DISCO solved the optimal parking lot placement problem for every electrical feeder to minimize the total cost of planning problem over the planning time horizon. In addition, the GENCO optimally managed the charging time of PEVs parked in the parking lots to maximize its daily profit by deferring the more expensive and pollutant generation units. It was proven that the drivers' behavioral model, their driving patterns, and even the type of PEVs can affect the optimal sizes and locations of the parking lots in the planning problem of DISCO, optimal value of incentive in both planning and operation problems of DISCO and GENCO, and minimum cost of DISCO and maximum profit of GENCO. Therefore, we modelled these factors in the traffic and system-based parking lot allocation planning and operation problems to find the optimal solution.

In our future work, we will focus on study the following problems: i) investigating the effects of presence of SHs on the electricity price volatility in a competitive power market for the first problem, ii) modelling the behavior all types of end user customers considering the price elasticity of demand and the social welfare of end users for the second problem, and iii) investigating other advantages of replacing conventional vehicles with PEVs on the power system and its related benefits for the drivers for the third problem. Our goal is to design efficient solutions for these three problems towards constructing a smart grid.

APPENDICES

APPENDIX A

Nomenclature for Problems I

Indices and sets:

h, H	Index and set of SHs
h', H'	Index and set of connected SHs to a SH
s, S, n_s	Index, set, and total number of scenarios related to solar irradiance
t_1, T_1, n_{t1}	Index, set, and total number of time in five-minute scale
t_2, T_2, n_{t2}	Index, set, and total number of time in one-hour scale
X	Set of continuous variables of problem
x	Set of discrete variables of problem

System and problem parameters and variables:

C^{E_DG}	Carbon emission cost of DG (¢)
C^{F_DG}	Fuel cost of DG (¢)
C^{SW_PEV}	Switching cost of battery of PEV (¢)
C^{STU_DG}	Start up cost of DG (¢)
C^{SHD_DG}	Shut down cost of DG (¢)
Cap^{PEV}	Capacity of battery of PEV (kWh)
DOD^{PEV}	Depth of discharge limit for battery of PEV (%)
F	Time step objective function
F^{FL}	Forward-looking objective function

$\mathbb{F}^{FL}$	Stochastic forward-looking objective function
MUT^{DG}	Minimum up time limit of DG (minute)
MDT^{DG}	Minimum down time limit of DG (minute)
$n\tau$	Number of time steps in optimization time horizon of MPC
P^{A}	Available extra power of a connected SH (kW)
$P^{PEV}, \overline{P^{PEV}}$	Power and rated power of battery of PEV (kW)
$\underline{P^{DG}}, \overline{P^{DG}}$	Minimum and maximum power limits of DG (kW)
P^{PV}	Estimated power for PV panels (kW)
P^{N}	Transacted power with a connected SH (kW)
P^{Grid}	Transacted power with DISCO through grid (kW)
P^{L}	Load demand (kW)
SOC^{PEV}	State of charge of battery of PEV (%)
t_{Arr}	Time that PEV arrives and connects to SH
t_{Dep}	Time that PEV disconnects from SH and departs
$\Delta t_{Dep-Arr}$	Time interval that PEV is not connected to SH
Δt^{DG_ON}	The duration that DG is continuously "on"
Δt^{DG_OFF}	The duration that DG is continuously "off"
$\acute{x}^{PEV}$	Indicator for switching battery of PEV
x^{PEV}	Status of battery of PEV
x^{DG}	Status of DG
z_1^F, z_2^F, z_3^F	Fuel cost coefficients of DG (¢/kWh^2, ¢/kWh, ¢)

z_1^E, z_2^E, z_3^E	Carbon emission coefficients of DG (¢/kg^2, ¢/kg, ¢)
π^{DISCO}	Electricity price proposed by local DISCO (¢/kWh)
$\acute{\pi}^{DISCO}$	Revised electricity price by local DISCO (¢/kWh)
π^N	Price of transacted power between neighboring SHs (¢/kWh)
Pr^{PEV}	Price of battery of PEV (¢)
μ^{Er}, σ^{Er}	Mean and standard deviation of prediction errors
Ω	Occurrence probability of a scenario of solar irradiance (%)
φ	Electricity price coefficient based on net energy metering (NEM) plan
β^E	Value of penalty for carbon emissions
ξ^{PEV}	Total cumulative ampere-hours throughput of battery of a PEV in its life cycle (Ah)
$\tilde{\rho}$	Forecasted value of solar irradiance (W/m^2)
ρ	Estimated solar irradiance (W/m^2)
ρ^s	Solar irradiation in the standard environment set as 1000 W/m^2
ρ^c	Certain solar irradiation point set as 150 W/m^2

APPENDIX B

Nomenclature for Problem II

Indices and sets:

$Model$	Behavioral model of an end user
g, Ng	Index and total number of generation units

t, Nt	Index of time and total number of hours in a day

System and problem parameters and variables:

$C^{STU}, Cost^{STU}$	Start-up cost of a generation unit
$C^{SHD}, Cost^{SHD}$	Shut down cost of a generation unit
$Cost^{F}$	Fuel cost of a generation unit
$Cost^{E}$	Greenhouse gas emissions cost of a generation unit
D^{PASS}	Demand of passive end users
D^{SHS}	Demand of active end users (smart homes)
$Income^{SELL}$	Income due to selling electricity
MDT, MUT	Minimum down time and minimum up time of a generation unit
OF	Objective function of a GENCO
$OFFT, ONT$	Duration that a generation unit has been kept "off" and "on"
P	Power of a generation of unit
P^{min}, P^{max}	Minimum and maximum power limit of a generation unit
RDR, RUR	Ramp down rate and ramp up rate of a generation unit
SR	Spinning reserve amount
x^{G}	Binary variable as commitment status of a generation unit
$\alpha_1^F, \alpha_2^F, \alpha_3^F$	Fuel cost coefficients of a generation unit
$\alpha_1^E, \alpha_2^E, \alpha_3^E$	Greenhouse gas emissions coefficients of a generation unit
β^{E}	Greenhouse gas emissions cost factor
π	Price of electricity before energy management

$\tilde{\pi}$	Price of electricity after energy management
ρ^{EM}	Variable for modifying electricity prices at peak period

APPENDIX C

Nomenclature for Problem III

Indices and sets:

b, Nb	Index and total number of buses of a system
br, Nbr	Index and total number of branches of a feeder
d	Index of year
e, N_{Tot}^{PEVs}	Index and total number of PEVs in an area
$Model$	Behavioral model of drivers with respect to value of incentive including linear (Lin), power (Pow), exponential (Exp), and logarithmic (Log)
t	Index of time in hour
y, Ny	Index of year and time horizon of planning period (year)

System and problem parameters and variables:

C^{PEV}	Capacity of battery of a PEV
C^{INV}	Amount of investment for equipping a parking lot for one PEV
C^{MAINT}	Amount of yearly maintenance cost of a parking lot for one PEV
$Cost^{INV}$	Total investment cost for installing parking lots in the optimal locations
$Cost^{MAINT}$	Maintenance cost of installed parking lots over operation period
$\widetilde{Cost^{MAINT}}$	Present worth value of maintenance cost of installed parking lots over

	operation period
$Cost^{INC}$	Cost of incentive (due to considering discount on charging fee of PEVs by a DISCO over planning period and extra credit by a GENCO over operation period)
$Cost^{EL}$	Energy loss cost of a feeder over operation period
$\widetilde{Cost^{EL}}$	Present worth value of energy loss cost of a feeder over operation period
$Cost^{EENS}$	Expected energy not supplied cost of a feeder over operation period
$\widetilde{Cost^{EENS}}$	Present worth value of expected energy not supplied cost of a feeder over operation period
D^{PL}	Hourly demand of parking lot
D^{EU}	Hourly demand of end users
EL	Value of energy loss of a feeder over planning horizon
$EENS$	Value of expected energy not supplied of a feeder over operation period
$\|I\|$	Magnitude of current flowing through a branch
$Income^{SELL}$	Income of GENCO due to selling electricity
IFR	Value of inflation rate (%)
ITR	Value of interest rate (%)
km^{kWh}	Amount of distance in kilometer that a PEV can travel per 1 kWh energy of its battery
LNS^{FL}	Value of load not supplied during locating a fault
LNS^{FR}	Value of load not supplied during repairing a fault

MVA^{BASE}	Value of base power in per unit system
$\|MVA^{BR}\|$	Magnitude of apparent power flowing through a branch
$\overline{\|MVA^{BR}\|}$	Allowable magnitude of apparent power of a branch
N_{Model}^{PEVs}	Number of PEVs' drivers that charge their PEVs through a parking lot in planning problem of a DISCO and number of PEVs' drivers that let the GENCO to decide on charging time of PEVs in operation problem of a GENCO
OF	Objective function
R	Value of resistance of a branch
SOC^{PEV}	State of charge of a PEV
$\|V^{B}\|$	Magnitude of voltage of a bus
$\overline{\|V^{B}\|}$	Allowable magnitude of voltage of a bus
x^{PEV}, y^{PEV}	Hourly position data of a PEV
γ	Value of incentive (discount on charging fee of PEVs considered by a DISCO and extra credit considered by a GENCO)
λ	Value of failure rate of a branch in planning problem of DISCO and marginal cost of system in generation scheduling problem of GENCO
ξ_{Model}	Percentage of drivers that charge their PEVs through a parking lot in planning problem of a DISCO and percentage of drivers that let the GENCO to decide on charging time of PEVs in operation problem of a GENCO

τ^{FL}	Failure locating duration (hour)
τ^{FR}	Failure repairing duration (hour)
π^{E}	Electricity price (Cent/kWh)
π^{ENS}	Energy not supplied cost of customers (Cent/kWh)
σ^{V}	Allowable tolerance for magnitude of voltage of a bus (%)
$\overline{\beta}$	Average daily distance of a PEV from a bus of feeder

APPENDIX D

Genetic Algorithm (GA) Parameters

a	Acceptance indicator of a chromosome
fit_c	Fitness of a chromosome
n_c	Number of chromosomes in population
r	A random number between [0,100]
θ^{Mut}	Value of mutation probability of genes (%)
θ^{PFBS}	Value of selection probability of a chromosome (%)

APPENDIX E

Quantum-Inspired Simulated Annealing (QSA) Algorithm Parameters

f^{BOLTZ}	Boltzmann function
k, Nk	Index and total number of trials for producing new solution at every temperature

O	Value of observed Q-bit
r	A random number between [0,1]
Rot	Rotation gate
z	A factor for decreasing temperature of molten metal
α	Square of probability amplitude that the Q-bit will be observed in '0' state
β	Square of probability amplitude that the Q-bit will be observed in '1' state
$\Delta\varphi$	Rotation angle
$\|\psi\rangle$	Superposition of states
μ	Sigmoid heating function
$\mathbb{Q}$	Q-bit matrix of problem variables
θ_0, θ	initial and current temperature of molten metal
ε	Value of internal energy of molten metal
ω_1, ω_2	Parameters of sigmoid heating function

APPENDIX F

Abbreviations

DISCO	Distribution company
DG	Diesel generator
DOD	Depth of discharge
EM	Energy management
GA	Genetic algorithm

GA-LP	Genetic algorithm-linear programming
GENCO	Generation company
MINLP	Mixed-integer nonlinear programming
MPC	Model predictive control
PEV	Plug-in electric vehicle
PV	Photovoltaic
QSA	Quantum-inspired simulated annealing
SH	Smart home
SOC	State of charge
UC	Unit commitment

REFERENCES

[1] International Energy Agency (IEA), Technology Roadmap, Smart Grids, 2011. [Online].Available:https://www.iea.org/publications/freepublications/publication/smartgrids_roadmap.pdf

[2] D. Pengwei and L. Ning, "Appliance commitment for household load scheduling," *IEEE Trans. Smart Grid*, vol. 2, pp. 411-419, 2011.

[3] A. Zipperer, P. A. Aloise-Young, S. Suryanarayanan, R. Roche, L. Earle, D. Christensen, P. Bauleo, and D. Zimmerle, "Electric energy management in the SH: Perspectives on enabling technologies and consumer behavior," *Proceedings of the IEEE*, vol. 101, no. 11, pp. 2397-2408, 2013.

[4] U.S. Energy Information Administration, "Annual energy review 2011," Washington, DC, EIA-0384, Sep. 2012.

[5] OECD/IEA, International Energy Agency, 2013. [Online]. Available: http://www.iea.org/aboutus/faqs/energyefficiency.

[6] R. Harper, "Inside the Smart Home," *Springer*, 2003.

[7] United States Congress, "Energy Independence and Security Act of 2007," *United States Government Printing Office*, July 2007.

[8] [Online]. Available: http://www.homes.com/blog/2012/08/7-recent-advances-in-home-security-technology/

[9] U.S. Congress, H. R. 6, "Energy Independence and Security Act of 2007," *110th Congress, 1st Session*, Jan. 4, 2007. [Online]. Available: http://www.gpo.gov/fdsys/pkg/BILLS-110hr6enr/pdf/BILLS-110hr6enr.pdf.

[10] L. Jiang, D. Y. Liu, and B. Yang, "Smart home research," *in Proc. 2004 Int. Conf. Mach. Learn. Cybern.*, vol. 2, pp. 659-663, 2004.

[11] Federal energy regulatory commission, [Online]. Available: http://www.ferc.gov/industries/electric/indus-act/section-1241.pdf.

[12] L. Chua and L. Yang, "Cellular neural networks," *IEEE international symposium on circuits and systems*, vol. 2, pp. 985–988, 1998.

[13] M. Lisovich, D. Mulligan, and S. B. Wicker, "Inferring personal information from demand response systems," *IEEE Security and Privacy Magazine*, 2010.

[14] C. O. Adika and L. Wang, "Autonomous appliance scheduling for household energy management," *IEEE Trans. Smart Grid*, vol. 5, no. 2, pp. 673-682, 2014.

[15] C. Chen, J. Wang, Y. Heo, and S. Kishore, "MPC-based appliance scheduling for residential building energy management controller," *IEEE Trans. Smart Grid*, vol. 4, no. 3, pp. 1401-1410, 2013.

[16] N. G. Paterakis, O. Erdinç, A. G. Bakirtzis, and J. P. S. Catalao, "Optimal household appliances scheduling under day-ahead pricing and load-shaping demand response strategies," *IEEE Trans. Indust. Info.*, vol. 11, no. 6, pp. 1509-1519, 2015.

[17] Z. Wu, S. Zhou, J. Li, and X. Zhang, "Real-time scheduling of residential appliances via conditional risk-at-value," *IEEE Trans. Smart Grid*, vol. 5, no. 3, pp. 1282-1291, 2014.

[18] A. Agnetis, G. Pascale, P. Detti, and A. Vicino, "Load scheduling for household energy consumption optimization," *IEEE Trans. Smart Grid*, vol. 4, no. 4, pp. 2364-2373, 2013.

[19] Y. Liu, S. Hu, H. Huang, R. Ranjan, A. Y. Zomaya, and Lizhe Wang, "Game-theoretic market-driven SH scheduling considering energy balancing," *IEEE System Journal,* DOI: 10.1109/JSYST.2015.2418032.

[20] M. A. A. Pedrasa, T. D. Spooner, and I. F. MacGill, "Coordinated scheduling of residential distributed energy resources to optimize SH energy services, *IEEE Trans. Smart Grid,* vol. 1, no. 2, pp. 134-143, 2010.

[21] N. Gatsis and G. B. Giannakis, "Residential load control: Distributed scheduling and convergence with lost AMI messages," *IEEE Trans. Smart Grid,* vol. 2, no. 3, pp. 1-17, Feb. 2012.

[22] T. Chang, M. Alizadeh, and A. Scaglione, "Real-time power balancing via decentralized coordinated home energy scheduling," *IEEE Trans. Smart Grid,* vol. 4, pp. 1490-1504, 2013.

[23] M. Rahmani-andebili and H. Shen, "Energy scheduling for a smart home applying stochastic model predictive control," *Proc. of 6th International Workshop on Context-aware Performance Engineering for the Internet of Things (ContextQoS) in conjunction with ICCCN 2016,* Waikoloa, Hawaii, USA, Aug. 1-4, 2016.

[24] [Online]. Available: http://www.globalissues.org/article/595/energy-security.

[25] IEA, Strategic plan for the IEA demand-side management program 2008-2012, [Online]. Available: http://www.ieadsm.org.

[26] Worldwide survey of network-driven demand-side management projects, Task XV, IEA-DSM Res. Rep. 1, 2006.

[27] M. Muslu, "Economic dispatch with environmental considerations: Tradeoff curves and emission reduction rates," *Electr. Power Syst. Res.* vol. 71, pp. 153-158, 2004.

[28] A. J. Wood and B. F. Wollenberg, Power Generation, Operation, Control. New York, NY, USA: Wiley, 1984.

[29] C. Goldman, M. Reid, R. Levy, and A. Silverstein, "Coordination of energy efficiency and demand response," *A Resource of the National Action Plan for Energy Efficiency*, Jan. 2010.

[30] P. Cappers, C. Goldman, and D. Kathan, "Demand response in U.S. electricity markets: Empirical evidence," *Energy,* vol. 35, pp. 1526-1535, 2010.

[31] J. H. Yoon, R. Bladick, and A. Novoselac, "Demand response for residential buildings based on dynamic price of electricity," *Energy and Buildings*, vol. 80, pp. 531-541, 2014.

[32] M. Rastegar and M. Fotuhi-Firuzabad, "Load management in a residential energy hub with renewable distributed energy resources," *Energy and Buildings*, vol. 107, pp. 234–242, 2015.

[33] A. Taniguchia, T. Inouea, M. Otsukia, Y. Yamaguchia, Y. Shimoda, A. Takamic, and K. Hanaoka, "Estimation of the contribution of the residential sector to summer peak demand reduction in Japan using an energy end-use simulation model," *Energy and Buildings,* vol. 112, pp. 80–92, 2016.

[34] F. Brahman, M. Honarmand, and S. Jadid, "Optimal electrical and thermal energy management of a residential energy hub, integrating demand response and energy storage system," *Energy and Buildings*, vol. 90, pp. 65–75, 2015.

[35] A. Keshtkara, S. Arzanpoura, F. Keshtkarb, and P. Ahmadi, "Smart residential load reduction via fuzzy logic, wireless sensors, and smart grid incentives," *Energy and Buildings*, vol. 104, pp. 165–180, 2015.

[36] Z. Zhao and L. Wu, "Impacts of high penetration wind generation and demand response on LMPs in day-ahead market," *IEEE Trans. Smart Grid*, vol. 5, pp. 220-229, 2014.

[37] C. D. Jonghe, B. F. Hobbs, and R. Belmans, "Value of price responsive load for wind integration in unit commitment," *IEEE Trans. Power Syst.*, vol. 29, pp. 675-85, 2014.

[38] S.H. Madaeni and R. Sioshansi, "Using demand response to improve the emission benefits of wind," *IEEE Trans Power Syst.*, vol. 28, no. 2, pp. 1385–94, 2013.

[39] F.H. Magnago, J. Alemany, and J. Lin, "Impact of demand response resources on unit commitment and dispatch in a day-ahead electricity market," *Electrical Power and Energy Systems*, vol. 68, pp. 142–149, 2015.

[40] M. Rahmani-andebili, M. P. Moghaddam, A. Abdollahi, "An investigation of implementing emergency demand response programs in unit commitment problem," *IEEE PES General Meeting*, USA, July 2011.

[41] M. Rahmani-andebili and G. K. Venayagamoorthy, "Combined emission and economic dispatch incorporating demand side resources," *IEEE Clemson PSC*, Clemson, SC, USA, Mar. 2015.

[42] M. Rahmani-andebili, "Investigating effect of responsive loads models on UC collaborated with demand side resources", *IET Generation, Transmission & Distribution*, vol. 7, no. 4, pp. 420-430, Apr. 2013.

[43] M. Rahmani-andebili, "Nonlinear demand response programs for residential customers with nonlinear behavioral models," *Energy and Buildings (Elsevier)*, vol. 119, pp. 352-362, 2016.

[44] U.S. Department of Energy, "Benefits of demand response in electricity markets and recommendations for achieving them," A report to the U.S. congress, section 1252, energy policy act of 2005, Feb. 2006.

[45] L. Wu "Impact of price-based demand response on market clearing and locational marginal prices," *IET Gener Transm Distrib*, vol. 7, no. 10 pp. 1087–95, 2013.

[46] S.F. Tie, C.W. Tan, "A review of energy sources and energy management system in electric vehicles," *Renewable and Sustain Energy Reviews*, vol. 20, pp. 82-102, 2013.

[47] W. Kempton, et al., "A test of vehicle-to-grid (V2G) for energy storage and frequency regulation in the PJM system," Newark, DE: Univ. Delaware, 2008.

[48] Canadian Automobile Association Electric Vehicles: What You Need to Know. [Online]. Available: <http://electricvehicles.caa.ca/government-incentives/>

[49] According to BC Hydro's Draft Integrated Resource Plan, Appendix 2A–2011 Electric Load Forecast. [Online]. Available: <https://www.bchydro.com/content/dam/hydro/medialib/internet/documents/environment/EVcharging_infrastructure_guidelines09.pdf>

[50] A.S. Masoum, S. Deilami, P.S. Moses, M.A.S. Masoum, A. Abu-Siada, "Smart load management of plug-in electric vehicles in distribution and residential networks with charging stations for peak shaving and loss minimization considering voltage regulation," *IET Gener. Transm. Distrib.* vol. 5, pp. 877–888, 2011.

[51] L.P. Fernandez, T.G. San Roman, R. Cossent, C.M. Domingo, P. Frias, Assessment of the impact of plug-in electric vehicles on distribution networks, *IEEE Trans. Power Syst.* vol. 26, pp. 206–213, 2011.

[52] J.C. Ferreira, et al., "Vehicle-to-anything application (V2Anything App) for electric vehicles," *IEEE Trans Ind Informat*., vol. 10, pp. 1927–1937, 2014.

[53] J. Kiviluoma, P. Meibom, "Methodology for modelling plug-in electric vehicles in the power system and cost estimates for a system with either smart or dumb electric vehicles," *Energy*, vol. 36, pp. 1758-1767, 2011.

[54] J. Liu, "Electric vehicle charging infrastructure assignment and power grid impacts assessment in Beijing," *Energy Policy*, vol. 51, pp. 544–557, 2012.

[55] T.D. Chen, K.M. Kockelman, M. Khan, "Locating electric vehicle charging stations parking-based assignment method for Seattle," *Washington. Transp Res Rec*, vol. 2385, pp. 28–36, 2013.

[56] A.P. Antunes, G. Gonçalves, A. Ribeiro, I. Frade, "Optimal location of charging stations for electric vehicles in a neighborhood in Lisbon," *Portugal. Transp Res Rec*, vol. 2252, pp. 91–98, 2011.

[57] J. Wirges, S. Linder, A. Kessler, "Modelling the development of a regional charging infrastructure for electric vehicles in time and space," *Eur J Transport Infrastruct Res*, vol. 12, pp. 391–416, 2012.

[58] D.Q. Oliveira, A.C. Zambroni de Souza, L.F.N. Delboni, "Optimal plug-in hybrid electric vehicles recharge in distribution power systems," *Elect Power Syst Res*, vol. 98, pp. 77– 85, 2013.

[59] Z. Liu, F. Wen, G. Ledwich, "Optimal planning of electric-vehicle charging stations in distribution systems," *IEEE Trans Power Del*, vol. 28, pp. 102-110, 2013.

[60] E. Sortomme, M. Hindi, S. MacPherson, S. Venkata, "Coordinated charging of plugin hybrid electric vehicles to minimize distribution system losses," *IEEE Trans Smart Grid*, vol. 2, pp. 198–205, 2011.

[61] M.H. Moradi, M. Abedini, S.M. Reza Tousi, S. M. Hosseinian, "Optimal siting and sizing of renewable energy sources and charging stations simultaneously based on Differential Evolution algorithm," *Electrical Power and Energy Systems*, vol. 73, pp. 1015–1024, 2015.

[62] F. Fazelpour, M. Vafaeipour, O. Rahbari, M.A. Rosen, "Intelligent optimization to integrate a plug-in hybrid electric vehicle smart parking lot with renewable energy resources and enhance grid characteristics," *Energy Conversion and Management*, vol. 77, pp. 250–261, 2014.

[63] M. Rahmani-andebili, G.K. Venayagamoorthy, "SmartPark placement and operation for improving system reliability and market participation," *Elect. Power Syst. Res.*, vol. 123, pp. 21-30, 2015.

[64] K. Hedegaard, H. Ravn, N. Juul, P. Meibom, “Effects of electric vehicles on power systems in Northern Europe,” *Energy*, vol. 48, pp. 356-368, 2012.

[65] S. Guo, H. Zhao, “Optimal site selection of electric vehicle charging station by using fuzzy TOPSIS based on sustainability perspective,” *Applied Energy*, vol. 158, pp. 390–402, 2015.

[66] M. Rahmani-andebili “Spinning reserve supply with presence of plug-in electric vehicles aggregator considering compromise between cost and reliability,” *IET Gener Trans Distrib.*, vol. 7, pp. 1442-1452, 2013.

[67] M. Rahmani-andebili, “Optimal power factor for optimally located and sized solar parking lots applying quantum annealing,” *IET Gener. Transm. Distrib.* vol. 10, pp. 2538-2547, 2016.

[68] Y. Fan, and L. Furong, “An exploration of a probabilistic model for electric vehicle residential demand profile modeling,” *IEEE Power Energy Soc. Gen. Meet.,* San Diego, CA, USA, Jul. 2012.

[69] B. Zhang and M. Kezunovic, “Impact of available electric vehicle battery power capacity on power system reliability,” *IEEE Power Energy Soc. Gen. Meet.,* pp.1–5, Jul. 2011.

[70] S.M. Mohammadi H., A. Fereidunian, H. Lesani, and M. Hashemi, “Enhancement of self-healing property of smart grid in islanding mode using electric vehicles and direct load control,” SGC 2014, Iran, Dec. 2014.

[71] J. J. Grainger and W. D. Stevenson, Jr., “Power system analysis,” New York: McGraw-Hill, 1994.

[72] J. B. Rawlings and D. Q. Mayne, "Model predictive control: Theory and design," Nob Hill Publishing, LLC, Madison, WI, 2009. [Online]. Available: http://jbrwww.che.wisc.edu/home/jbraw/mpc/electronic-book.pdf.

[73] M. Rahmani-andebili and G. K. Venayagamoorthy, "Stochastic optimization for combined economic and emission dispatch with renewables," *IEEE Symposium Series on Computational Intelligence*, Cape Town, pp. 1252-1258, 2015.

[74] M. Mitchell "An Introduction to Genetic Algorithms," Cambridge, MA: MIT Press. ISBN 9780585030944, 1996.

[75] R. H. Liang and J. H. Liao, "A fuzzy-optimization approach for generation scheduling with wind and solar energy systems," *IEEE Trans. Power Syst.*, vol. 22, no. 4, pp. 1665-1674, 2007.

[76] U.S. energy information administration (EIA), [Online]. Available: http://www.eia.gov/todayinenergy/detail.cfm?id=9310. <Accessed Oct. 2015>.

[77] H. Saadat, "Power System Analysis," McGraw-Hill, Apr. 2009.

[78] https://en.wikipedia.org/wiki/Speed_limits_in_the_United_States.

[79] Z. Chen and P. Luo, "Incorporating quantum computation into simulated annealing for optimization problems," *IEEE Congress on Evolutionary Computation (CEC)*, New Orleans, LA, 2011.

[80] M. Nielsen and I. Chuang, "Quantum computation and quantum information," 10th Anniversary Edition. Cambridge University Press, 2010.

[81] P. A. M. Dirac, "The Principles of Quantum Mechanics," 4th ed. Oxford University Press, USA, February 1982.

[82] IEEE Guide for Electric Power Distribution Reliability Indices, IEEE Std., pp. 1366–2003, 2004.

[83] R. Billinton and R. N. Allan “Reliability evaluation of power system,” 2nd ed. New York: Plenum Press; 1996.

[84] D. Newbery, “The Economics of Electric Vehicles,” EPRG and Imperial College London, E&E Seminar, Cambridge, Jan. 2013. [Online]. Available: http://www.eprg.group.cam.ac.uk/wp-content/uploads/2013/01/EEJan13_EconomicsEVs.pdf.

[85] U.S. energy information administration (EIA), [Online]. Available: http://www.eia.gov/electricity/monthly/epm_table_grapher.cfm?t=epmt_5_6_a, Accessed Jun. 2015.